



Applicability of existing fibre optic cable solutions for strain measurements in mastic asphalt

Anwendbarkeit bestehender Glasfaserkabelösungen für Dehnungsmessungen in Gussasphalt

Applicabilité des solutions existantes de câbles à fibres optiques pour les mesures de déformation dans l'asphalte coulé

**ETH Zürich, Institute for Geotechnical Engineering
Alexander Puzrin, Prof. Dr.
Dominik Hauswirth, Dr.
Urias Morf, MSc ETH
Andrey Molinari**

Forschungsprojekt TRU_20_01B_01 auf Antrag der Arbeitsgruppe Trasse und Umwelt (TRU)

Oktober 2022

1733

Der Inhalt dieses Berichtes verpflichtet nur den (die) vom Bundesamt für Strassen unterstützten Autor(en). Dies gilt nicht für das Formular 3 "Projektabschluss", welches die Meinung der Begleitkommission darstellt und deshalb nur diese verpflichtet.

Bezug: Schweizerischer Verband der Strassen- und Verkehrsfachleute (VSS)

Le contenu de ce rapport n'engage que les auteurs ayant obtenu l'appui de l'Office fédéral des routes. Cela ne s'applique pas au formulaire 3 « Clôture du projet », qui représente l'avis de la commission de suivi et qui n'engage que cette dernière.

Diffusion : Association suisse des professionnels de la route et des transports (VSS)

La responsabilità per il contenuto di questo rapporto spetta unicamente agli autori sostenuti dall'Ufficio federale delle strade. Tale indicazione non si applica al modulo 3 "conclusione del progetto", che esprime l'opinione della commissione d'accompagnamento e di cui risponde solo quest'ultima.

Ordinazione: Associazione svizzera dei professionisti della strada e dei trasporti (VSS)

The content of this report engages only the author(s) supported by the Federal Roads Office. This does not apply to Form 3 'Project Conclusion' which presents the view of the monitoring committee.

Distribution: Swiss Association of Road and Transportation Experts (VSS)



Applicability of existing fibre optic cable solutions for strain measurements in mastic asphalt

Anwendbarkeit bestehender Glasfaserkabelösungen für Dehnungsmessungen in Gussasphalt

Applicabilité des solutions existantes de câbles à fibres optiques pour les mesures de déformation dans l'asphalte coulé

**ETH Zürich, Institute for Geotechnical Engineering
Alexander Puzrin, Prof. Dr.
Dominik Hauswirth, Dr.
Urias Morf, MSc ETH
Andrey Molinari**

Forschungsprojekt TRU_20_01B_01 auf Antrag der Arbeitsgruppe Trasse und Umwelt (TRU)

Imprint

Forschungsstelle und Projektteam

Projektleitung

Alexander M. Puzrin, Prof. Dr.

Mitglieder

Dominik Hauswirth, Dr.

Urias Morf, MSc ETH

Andrey Molinari

Begleitkommission

Präsidentin

Christiane Raab, Prof. Dr.

Mitglieder

Michael Iten, Dr.

Massimo Facchini, Dr.

Nicolas Bueche, Prof. Dr.

Samuel Probst

Fabian Traber

Antragsteller

Arbeitsgruppe Trasse und Umwelt (TRU)

Bezugsquelle

Das Dokument kann kostenlos von <http://www.mobilityplatform.ch> heruntergeladen werden.

Table of contents

Imprint	4
Zusammenfassung	7
Résumé	11
Summary	15
1 Introduction	17
1.1 Initial position.....	17
1.1.1 Mastic asphalt development.....	17
1.1.2 In-situ performance testing of mastic asphalt	17
1.1.3 Distributed fibre optic sensors.....	17
1.1.4 Potential application of distributed fibre optic sensors in mastic asphalt.....	18
1.2 State-of-the-art	18
1.2.1 Traditional technologies	18
1.2.2 Fibre optic point sensors in pavements	18
1.2.3 Distributed fibre optic sensors in pavements	19
1.2.4 Embedment solutions.....	19
1.2.5 Conclusions and further research	20
1.3 Research question	20
2 Measurement technology and cables solutions	21
2.1 Distributed fibre-optic sensing.....	21
2.2 Cables	23
2.2.1 Initial position.....	23
2.2.2 Requirements on the cable types.....	24
2.2.3 Selected cable solutions	25
2.2.4 Effects of thermal exposure	27
2.3 Modifications	29
2.3.1 Additional protective layer	29
2.3.2 Coated fibre casted in protective material.....	30
2.3.3 Embedment procedure.....	31
2.4 Testing program	32
3 Temperature exposition and strain test	33
3.1 Introduction and purpose	33
3.2 Temperature exposition	33
3.3 Strain test	34
3.4 Results	36
3.4.1 NM1	36
3.4.2 NM2.....	37
3.4.3 PK.....	37
3.4.4 M1	38
3.4.5 M2	38
3.4.6 M3	39
3.4.7 M4	39
3.5 Discussion	40
4 Embedment of cable solutions	45
4.1 Introduction and purpose	45
4.2 Embedment procedure.....	45
4.3 Bending test	49
4.3.1 Test equipment	49
4.3.2 Preparation.....	50
4.3.3 Test procedure	51

4.3.4	Numerical comparison	52
4.4	Results	53
4.4.1	Embedment.....	53
4.4.2	Bending test	53
4.5	Discussion.....	58
4.5.1	Embedment.....	58
4.5.2	Bending test	58
5	Conclusion and recommendations	61
5.1	Conclusions	61
5.1.1	Cables	61
5.1.2	Modification methods 1 and 2 (protective layers)	62
5.1.3	Modification method 3 (embedment procedure).....	62
5.2	Recommendations	62
5.3	Outlook.....	63
5.4	Acknowledgement.....	63
	Appendix.....	65
	Glossary.....	71
	References.....	73
	Project closure	75

Zusammenfassung

Mit einigen der jüngeren Entwicklungen der Bautechnik wird eine breitere Verwendung von Gussasphalt in Straßenbelägen angestrebt. Damit einhergehend wird auch eine eingehendere Untersuchung seiner Eigenschaften und seines Verhaltens vor Ort in der Strasse wichtig werden. Das vorliegende Forschungsprojekt zielt darauf ab, die Frage zu beantworten, ob die derzeit kommerziell verfügbare Glasfasertechnologie ein geeignetes Instrument für diese Aufgabe darstellt. Insbesondere geht es darum, ob die Glasfaserkabel den hohen Temperaturen von bis zu 240°C standhalten und eine ausreichende thermische und mechanische Robustheit unter Beibehaltung der notwendigen Dehnungsübertragungseigenschaften aufweisen. Technisch gesehen kann der Kern der Kabel viel höheren Temperaturen standhalten, aber das Problem liegt in den umgebenden Schutzschichten, die ihren Verbund verlieren können und daher anfällig auf Schlupf zwischen den verschiedenen Schichten sind. Es gibt nur wenige Kabellösungen auf dem Markt, die eine Betriebstemperatur von über 240°C aufweisen. Dabei handelt es sich um sehr dünne Kabel oder Fasern mit sehr widerstandsfähigen Beschichtungen, die jedoch insgesamt nicht über die mechanische Robustheit für ein praktikables Messinstrument auf einer Baustelle verfügen. Resultate anderer Untersuchungen zeigten aber, dass einige existierende Kabellösungen in der Lage sind, ein kurzfristiges deutliches Überschreiten der Betriebstemperaturen relativ unbeschadet zu überstehen. Für andere Fälle wird aber auch die Machbarkeit einfacher Modifikationen zur Verbesserung der thermischen oder mechanischen Robustheit untersucht.

In einem ersten Schritt werden mögliche Kabellösungen identifiziert. Die Kabel mit einer niedrigeren Betriebstemperatur werden dann auf ihre Dehnungsübertragung vor und nach der Exposition gegenüber hohen Temperaturen getestet. Beim Dehnungsversuch werden die Kabel in einer Ausziehbox montiert und über Fixierungen mit einem Schrittmotor verbunden. Mit diesem Motor werden kleine Verschiebungsschritte erzwungen und dabei die spektrale Verschiebung in den Kabeln mit einem optischen Rückstreureflektometer (OBR) gemessen. Zeigen diese Messungen eine konstante Verschiebung über den gespannten Abschnitt, ist die Dehnungsübertragung intakt. Nach dem Testen des originalen Kabels wird es in einen Ofen gelegt und auf 240°C erhitzt. Da bekannt ist, dass einige Kabel nach diesen Temperaturen zum Schrumpfen neigen, wird die Hälfte des Kabels um ein Metallrohr im Ofen vorgespannt. Dadurch wird eine dauerhafte Schrumpfung und der damit verbundene mögliche Signalverlust durch Mikrokrümmung verhindert. Sowohl der gespannte als auch der lose Abschnitt werden dann erneut auf ihre Dehnungsübertragung geprüft. Von den sieben getesteten Kabeln zeigten vier einen starken Verbundverlust nach der thermischen Belastung, was durch spektrale Verschiebungen außerhalb des gespannten Abschnitts erkannt wird.

Aus diesem Grund wurden optionale Modifikationen ausgearbeitet. Als erste Option wird dem Kabel eine zusätzliche Schutzschicht in Form eines Schrumpfschlauches hinzugefügt. Allerdings ist es auch bei Schrumpfschläuchen schwierig, Lösungen zu finden, die bei den hohen Temperaturen funktionieren. Es wurden nur zwei spezielle Schrumpfschläuche gefunden, die eine ausreichende Betriebstemperatur aufweisen. Dennoch werden andere Schrumpfschläuche getestet, um die Temperatur im Inneren der geschützten Kabellösungen zu reduzieren. Weiter wird untersucht, ob die Platzierung der Sensoren an bestimmten Stellen im Gussasphalt, wie z.B. am Boden oder zwischen zwei Schichten, den thermischen Einfluss minimiert und die Eigenschaften als verteilter Dehnungssensor verbessert. Schließlich wird eine dritte Möglichkeit für die dünnen und hochtemperaturbeständigen Kabellösungen untersucht, indem eine schützende Epoxidschicht um die Kabel gegossen wird.

Die Kabellösungen und ihre jeweiligen Modifikationen werden dann in Proben aus Gussasphalt eingebettet. Jede modifizierte Kabellösung wird auf drei verschiedenen Höhen in die jeweilige 80cm x 30cm x 10cm große Probe eingebettet. Die unterste Schicht wird an der Unterfläche platziert und in die erste 3cm dicke Gussasphaltschicht eingebettet. Sobald diese Schicht abgekühlt ist, wird eine Aussparung geschaffen, in welche die mittlere Lage mit einem Bitumen als Schutz eingegossen wird. Die dritte und oberste Kabellage

wird in der Mitte der zweiten Gussasphaltschicht eingegossen. Jedes Kabel wird vor der Einbettung vorgespannt, um die genaue Positionierung zu verbessern. Leider rissen die selbst gegossenen Kabel unter den kalten Bedingungen auf der Baustelle sofort. Außerdem zeigten drei Kabellösungen eine unzureichende Verarbeitbarkeit und einen Verlust des optischen Signals. Letztendlich wurden 17 der 22 vorgesehenen Kabellösungen erfolgreich eingebettet und ermöglichten die Dehnungsmessung in jeder der drei Kabellagen. Außerdem wurden Temperaturmessungen mit Punktsensoren an den drei Kabelstellen vorgenommen. Diese Temperaturen zeigen, dass die Zeit der erhöhten Temperaturen sehr kurz ist und praktisch sofort unter 200°C abkühlt. Diese schnelle Abkühlung kann in einem normalen Ofen im Labor nicht erreicht werden. Daher liegt die Temperaturexposition im Ofen im vorherigen Dehnungsversuch stark auf der konservativen Seite.

Im letzten Versuch werden die fünf Gussasphaltproben, die jeweils vier Kabellösungen auf drei verschiedenen Lagen enthalten, in einem Dreipunkt-Biegeversuch geprüft. Außerdem werden die Proben für zusätzliche Vergleichsmessungen mit externen Glasfaserkabeln ausgestattet und mit den eingebetteten Kabeln in Reihe geschaltet, um deren synchronisierte Messung zu ermöglichen. Um die Kriechdehnungen unter Eigengewicht zu minimieren, werden die Proben an ihren Viertelpunkten abgestützt und in der Mitte der Spannweite mit einer elektrischen Presse belastet. Sobald die Kriechdehnung abgeklungen ist, werden die Proben schrittweise mit 50N bis 3200N belastet, gefolgt von einer sofortigen OBR-Messung. Diese Belastung verursacht Dehnungen zwischen 20µε und 2000µε an der Unterkante in der Mitte der Spannweite. In einem ersten Schritt werden die Messungen der externen faseroptischen Sensoren ausgewertet, um eine Referenzdehnung zu schätzen, die in der unteren Mitte der Spannweite auftritt. Dazu werden die Dehnungen, die sich aus einem numerischen Modell mit einem idealen elastischen Material ergeben, so skaliert, dass sie am besten zu den Messungen der externen Sensoren passen. Mit der Referenzdehnung der jeweiligen Probe und des jeweiligen Lastniveaus können die Dehnungsmessungen der eingebetteten Kabel normalisiert werden und erlauben einen Vergleich zwischen den verschiedenen Proben und Lastniveaus ermöglichen. Diese normalisierten Dehnungen können auf Konstanz zwischen den Lastschritten und auf Übereinstimmung mit dem numerischen Modell geprüft werden.

Viele Kabellösungen zeigen die Dehnungsverteilung genau an, aber es werden auch eine Reihe von Problemen festgestellt. Einige Kabel zeigen Schlupf oder eine inkonstante Dehnungsübertragung. Ein weiteres offensichtliches Problem ist die ungenaue Positionierung, die insbesondere bei dicken Schrumpfschläuchen oder grosser temporärer Temperatureausdehnung auftritt. Die beiden steifen Kabel und ihre jeweiligen Modifikationen schienen eine Art Bewehrung der Probekörper zu zeigen und neigten dazu, seine Reaktion zu verändern. Alle Kabellösungen, die eines dieser Probleme aufweisen, eignen sich nur bedingt als zuverlässige Dehnungssensoren. Aber etwa die Hälfte der Kabellösungen zeigt eine sehr genaue Dehnungsverteilung. Außerdem zeigen einige eingebettete Kabel sogar die vom numerischen Modell vorhergesagten diskontinuierlichen Zonen mit erstaunlicher Genauigkeit an. Die Messung der diskontinuierlichen Zonen kann als das höchste Maß für die Messqualität der eingebetteten Kabel angesehen werden, da hier die größten Dehnungsgradienten auftreten, was eine besonders starke Verbindung zwischen den verschiedenen Kabelschichten und auch mit dem Gussasphalt erfordert.

Die Ergebnisse des Biegetests deuten darauf hin, dass die genaue Positionierung eines Kabels über große Spannweiten eine praktische Herausforderung bleibt, die weitere Aufmerksamkeit erfordert. Die Vorspannung könnte potenziell anfällig für Positionsänderungen unter thermischer Dehnung sein. Daher sollte die Untersuchung anderer Optionen wie eine kraftgesteuerte oder eine wiederholte Vorspannung in Betracht gezogen werden. Ansonsten ist die Einbettung an der Schnittstelle zwischen zwei Asphaltsschichten oder an der Bodenoberfläche eine vielversprechende Option. Weiter zeigt sich, dass die untersuchten Modifikationen nicht zwingend notwendig sind und dass die dicken und die hochtemperaturbeständigen Schrumpfschläuche Probleme bei der Positionierung und der Dehnungsübertragung verursachen können. Lediglich die weitverbreiteten Polyolefin-Schrumpfschläuche erhöhen die mechanische Festigkeit ohne erkennbare Nachteile. Die zweite Modifikationsmöglichkeit mit den dünnen,

hochtemperaturbeständigen Kabeln mit zusätzlichem Schutz erwies sich als wenig praktikable Lösung. Letztlich zeigt sich, dass die Dehnungsverteilung mit höherer Genauigkeit als erwartet gemessen werden kann. Dies eröffnet die Möglichkeit für eine genauere Untersuchung der Lasteinleitung in der Zukunft. Insbesondere zwei der getesteten Kabel liefern sowohl im Dehnungsversuch als auch im Biegeversuch sehr gute Ergebnisse, mit und ohne Schrumpfschläuche als zusätzlichen Schutz. Zusammenfassend lässt sich sagen, dass die faseroptische Technologie kommerziell verfügbar ist, um das Verhalten von Gussasphalt zu untersuchen.

Résumé

Le développement récent des techniques de construction ouvre la voie à une utilisation plus large de l'asphalte coulé dans les revêtements routiers. Par conséquent, une étude plus élaborée de ses propriétés et caractéristiques est nécessaire. Le présent projet de recherche vise à répondre à la question de savoir si la technologie de la fibre optique actuellement disponible dans le commerce constitue un instrument approprié pour cette tâche. En particulier, les principales préoccupations sont de savoir si les câbles à fibres optiques peuvent supporter des températures élevées allant jusqu'à 240°C et fournir une robustesse thermique et mécanique suffisante, tout en maintenant les caractéristiques de transfert de contrainte nécessaires. Techniquement, l'élément centrale des câbles peut supporter des températures beaucoup plus élevées, mais le problème réside dans les revêtements de protection environnants qui peuvent perdre leur adhérence et sont donc susceptibles de glisser entre les différentes couches. Il n'y a que quelques solutions de câbles sur le marché qui indiquent une température de fonctionnement supérieure à 240°C. Il s'agit de câbles très fins avec des revêtements très résistants, mais qui n'ont pas la robustesse mécanique nécessaire pour fournir un instrument de mesure utilisable sur un chantier de construction. Cependant, les résultats d'autres investigations ont montré que certaines solutions de câbles existantes sont capables de supporter relativement indemnes un dépassement significatif à court terme des températures de fonctionnement. Pour d'autres cas, cependant, la faisabilité de modifications simples pour améliorer la fiabilité thermique ou mécanique est également à l'étude.

Dans un premier temps, les solutions possibles pour les câbles sont identifiées. Les câbles ayant une température de fonctionnement plus basse sont ensuite testés pour évaluer la transmission de l'allongement avant et après une exposition à des températures élevées. Dans l'essai de transmission de l'allongement, les câbles sont montés dans une boîte d'extraction et reliés par des fixations à un moteur pas-à-pas. De petits incréments de déplacement sont imposés par ce moteur et le décalage spectral des câbles est mesuré à l'aide d'un réflectomètre à rétrodiffusion optique (OBR). Si ces mesures indiquent un décalage constant sur la section tendue, leur transmission de l'allongement est intact. Après avoir été testé, le câble original est placé dans un four et chauffé jusqu'à 240°C. Comme on sait que certains câbles ont tendance à se rétracter lorsqu'ils sont exposés à ces températures, la moitié du câble est précontrainte autour d'un tube métallique dans le four. Le rétrécissement permanent et la perte de signal qui en découle en raison de la microflexion sont ainsi évités. La section tendue et la section lâche sont ensuite testées une nouvelle fois pour vérifier leur transmission de l'allongement. Sur les sept câbles testés, quatre ont montré une forte perte de liaison après l'exposition thermique, ce qui est indiqué par des décalages spectraux en dehors de la section tendue.

Pour cette raison, des modifications optionnelles ont été élaborées. La première option consiste à ajouter une couche de protection supplémentaire au câble constituée d'une gaine thermorétractable. Cependant, même pour les gaines thermorétractables, il est difficile de trouver des solutions qui fonctionnent à des températures élevées. Seules deux gaines thermorétractables spéciales ayant une température de fonctionnement adéquate ont été trouvées. Néanmoins, d'autres gaines thermorétractables sont testées dans le but de minimiser la température à l'intérieur des solutions de câbles protégés. En outre, on cherche à savoir si le placement des capteurs à des endroits particuliers de l'asphalte coulé, par exemple au fond ou entre deux couches, minimise l'influence thermique et améliore les caractéristiques des capteurs de contrainte répartis. Enfin, une troisième option est étudiée pour les solutions de câbles minces et très résistants à la température, en coulant une couche d'époxy protectrice autour des câbles.

Les solutions de câbles et leurs modifications respectives sont ensuite noyées dans des échantillons d'asphalte coulé. Chaque solution de câble modifiée est installée à trois hauteurs différentes dans l'échantillon respectif de 80cm x 30cm x 10cm. La couche inférieure est placée à la surface du sol et noyée dans la première couche de 3cm d'épaisseur d'asphalte coulé. Une fois que cette couche a refroidi, une entaille est créée et la couche intermédiaire est coulée dans celle-ci en utilisant un bitume comme protection.

La troisième et dernière couche de câbles est coulée au milieu de la deuxième couche d'asphalte coulé. Chaque câble est pré-tendu avant l'encastrement pour améliorer la précision du positionnement. Malheureusement, les solutions de câbles développés en train de cette étude se sont immédiatement rompues dans les conditions froides du site. De plus, trois solutions de câbles ont indiqué une maniabilité insuffisante et une perte du signal optique. En fin de compte, 17 des 22 solutions de câble prévues ont été intégrées avec succès et ont permis de mesurer la déformation dans chacune des trois couches de câble respectives. De plus, des mesures de température sont effectuées à l'aide de capteurs ponctuels aux trois emplacements du câble. Ces températures montrent que la durée des températures élevées est très courte et que le refroidissement est pratiquement immédiat en dessous de 200°C. Ce refroidissement rapide ne peut pas être obtenu dans un four ordinaire en laboratoire. Par conséquent, l'exposition à la température dans l'essai de transmission de l'allongement précédent est fortement conservatrice.

Dans la dernière expérience, les cinq échantillons d'asphalte coulé, contenant chacun quatre solutions de câbles sur trois couches différentes, sont testés dans un essai de flexion à trois points. En outre, les échantillons sont équipés de câbles à fibres optiques externes pour des mesures comparatives supplémentaires de la déformation et sont épissés en série avec les câbles intégrés pour permettre leur mesure synchronisée. Pour minimiser les déformations de fluage sous l'effet du poids propre, les spécimens sont soutenus au niveau de leurs quarts de point et chargés au centre de la portée par une presse électrique. Une fois que le taux de déformations de fluage s'est estompé, les spécimens sont chargés progressivement de 50N à 3200N, suivis par une mesure OBR dynamique. Ce chargement provoque des déformations entre 20 $\mu\epsilon$ et 2000 $\mu\epsilon$ à la surface inférieure au centre de la travée. Dans un premier temps, les mesures des capteurs à fibre optique externes sont évaluées pour estimer une déformation de référence se produisant au centre inférieur de la travée. Pour ce faire, les déformations résultant d'un modèle numérique utilisant un matériau élastique idéal sont mises à l'échelle afin de s'adapter au mieux aux mesures des capteurs externes. En divisant les mesures de déformation dans les câbles intégrés par la déformation de référence du niveau de charge respectifs, on obtient des résultats normalisés qui permettent une comparaison entre les différentes éprouvettes et niveaux de charge. Ces déformations normalisées peuvent être comparées au résultat du modèle numérique idéal, qui s'avère fournir une comparaison très précise.

De nombreuses solutions de câbles indiquent la distribution des déformations avec précision, mais divers problèmes sont également identifiés. Certains câbles indiquent un glissement ou une transmission de l'allongement inconstant. Un autre problème apparent est la localisation imprécise des événements déformatifs, qui est associé en particulier à la présence d'une gaine thermorétractable épaisse ou à de gradients de température rapides. Les deux câbles rigides et leurs solutions respectives ont renforcé l'éprouvette et ont fortement modifié sa réponse. Toutes les solutions de câbles qui indiquent l'un de ces problèmes ne servent pas de capteur d'allongement fiable. Mais environ la moitié des solutions de câbles indiquent une distribution très précise de la déformation. De plus, certains câbles enchâssés indiquent même les zones discontinues prévues par le modèle numérique avec une précision étonnante. La mesure des zones discontinues peut être considérée comme la mesure ultime de la performance des câbles enchâssés, car elle implique les plus grands gradients de déformation, ce qui nécessite une liaison particulièrement forte entre les différentes couches de câbles et également avec l'asphalte coulé.

Les résultats de l'essai de flexion indiquent que le positionnement précis d'un câble sur de grandes portées reste un défi pratique qui nécessite une attention particulière. La précontrainte pourrait potentiellement être sensible aux changements de position sous l'effet de l'élongation thermique. Par conséquent, l'étude d'autres options telles qu'une précontrainte contrôlée par la force ou une précontrainte répétée doit être envisagée. Sinon, l'encastrement à l'interface entre deux couches d'asphalte ou à la surface du sol constitue une option prometteuse. En outre, on constate que les modifications étudiées ne sont pas entièrement nécessaires. On peut affirmer que les gaines thermorétractables épaisses et très résistantes à la température peuvent causer des problèmes de positionnement et de transmission de l'allongement. Seules les gaines thermorétractables communes ont augmenté la résistance mécanique sans inconvénient apparent. La

deuxième option de modification utilisant des câbles fins et très résistants à la température avec une protection supplémentaire s'est avérée être une solution peu pratique et sujette à la rupture. En fin de compte, il est démontré que la distribution de la déformation peut être mesurée avec une précision plus précise que prévu. Cela ouvre la porte à une étude plus approfondie de la mesure de distribution des efforts mécaniques dans l'asphalte en avenir. En particulier, deux des câbles testés donnent de très bons résultats dans l'essai de transmission de l'allongement ainsi que dans l'essai de flexion, avec ou sans gaines thermorétractables pour une protection supplémentaire. En conclusion, la technologie des fibres optiques est disponible dans le commerce pour étudier le comportement de l'asphalte coulé.

Summary

Some recent developments of construction technology open the door for a potentially broader usage of mastic asphalt in road pavements. Therefore, a more elaborate investigation of its in-situ properties and characteristics will become more important. The present research project aims at answering the question whether the currently commercially available fibre optic technology provides, amongst others, a suitable instrument for this task. In particular the main concerns are whether the fibre optic cables can sustain the high temperatures of up to 240°C and provide a sufficient thermal and mechanical robustness while maintaining the necessary strain transfer characteristics. Technically the fibre core of the cables can sustain temperatures much higher than this, but the problem lies in the surrounding protective coatings which can lose the bond and are therefore prone to slippage between the different layers. There are only a few cable solutions on the market which indicate an operating temperature above 240°C. These are very thin cables with highly resistant coatings which do not have the mechanical robustness to provide a workable measurement instrument on a construction site. However, results of other studies showed, that some cable solutions are able to withstand short term temperatures which are clearly higher than the operating temperatures and this without detrimental effects. For other cases, however, the feasibility of simple modifications to improve the thermal or mechanical robustness are also investigated.

In a first step possible cables solutions are identified. The cables with a lower operating temperature are then tested for their strain transfer before and after an exposition to high temperatures. In the strain test the cables are mounted into a pull-out box and connected by fixations to a step motor. Small displacement increments are forced with this motor and the spectral shift in the cables is measured using an optical backscatter reflectometer (OBR). If these measurements indicate a constant shift over the tensioned section, their strain transfer is intact. After testing the original cable it is placed into an oven and heated up to 240°C. As it is known that a few cables are prone to shrinkage after being exposed to these temperatures, half of the cable is pre-tensioned around a metal tube in the oven. Thereby permanent shrinkage and the potentially associated loss of signal due to micro-bending is hindered. Both the tensioned and the loose section are then again tested for their strain transfer. Out of the seven tested cables four showed a strong loss of bond after the thermal exposition which is indicated by spectral shifts outside the tensioned section.

For this reason optional modifications were elaborated. As a first option an additional protective layer is added to the cable by a shrinkage tube. However, also for shrinkage tubes it is hard to find solutions which work at the elevated temperatures. Only two special purpose shrinkage tubes with an adequate operating temperature have been found. Nevertheless other shrinkage tubes are tested for the purpose of minimizing the temperature inside the protected cable solutions. Further, it is investigated whether the placement of the sensors at particular positions within the mastic asphalt, such as at the bottom or between two layers, reduces the thermal influence and improves the characteristics as a distributed strain sensor. Ultimately, a third option is investigated for the thin and highly temperature-resistant cable solutions, by casting a protective epoxy layer around the cables.

The cables solutions and their respective modifications are then embedded into samples of mastic asphalt. Each modified cable solution is embedded at three different heights in the respective 80cm x 30cm x 10cm sample. The bottom layer is placed at the bottom surface and embedded in the first 3cm thick layer of mastic asphalt. Once this layer has cooled off, a notch is created and the middle layer is casted into it using a bitumen as protection. The third and top cable layer is casted in the middle of the second mastic asphalt layer. Each cable is pre-tensioned before the embedment to improve the accurate positioning. Unfortunately, the self-casted cable solutions immediately ruptured in the cold conditions at the site. Further, three cable solutions indicated an insufficient workability and a loss of the optic signal. Ultimately, 17 out of the 22 intended cable solutions were embedded successfully and allowed for the strain measurement in each of the respective three cable layers. Further, temperature measurements are taken using point sensors at the three cable locations. These temperatures show that the time of elevated temperatures

is very short and cool off practically immediately below 200°C. This rapid cool-down cannot be achieved inside a regular oven in the laboratory. Therefore, the temperature exposition in the oven in the previous strain test lies strongly on the conservative side.

In the last experiment the five casted samples of mastic asphalt, each containing four cable solutions on three different layers, are tested in a three-point bending test. Further, the specimens are equipped with external fibre optic cables for additional comparative strain measurements and spliced into a series with the embedded cables to allow for their synchronized measurement. To minimize the creeping strains under self-weight the specimens are supported at their quarter points and loaded at the centre of the span by an electrical press. Once the rate of creeping strains has faded the specimens are loaded stepwise from 50N up to 3200N followed by an immediate OBR measurement. This loading causes strains between $20\mu\epsilon$ and $2000\mu\epsilon$ at the bottom surface at the centre of the span. In a first step, the measurements from the external fibre optic sensors are evaluated to estimate a reference strain occurring at the bottom centre of the span. This is done by scaling the strains resulting from a numerical model using an ideal elastic material to best fit the measurements in the external sensors. By dividing the strain measurements in the embedded cables by the reference strain from the respective specimen and load level, normalized results are obtained which allow for a comparison between the different specimens and load levels. These normalized strains can be compared to the result of the ideal numerical model, which is shown to provide a very accurate comparison.

Many cable solutions indicate the strain distribution accurately, but also a variety of problems are identified. Some cables indicate slippage or an inconstant strain transfer. Another apparent problem is the inaccurate positioning, which is associated in particular with the thick shrinkage tube. The two stiff cables and their respective solutions seemed to reinforce their specimen and tended to change its response. All the cable solutions which indicate one of these problems are only suitable to a limited extent to serve as strain sensor. But about half of the cables solutions indicate a very accurate strain distribution. Further, some embedded cables even indicate the discontinuous zones predicted by the numerical model with astonishing accuracy. The measurement of the discontinuous zones can be considered the ultimate measure of the performance of the embedded cables as it involves the largest strain gradients, which requires a particularly strong bond between the different cable layers and also with the mastic asphalt.

The results of the bending test indicate that the accurate positioning of a cable along large spans remains a practical challenge which requires further attention. Pre-tensioning could potentially be susceptible to position changes under thermal elongation. Therefore, the investigation of other options such as a force-controlled pre-stressing or a repeated pre-straining should be considered. Otherwise, the embedment on the interface between two asphalt layers or at the bottom surface provide a promising option. Further, it is seen that the investigated modifications are not entirely necessary. It can be stated that the thick and the highly temperature resistant shrinkage tubes can cause problems in the positioning and the strain transfer. Only the common shrinkage tubes increased the mechanical resistance without apparent disadvantages. The second modification option using the thin, highly temperature resistant cables with additional protection proved to be an impractical solution and prone to breakage. Ultimately, it is shown that the strain distribution can be measured with higher accuracy than expected. This opens the door for a further investigation of the load introduction in the future. In particular two of the tested cables provide very good results in the strain transfer as well as in the bending test, with or without shrinkage tubes for additional protection. Conclusively, the fibre optic technology is commercially available to investigate the behaviour of mastic asphalt.

1 Introduction

1.1 Initial position

Currently, efforts are made for broadening the future application range of mastic asphalt in road construction. This intended new application range of mastic asphalt requires measuring and analysing its structural behaviour in field under traffic loads. A potential measurement tool for assessing the in-situ performance of mastic asphalt are distributed fibre optic sensors. This class of sensors enables to gather a unique amount of strain data within the pavement and it was already successfully applied in hot mix asphalt. However, the temperature range during laying of mastic asphalt is clearly higher, endangering the functionality of fibre optic cable solutions proven in hot mix asphalt. The present research projects has the goal to test the suitability of existing fibre optic cable solution for the higher temperatures present in mastic asphalt. Furthermore, first installation concepts for embedding the fibre in mastic asphalt will be investigated. The present research project is rather small and was conducted in short time in order to deliver recommendations for the potential application of distributed fibre optic sensors in mastic asphalt soon.

1.1.1 Mastic asphalt development

Mastic asphalt represents in principle a pavement material with promising properties for the construction of roads, this especially when taking into account the full life cycle analysis of road construction materials. However, its application was limited so far to rather specific purposes as e.g. bridges or specific surface courses. Recent developments concerning the machinery for casting the mastic asphalt and encouraging results from an initial project gave rise for intentions to investigate the mastic asphalt application for a wider application range in general open road stretches. Further research projects are expected in near future, addressing in particular the placement of the mastic layer as well as its performance under traffic loads.

1.1.2 In-situ performance testing of mastic asphalt

Before applying new materials or procedures in road engineering, usually its behaviour is tested in the laboratory on samples and in the field with full scale tests. There are several existing testing procedures to analyse the in-situ behaviour of roads. In order to measure the structural behaviour, e.g. static or dynamic measurements of the deflection bowl under load may be conducted or strains within the pavement may be measured and analysed. Such strains within the pavement may be gathered by applying electrical strain gages in certain points of interest. In the past years, also fibre optic point sensors were applied for this purpose. However, these sensors can only provide strains in predefined locations, which represents a certain limitation since the strain field present in an asphalt layer has a rather high spatial variability and it is often not clear in advance, where exactly e.g. a strain peak is expected.

1.1.3 Distributed fibre optic sensors

In contradiction to fibre optic point sensors, distributed fibre optic sensors may overcome this limitation since they allow for a continuous measurement of strain along an optical fibre. The required spatial resolution as well as the necessary temporal resolution of the measurements became available in the form of commercial devices over the last years. Currently, sub-centimetre spatial resolution as well as measurement rates of 100Hz up to 250Hz (depending on the sensor length) are available in the form of measurement instruments, enabling for measuring strains in the range of a few microstrains up to several thousand microstrains. In principle, these properties make distributed fibre optic sensors an ideal candidate for measuring the performance of pavements, since a very large amount of measurements data (corresponding to thousands of conventional strain gages) can be acquired within short time. In addition, owing to its continuous nature, it is furthermore ensured that not only relevant strain maxima are being captured in the measurement but

also the spatial distribution of strains can be gathered. However, the particular environment in pavements as well as the harsh conditions on construction sites require an adequate protection of the vulnerable thin silica fibre. For this purpose, commercially available fibre optic cables with different level of robustness were successfully tested in rolled asphalt in a former project [1] (VSS 2014/501).

1.1.4 Potential application of distributed fibre optic sensors in mastic asphalt

Whereas embedment temperatures of rolled asphalt are somewhere around 140°C to 160°C, temperatures for casting mastic asphalt are typically higher. In the current project call, temperatures of 190°C to 240°C are defined as an expected temperature range for mastic asphalt, but 240°C as well as a reserve of 10°C should be considered. This is not a problematic temperature range for the silica fibre, which is acting as optical waveguide and as the sensing element for distributed fibre optic sensors. However, the material of some of the protective and buffer layers, used in usual fibre optic cable solutions, is expected to melt at these temperatures, having potentially detrimental effects on the properties of the cable. In order to exclude such potentially disadvantageous influence on the measurements, existing fibre optic cable solutions should be tested in the relevant temperature range in order to ensure its functionality before embedding them for in-situ performance measurements in mastic asphalt. In addition, an adequate embedment procedure may differ from that applied for hot mix asphalt and should be investigated before applying it in the field.

1.2 State-of-the-art

Since around three decades, various types of fibre optic sensors were increasingly used for measurement and monitoring purpose in civil engineering research. In the past decade, this class of sensors became also increasingly applied in commercial civil engineering projects. By sending light through a fibre and investigating the back-reflected light with different analyses techniques, fibre optic sensors can be applied for different measurement purposes. Various application purposes are also present in the field of road engineering, where e.g. in [2] or [3] weigh-in-motion fibre optic sensors are showed, based on loss measurements caused by bending or micro-bending. A section of a road, equipped with fibre optic strain sensors, can also be used as sensor on a larger scale, as was demonstrated in [4] for the detection of landslide movements. Recently also traffic monitoring systems, based on a fibre optic sensor placed along the road, became commercially available.

1.2.1 Traditional technologies

The present research project aims to use fibre optic sensors for measuring the structural behaviour of the mastic asphalt layers of the road. The assessment of the behaviour and the condition of a road on basis of measuring its structural in-situ performance under load, is a topic of large interest in the field of road engineering. This is reflected in the development of many test devices and a large number of studies, devoted to this subject. In the past, devices as e.g. Benkelman Beam or ETH Delta were developed for measuring the static deflection bowl under load and devices as e.g. Falling Weight Deflectometer or geophones were used to analyse effects of a dynamic impact. Furthermore, classical electrical strain gauges were applied in order to measure strains in certain pre-defined locations caused by various pavement loading.

1.2.2 Fibre optic point sensors in pavements

Such a pointwise strain measurement can also be conducted by means of fibre optic sensors. Fibre Bragg gratings (FBG) enable for strain or temperature measurements in points where a grating is created in the core of the fibre. The rest of the fibre is acting as waveguide for the transmission of light (point sensor). However, multiplexing enables for several gratings along the same fibre, forming already a quasi-distributed sensor, which

can be readout in the kilohertz range. Applications of FBG sensors for measuring strains in roads are reported e.g. in [5], [6] or [7].

1.2.3 Distributed fibre optic sensors in pavements

In this project, distributed fibre optic sensors and no fibre optic point sensors were applied. A brief overview about the application of this sensor class in pavements is provided here. More general information about this sensor class is given in section 2.1.

Fully distributed fibre optic sensors have the advantage that the whole length of the fibre is acting as sensor and hence, strain or temperatures can be monitored gapless along the fibre. On the other hand, earlier measurement techniques had a rather coarse spatial resolution and the time required for a measurement was rather long. However, recent developments made on this class of sensors lead to sub-centimetre spatial resolution and, for short sensors in the range of several meters, to measurement rates of hundred up to several hundred Hertz. In principle, this enables for replacing several hundred to thousand classical strain gages by a single optical fibre and makes these technologies in particular interesting for measuring and assessing the behaviour of structures. The application of distributed fibre optic sensors in pavements based on Brillouin optical time domain analysis (BOTDA) is reported e.g. in [8], [9] or [10]. However, the spatial resolution of this technique is rather coarse for monitoring the structural behaviour. By applying PPP-BOTDA (pulse prepump BOTDA), in [11] the achievement of 0.1m spatial resolution (2cm applicable as a minimum) is reported, which was used for the detection of cracks in a laboratory test on concrete pavement slabs. Beside of distributed sensors, which are based on Brillouin scattering effects in the fibre, there are also distributed fibre optic sensors, which are based on Rayleigh scattering effects. In [12], [13] and [14] such Rayleigh scattering based sensors were used for the purpose strain measurements with high spatial resolution in the asphalt pavement. Such Rayleigh scattering based sensors enable for measurements with sub-centimetre spatial resolution and they were also applied in the project VSS 2014/501 [1]. An overview about recent applications of fibre optic sensors is furthermore provided in [15].

1.2.4 Embedment solutions

Clearly, in almost every study dealing with fibre optic sensor application for the purpose of strain sensing within the pavement, the protection of the fibre from the harsh environment and its performance is briefly addressed. However, important details about cable type, involved materials or procedure are often missing. In the case of FBG applications, the protection is rather simple, because the issue of good strain transfer as well as protection against crushing or detrimental temperature effects needs only to be sorted out around the point of the grating location. In [6], carrying out initially two static roller compaction passages before additionally vibrating with the roller was suggested. In [8], a flexible encapsulation system around the grating location was used for the FBG solution, in between an armoured cable was used. For the BOTDA application they suggested a similar procedure, however, it is not clear how it should be applied for measuring strains continuously with sub-centimetre resolution. Their sensors were embedded in asphalt concrete pavement (and Macadam layer) which was constructed without a paver and only rollers were used (75% survival rate reported). In [7], a resin encapsulated FBG sensor for asphalt concrete applications was used.

Regarding distributed fibre optic sensors, the authors of [12] were using a telecommunication fibre optic cable instead a special fibre optic measurement cable. For their application of crack detection in asphalt concrete (around 170°C), they concluded that high accuracy of strain measurements is not absolutely required. The authors of [13] and [14] were using well-protected fibre optic measurement cables in asphalt concrete, for which they did not observed detrimental effects for a short term temperature exposition up to 140°C (see also research report to VSS 2014/501, [1]). In [9], the authors were wrapping an optical fibre into several thin layers of asphalt mastic before embedding it into asphalt concrete. This in order to protect the fibre from crushing during embedment into asphalt concrete. Detrimental effects of lateral pressure on the fibre were not reported.

1.2.5 Conclusions and further research

No application in mastic asphalt was reported in the studies above. Hence, the typical temporary temperature range in these studies is lower than in mastic asphalt. Hence, it seems not to be clear, whether commercially available, mechanically well-protected fibre optic measurement cable for strain sensing can be exposed to the temperature range of mastic asphalt without suffering from detrimental effects on their performance afterwards. Solutions based on fibres within telecommunication cables may have insufficient strain transfer for in-situ measurement of structural behaviour. Wrapping an optical fibre, which has in principle a high resistance against temperature, into asphalt mastic before embedding in the field, is an interesting approach. However, detrimental effects from lateral pressures should be investigated before using it. Such a prior wrapping of a well-protected fibre optic measurement cables with an asphalt material, could potentially be a promising solution, if this would allow reducing the temperature, acting on the cable during construction of asphalt mastic layer.

1.3 Research question

The present research project is a rather small and short project with a clear focus. It was formulated in order to deliver quickly an answer whether commercially available fibre optic cable solutions may be applied in the temporary high temperature environment of mastic asphalt. This in order to provide an additional tool for measuring and assessing the structural short term response of mastic asphalt in-situ and to contribute to the currently ongoing efforts undertaken to apply mastic asphalt in a broader range of application. In order to provide a fast answer to this question, no development of a new optimized cable design was foreseen.

The focus in the research project is clearly put on studying potentially detrimental effects of the high emplacement temperatures of mastic asphalt on the cable performance regarding its embedment and the transfer of axial strains. For this purpose a measurement device based on Rayleigh backscattering along a conventional single mode fibre was used. Owing to its limited size and short duration, this study cannot answer all further questions regarding embedment and measurement strategies, adequate measurement technology or compensation strategies for other environmental effects, regarding the potential future application of such distributed fibre optic sensors in mastic asphalt.

2 Measurement technology and cables solutions

2.1 Distributed fibre-optic sensing

In the past three decades, the field of distributed fibre optic sensing has experienced a large progress and many measurement technologies and sensor concepts have made the leap from laboratory to industrial applications. A brief overview is provided here, more information about the technology and its application can be found elsewhere as e.g. in [16] or [17]. Measurement interrogators are using connected standard optical silica fibres to detect and measure quantities as strains or temperatures along these fibres. In contrast to fibre optic point sensors, which can measure such quantities in pre-defined points, distributed fibre optic sensors turn the whole length of an optical fibre into a sensing element.

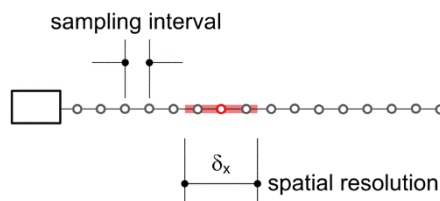


Fig. 1 Distributed fibre optic sensor, after [18] and [19].

Distributed fibre optic sensor technologies are often characterized by a spatial resolution of the measurand and a sampling interval. The first can be interpreted as the minimum length of the measurand event which is required to have a readout with full accuracy. Within this length some sort of the average of the measurand is obtained representing the quantity of the measurand in this zone. Events smaller than this length may not be accurately quantified. The second is simply the spatial distance between two points where the measurand is being computed. Referring to conventional strain measurements using electrical strain gauges, the first one is also called “gauge length” and the second one “sensor spacing”. By choosing the sampling interval equal or smaller than the spatial resolution, one obtains a gapless, continuous measurement along the optical fibre. Beside of the two quantities spatial resolution and sampling interval, also the maximum sensor length as well as measurement rate are important quantities to characterize a distributed sensor.

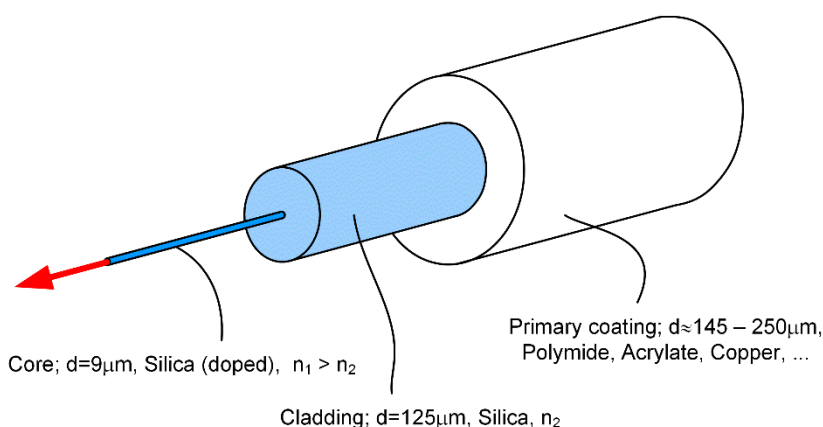


Fig. 2 Optical single mode fibre.

Many distributed fibre optic sensing technologies are using standard single mode (SMF) or multimode fibres (MMF) originating from telecommunication industry. In case of a standard SMF, the fibre consists of a silica core ($9\mu\text{m}$) including some dopants which is surrounded by a cladding ($125\mu\text{m}$), consisting of silica as well (Fig. 2). These silica layers are usually protected by primary coating made from plastic (e.g. acrylate) up to a diameter of $250\mu\text{m}$.

The sensing technologies are based on different scattering phenomena such as Raman, Brillouin or Rayleigh scattering, occurring when a light pulse travels through the core down the fibre ([20], [21]). The light pulse is emitted from a laser, located in the interrogator. Some of these technologies are using stimulated scattering instead of spontaneous scattering which may require a closed loop of the fibre in order to stimulate the fibre from the other end as well as indicated in Fig. 3.

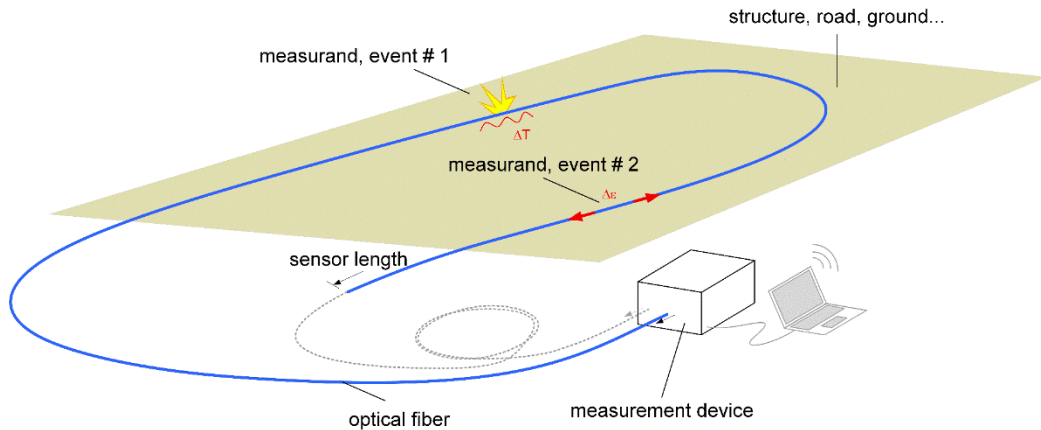


Fig. 3 Distributed fibre optic sensor layout.

Some technologies are sensitive to temperatures only (e.g. distributed temperature sensing DTS based on Raman scattering, e.g. [22]) others are sensitive to strain and temperatures (distributed strain sensing DSS or distributed temperature and strain sensing DTSS based on Brillouin or Rayleigh scattering, e.g. [23], [24] or [25]).

Many different technologies have emerged in the past decades, each of them having its own opportunities and limitations. Some distributed technologies as e.g. BOTDR or BOTDA (Brillouin Optical Time Domain Reflectometry / Analysis, [26], [27] or [28]) nowadays achieve spatial resolution in the sub-metre range and enable sensor lengths of several tens of kilometres. Further developments lead to an even more refined spatial resolution of Brillouin scattering based systems as e.g. PPP-BOTDA (pulse prepump BOTDA, e.g. [29] or [11]) with minimum spatial resolution in the range of several centimetres. On the other hand, development of Rayleigh scattering based measurement technologies as SWI / c-OFDR (Swept Wavelength Interferometry / coherent Optical Frequency Domain Reflectometry, e.g. [30], [31] or [32]) enables for spatial resolution in the sub-centimetre range and even to a limited dynamic measurements of strains but this at the cost of the sensor length, which is limited to several tens of metres. In the past decade further technologies have emerged which enable also for monitoring vibrations (Distributed Vibration / Acoustic Sensing DVS / DAS) enabling the detection of very small strain rates at high frequencies or systems enabling for measuring pressures, some of them based on engineered fibres. As this very brief overview shows, distributed fibre optic sensors form a rapidly developing field, providing many new solutions and opportunities to the field of monitoring structures and the environment.

For the purpose of the present project, a commercially available measurement device (OBR 4600, Luna Inc.) based on Rayleigh backscattering (SWI / c-OFDR) was used, since it best fitted to the goals of this project. This device enables for sensor lengths up to around 70m with spatial resolution in the sub-centimetre range and it is sensitive to strain and temperature changes. The practical strain resolution is in the range of around $1\mu\epsilon$. Data acquisition along the fibre can be conducted within seconds and it contains also an OTDR (Optical Time Domain Reflectometry) option. No dynamic strain measurements or temperature measurements were conducted within this study, however, using other devices and techniques, also this could be possible, but would require first a test with the involved cables.

The applied measurement technology based on Rayleigh backscattering is suited rather for local measurements with fine spatial resolution and relatively short sensor lengths up

to several tens of meters. For measurements involving larger perimeters, other technologies may be a more adequate choice (e.g. technologies based on Brillouin scattering), however, it has to be ensured, that the spatial resolution remains at a useful scale. Whereas many findings of this study are independent of the applied measurement technology, some detrimental effects of the temporary high temperature environment may potentially cause difficulties when applying other measurement technologies (e.g. technologies based on Brillouin scattering). In such a case, the performance of the cables over large sections would need to be analysed and potential other detrimental effects from the high temporary temperatures (e.g. on the Brillouin gain spectrum) would need to be excluded before applying the cable solutions discussed in this study with other technologies. This consideration was not subject of the present study and should be tested before the application.

Beside the usage of the adequate distributed measurement technology, also the choice of an appropriate and adequately packaged optical fibre is very important, since the measurement device can only measure the measurands (e.g. strain or temperature) in the way as they are present in the core of the fibre. Regarding a potential application of this technology in the temporary high temperature environment of mastic asphalt requires suitable cable embedment strategies and compensation methods for the separation of environmental effects of e.g. strain and temperature. Hence, the appropriate choice of the adequate distributed measurement technology is only a part of a successful measurement campaign. In particular if the time-dependent structural response of mastic asphalt is of importance.

2.2 Cables

2.2.1 Initial position

The potential usage of distributed fibre optic technology as a strain sensor in mastic asphalt for the purpose of measuring its short term structural response to external loads poses several requirements to the sensing element, which is the optical fibre. These requirements are:

1. Adequate robustness for field application on construction sites
2. Good strain transfer from the asphalt material to the fibre
3. High temperature resistance during casting of mastic asphalt ($T_{\max} = 240^{\circ}\text{C}$)
4. Limited axial cable stiffness in order not to act as a reinforcement

The present project does not aim to develop a new cable design. The goal is to rapidly find an answer to the question, whether existing, commercially available cable solutions could be applied for this purpose.

A product search, conducted on the websites of cable manufacturers, delivers many cable designs which fulfil two or even three out of these four requirements. There are many high temperature resistant, well-protected cable solutions (e.g. fibre in metal tube (FIMT)) for temperature monitoring. However, most of the time they consist of fibres in loose tube design to prevent or limit the strain transfer. On the other hand, there are many thin coated fibres for high temperature applications available, possessing good strain transfer properties, however, their robustness is limited. In order to find a cable design, which is meeting all four stated requirements, several cable manufacturers and cable suppliers, having promising designs in their portfolio, were contacted. However, in several cases these products were rather existing designs, requiring significant minimum order quantities, than cables available from stock. In addition to that, several companies did unfortunately not react on requests or, owing the pandemic situation, had to include very long delivery times, which were too long for this short project. Unfortunately, no existing solution meeting all requirements could be found within the short time of this project.

However, several promising fibres and cables could be purchased, which may form an acceptable distributed strain sensor for mastic asphalt application. In addition to that, there

exists also the option of protecting these cables with additional layers against the temporary high temperatures or of modifying the embedment procedure in a way that the cable is exposed not to the maximum temperatures, as discussed in section 2.3.3.

2.2.2 Requirements on the cable types

The above listed requirements identified for the fibre optic cables are briefly described in the following sections.

1. Robustness

A certain mechanical robustness of the cable is required for a successful handling on the construction site as well as for the process of installation. However, the required mechanical resistance against crushing from grains in the mastic asphalt or from mechanical stress owing to the production process of the mastic asphalt layers is expected to be lower than in the case of hot mix asphalt (ASTRA research project VSS 2014/501, [1]), since mastic asphalt does not require a compaction with vibrating rollers. Hence, in the absence of the ideal cable candidate, also quite vulnerable cable solutions may not be excluded from the beginning. Please note that in several cable designs, enhanced robustness contributes unfortunately also to increasing axial stiffness and affects also the strain transfer properties.

2. Strain transfer

In principle the distributed fibre optic strain sensor should indicate the strains present in the host material (mastic asphalt) as accurate as possible. This requires that the axial strains present in mastic asphalt around the cable are transmitted through the interface (host material – cable) through the cable sheath layers to the fibre core with only small alterations. However, there are of course limitations. First of all, mastic asphalt is a mixture of grains, bitumen and a small amount of voids. Hence, at a (sub-) millimetre scale, the quantity “strain” may become a very heterogeneous quantity in asphalts, whose correct mapping is not pursued in this project and the focus is on mapping the average strain in the matrix. Second, the spatial resolution of current distributed measurement devices is limited to a minimum of several millimetres. Above this stated boundaries, the strain transfer is mainly influenced by the surface properties of the cable (corrugated vs. smooth, bond to asphalt) as well as the internal strain transfer within the cable layer materials as well as their interfaces.

3. Axial stiffness

Each sensor, and with that also the fibre optic cable, reflects a disturbance to the host material, leading to a potential influence of the sensor on the local structural behaviour and the strain field surrounding the cable. In particular cables with axial stiffness higher than surrounding mastic asphalt may cause an effect similar to a reinforcement. This may strengthen the asphalt and modify its behaviour under load. Further, the transfer of longitudinal force from the cable to asphalt creates a measured axial strain which deviates from the strain present in the host material if the interface between cable and asphalt can transfer only limited shear stresses.

4. Thermal resistance

In contrast to hot mix asphalt, mastic asphalt is poured at significantly higher temperatures. Many efforts are currently undertaken in order to reduce emplacement temperatures of mastic asphalt. However, in order to comply with all situations, a relevant maximum temperature of 240°C was chosen for this project. The cooling curve over time appears to be dependent on laying procedure, layer thickness and environmental conditions, but 240°C represent a temperature which is present only for several minutes in the asphalt. In an ideal case, all involved cable layers are designed to withstand this temperatures also for a longer duration. However, also a temporary melting of the outermost layer may not be crucial, if it does not have disadvantageous effects on the later measurements. It should

be noted, that the optical fibre (silica) itself can sustain temperatures much higher than 240°C.

2.2.3 Selected cable solutions

The nine cable solutions which could be made available for the testing program of this project are summarized in Tab. 1. It is important to note, that none of these cables is initially foreseen by the supplier to this specific mastic asphalt application. In all cases some testing prior to application is required. This family of potentially promising solutions contains no cable which suits all specified requirements and could be ad hoc stated as the ideal cable for the mastic asphalt application. The selection contains solutions which should be stated rather as a coated optical fibre than a fibre optic cable but fulfil the temperature, strain transfer as well as stiffness requirements. However, the criterion of sufficient robustness for mastic asphalt application would need to be checked in this project. On the other hand, there are solutions which fulfil robustness, strain transfer and partially also stiffness requirements but their stated temperature range (product information from the supplier) does not reach the range necessary for mastic asphalt applications. However, not meeting the temperature requirements does not necessarily mean, that the cable is a priori not suited for measuring strains in mastic asphalt, since the high temperature exposure is only temporary during installation, whereas operating temperatures are expected to be smaller than those stated in the suppliers product information. In this case, the goal of this project is to check, whether these cables can withstand the transient high temperatures without damaging their properties to work as a strain sensor. A similar situation was met in [1], where cables were embedded into hot mix asphalt in a temporary high-temperature environment, exceeding the operating temperatures stated by the manufacturer, nevertheless leading to good measurement results. Throughout the whole report, the cables will not be identified by their product name but through their ID given in in Tab. 1.

Tab. 1 Tested cable solutions.

Cable type	ID	Comment
Coated fibre	PI	d = 0.145mm, Polyimide coated 9/125 SMF T < 350°C
Coated fibre	CO	d = 0.26mm, Copper alloy coating on a 9/200 SMF T < 450°C
Fibre with thin plastic jacket	PK	d = 0.9mm, Polyetheretherketon (PEEK) jacket T < 260°C
Non-metallic cable	NM1	d = 2.8mm, Ethylenpropylencopolymer (EPR) jacket; T < 85°C
Non-metallic cable	NM2	b x h = 2 x 3mm, 2 SMF in reinforced plastic sheath T < 70°C
Metallic cable	M1	d = 3.2mm, Polyamide (PA) jacket, thin metal tube T < 85°C
Non-metallic cable	M2	d = 4.5mm, 4 jacketed SMF, 2 SMF and 1MMF loose tube T < 70°C
Metallic cable	M3	d = 3.6mm, outer metal tube, 3 jacketed SMF T < 70°C
Metallic cable	M4	d = 7.2mm, Polyamide jacket, steel wires, thin metal tube T < 85°C

Cross-sections (in scale to each other) of the selected cables are shown in Fig. 4. Where available, some involved materials are also provided. The diameters of these cables range from 0.145mm to 7.2mm and their axial stiffness ranges from around 1kN to 500kN. Several cables involve multiple fibres, which may increase their redundancy. For the cable versions PI, CO and PK, the temperature range should not be a problem, however, their robustness may not a priori fulfil the specific requirements. On the other hand, there are the very robust versions M3 and M4, which on the other hand may be too stiff or may not be applicable to that temperature range.

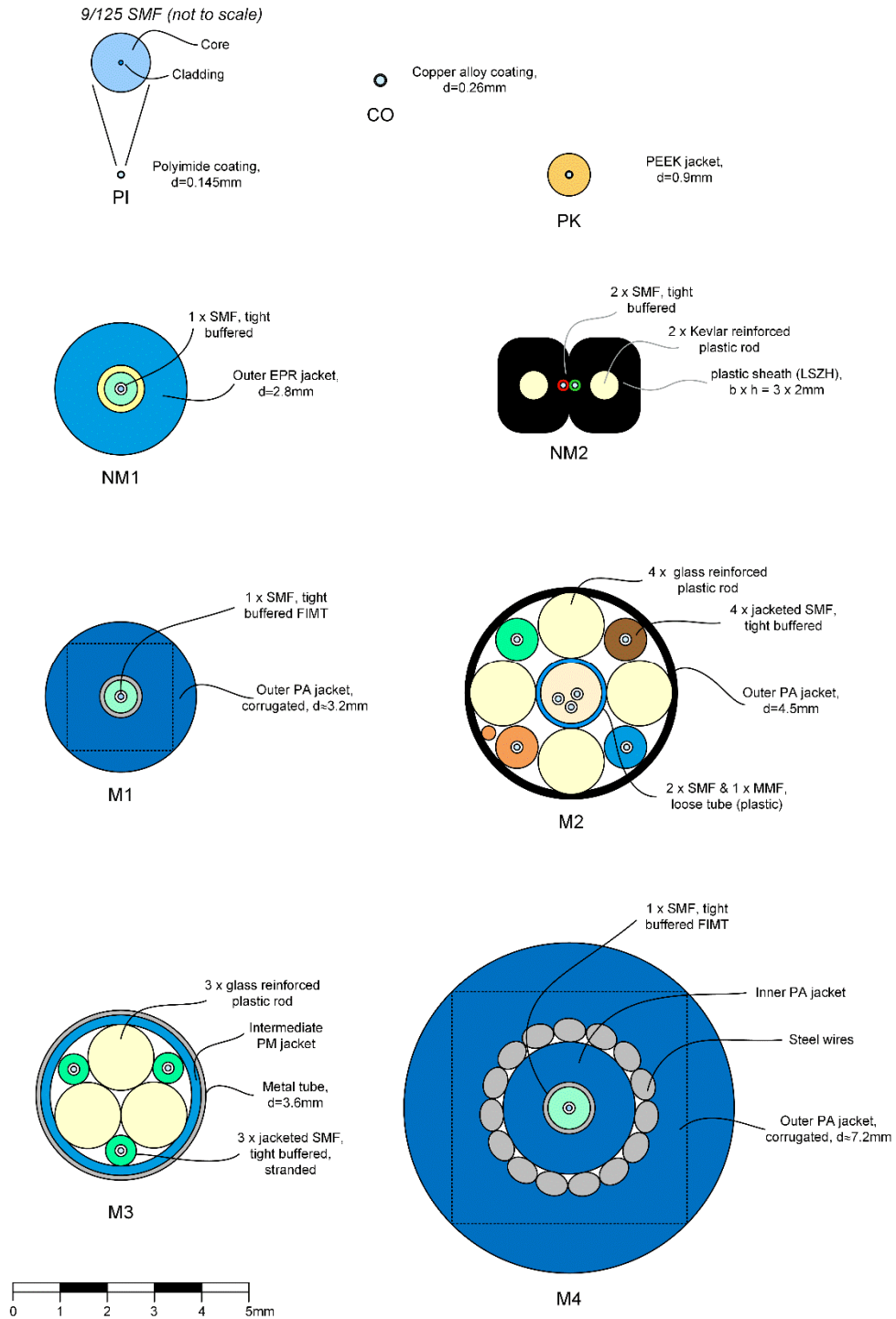


Fig. 4 Tested cable solutions (cross-section, only outer diameter to scale) with specifications from the product sheets.

For high temperature applications, the cable manufacturing industry is in principle using materials which, amongst other criteria, unite processability, flexibility, durability and high temperature resistance. For this purpose, e.g. high temperature acrylates, polyimide or metal alloys are used as coating materials on the fibre. Further materials used for cable sheaths in high temperature applications may be silicones, polytetrafluorethylene (PTFE) or thermoplastic elastomers (TPE-E) in order to name a few possibilities. The temperature application range of some of them is still not sufficient for the present applications (or they have other drawbacks), others reach far beyond the temperatures present while laying

mastic asphalt. However, it is not the goal of the present study to give further information about the cable production and the properties of the involved materials. More information about this subject can be found in the relevant literature and on the websites of the cable manufacturers.

2.2.4 Effects of thermal exposure

For the present project, initial temperature of mastic asphalt was defined as a maximum temperature of 240°C. However, it was not clear in advance, how fast it will cool down again. For this reason a rather conservative heating curve was defined in this project in order to simulate the thermal exposure of the cables in mastic asphalt. After a phase in which the oven is heating up to 240°C, the temperature was fixed for 10min to 240°C. Afterwards the temperature was set to 180°C for additional 35min, afterwards to 120°C for additional 45min and finally the oven was turned off. The resulting temperatures of this program are shown in Fig. 5 for positions at the bottom, in the centre and at the top of the oven. From this it may be concluded, that temperatures above 180° were acting on the cable for almost an hour.

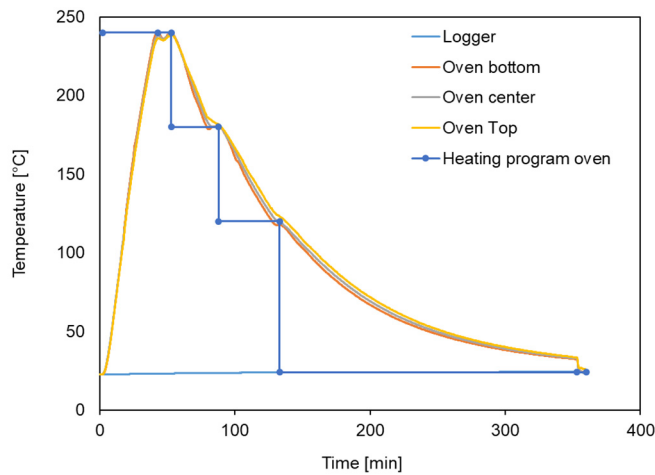


Fig. 5 Temperature exposition.

Fig. 6 shows samples of the nine tested cable solutions before they were exposed in the oven to the temperatures discussed in Fig. 5. A comparison of these cables between the state before and after thermal exposure is shown in Fig. 7 and Fig. 8. It becomes obvious that the melting range of several cable sheaths was exceeded. Other cable sheaths do not melt, but seem to shrink significantly or are experiencing other changes in state (brittle vs. ductile behaviour).

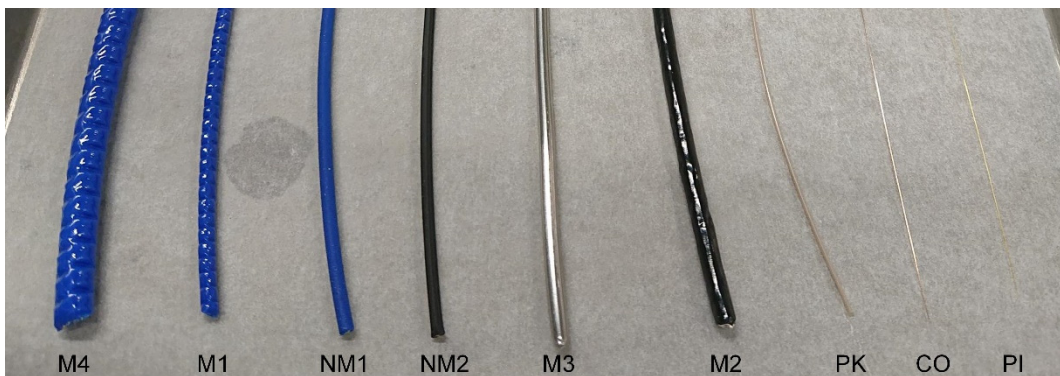


Fig. 6 Cable specimens before temperature exposition.

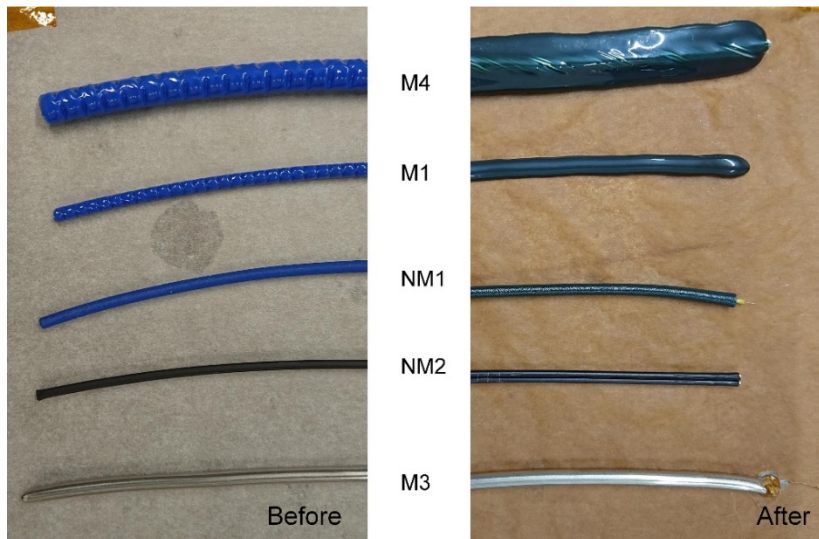


Fig. 7 Cable specimens (part 1) before and after thermal exposure.

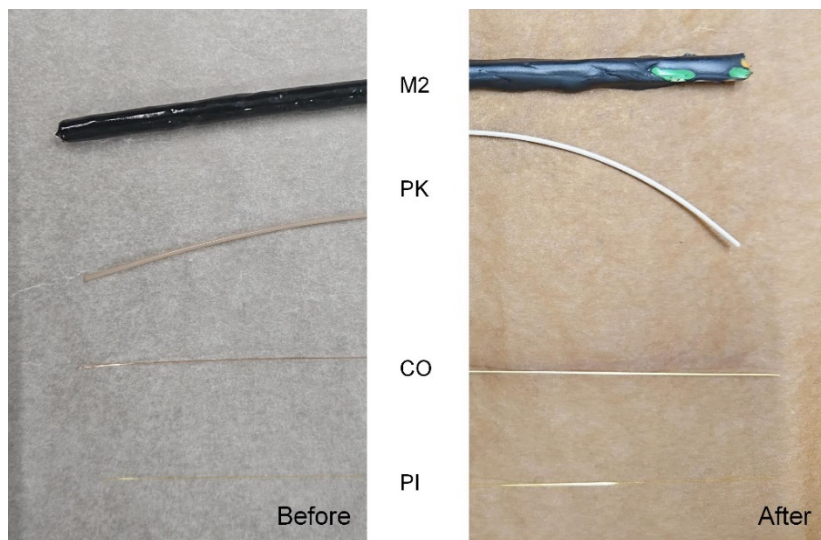


Fig. 8 Cable specimens (part 2) before and after thermal exposure.

Some details of the cable ends after temperature exposure are shown in Fig. 8. The protruding tension element or optical fibre (left side) indicated the significant longitudinal shrinkage of the cable sheath. Other effects like melting of the outer cable sheath and the fibre coating as well as other inner parts of the cable are shown in on the right side. Although some cables seem to suffer strongly from the temperature exposure, it is not clear in advance, to which extent this would finally harm the cable performance in mastic asphalt. A temporarily melted outer cable sheath may not necessarily be problem as long as the strain transfer within the cable does not suffer from that. It is also unclear whether the longitudinal shrinkage of the outer cable would occur in a similar manner, if longer and pre-stressed cable sections would be exposed to temperatures and whether it causes any detrimental effects on the cable behaviour (e.g. losses).

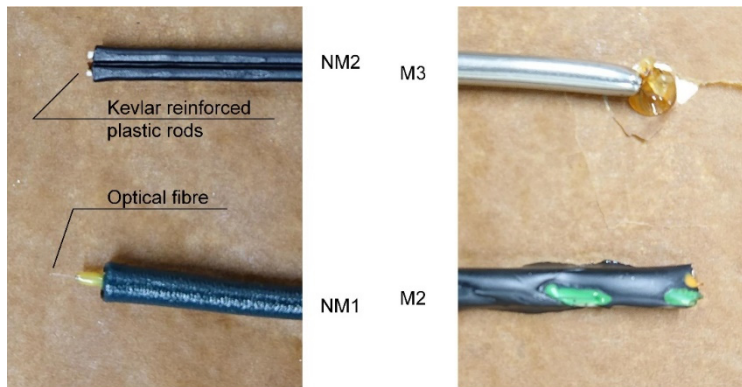


Fig. 9 Some detailed pictures of selected cables after the thermal exposure.

2.3 Modifications

The selected cable versions consist of some rather thin solutions (coated or jacketed fibres) which bring the required temperature resistance but in turn, may be not robust enough. On the other hand, there are several cable solutions which possess sufficient robustness but may not perform adequately after this temporary high temperature exposure. In both cases, the situation may be improved by modifying either the cable or the embedment procedure. A procedure, where a fibre was protected using thin mastic asphalt layers before it was embedded into a pavement, is shown in [9]. In the present project, three different potential modifications were analysed:

1. Protection of the cable with additional layers
2. Casting of a protective layer around a fibre
3. Embedment at locations where the temperature exposure is less pronounced

The different possibilities will be briefly discussed in the following subsections. It should be mentioned that in particular the first two modifications listed above can only be used for the purpose of instrumenting rather small test sections. As soon as the instrumentation requires more than several metres, the cable solution should be a result of an industrial process.

2.3.1 Additional protective layer

A common method to provide additional cable protection from the mechanical and thermal influences is the usage of shrinkage tubes. They are stripped over the cable and heated with a hot air dryer which causes the shrinkage tube to shrink and connect by its internal glue or by pure friction with the cable. Thereby, the cables diameter and its resistance is significantly increased but also another interface which can cause strain transfer problems is created. Owing to the manual production procedure, this modification is only suitable for short sensor lengths. A variety of products made of different materials and characteristics is commercially available. However, only PEEK and PTFE shrinkage tubes indicate an operating temperature in the range of 240°C which is expected during the embedment in the mastic asphalt. Further, also a selection of the more common Polyolefin shrinkage tubes are considered. The used materials are shown in Fig. 10.



Fig. 10 Polyolefin, PEEK and PTFE shrinkage tubes.

The PEEK shrinkage tubes are only rarely used and are usually not on stock in most distributions. Only for the size of 1mm shrinkage tubes were available. However, it comes without internal glue, which has to be manually inserted. The PTFE shrinkage tube has an internal layer which serves as a glue between the cable and the tube when heated. From the Polyolefin-based shrinkage tubes the common ETW and ATUM tubes are chosen as from experience they can sustain short peak temperatures much higher than the specified operating temperatures. Ultimately, also the very thick MDTA shrinkage tube is selected as a comparison to the thinner Polyolefin shrinkage tubes. An overview of all used shrinkage tubes is given in Tab. 2.

Tab. 2 Overview of the used shrinkage tubes.

Name	Material	Max. operating temperature	Diameter	Thickness	Glue	Additional Considerations
PEEK	PEEK	260°C	1mm	0.2mm	No	Glue is manually inserted
PTFE	PTFE	230°C	4mm	0.8mm	Yes	Very low external friction
ATUM	Polyolefin	110°C	3mm	0.5mm	Yes	-
ETW	Polyolefin	125°C	3mm	0.5mm	Yes	-
MDTA	Polyolefin	130°C	12mm	1.2mm	Yes	Large tube thickness

2.3.2 Coated fibre casted in protective material

The cables with the highest temperature resistance also are the smallest in size and are prone to breaking during the embedment process. To improve the workability of these cables, they are casted into an additional protective layer. A two component adhesive epoxy (Duralco® 4400) is used therefor. This modification is indicated by the abbreviation (+EPOX). It is attempted to also increase the bond by creating an uneven surface. The formwork is created by pressing an M1 cable into a wax-filled U-profile as shown in Fig. 11. After tensioning the coated fibre in the middle of the formwork it is filled by the mixed epoxy as shown in Fig. 12.



Fig. 11 Creation of the formwork.



Fig. 12 Casted cable solution.

After a day the epoxy has hardened and the cable can be taken out of the formwork. The resulting cable solution offers a workable robustness and bending stiffness. It can be bent into almost any shape at this point. However, the epoxy continues to harden and after an additional day it loses its entire flexibility and breaks rather fast as shown in Fig. 13. Therefore, the protected cable is best crafted on the day before the embedment. However, even a successfully embedded cable can break under the demands experienced within the asphalt during its operating time and hence, further protective materials should be investigated. However, owing to the time consuming manual production procedure, this modification would only be suitable for short sensor lengths.



Fig. 13 Ruptured casted cable solution.

2.3.3 Embedment procedure

The highest laying temperatures during mastic asphalt production may occur most likely in the centre of the casted layer. Furthermore, also the slowest decrease of temperatures with time is expected to be in this area. Towards the boundaries as e.g. the free surface or the interface to another construction layer, built earlier in time, lower temperatures and a faster decrease may be expected. Hence, the position of the embedment of the fibre optic cable in the mastic asphalt layer may potentially also be a parameter, which may help to milden the high temperature environment for particularly sensitive cables.

The distributed fibre optic sensor can be embedded in principle in three different embedment procedure types (Fig. 14). Type 1 refers to a situation, where the cable is put and fixated on an existing layer. In type 2, a notch is created (milling cut into an existing layer or moulding a warm layer) into which the cable is laid. The cable will afterwards be casted into this notch by using a temperature resistant curing compound, a hard bitumen or other suitable materials. Type 3 finally refers to an embedment procedure, where the cables is tried to be installed at a certain position somewhere within the asphalt layer.

*Embedment
procedure type*

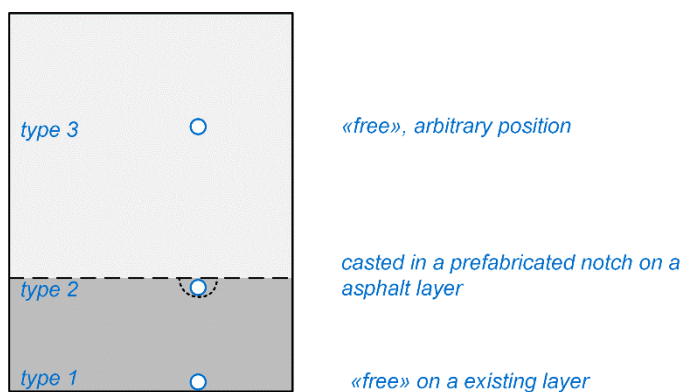


Fig. 14 Different embedment procedures, type 1 – 3.

The problems and benefits of these different embedment types will be discussed in section 5.1.3. At this position the different embedment procedures will only be qualified regarding the expected temperature exposure of the cables. Type 1 may benefit from the fact, that the temperature of the underground is lower and hence, the mastic asphalt is also expected to cool down rather fast. An even more protected situation may occur in a type 2 embedment procedure, where the cable is covered by a bitumen or a temperature resistant

curing compound and the level of protection against temperature can be controlled by the depth of the notch. The clearly most exposed situation is occurring in an embedment procedure according type 3.

As the embedment procedure seems to be also an important parameter, different embedment procedures will be considered when investigating the performance in mastic asphalt samples.

2.4 Testing program

In order to investigate, whether the existing cable solution can be directly used in mastic asphalt for the purpose of strain sensing, several tests were conducted in this study:

- Strain test before and after temperature exposition (chapter 3)
- Controlled temperature exposition in the laboratory oven (chapter 3)
- Embedment of different cable solutions using different modifications embedment procedures (chapter 4)
- Laboratory bending tests using the instrumented mastic asphalt samples (chapter 4)

In order to assess, whether the thermal exposure has any detrimental effects on the cable performance (strain transfer) the cable is tested a strain test bed before and after the temperature exposure. In between the cables are exposed to a relevant temperature-time curve in a laboratory oven in order to study the effects of the high temperatures on the cables. Since it appears rather likely, that the thermal exposure in the oven is rather conservative and furthermore, its boundary conditions for the cable are not identical to the situation in real mastic asphalt applications, an embedment of the most promising solutions into mastic asphalt was conducted. A simple functionality check conducted after the embedment into mastic asphalt showed that many of the involved cable solutions seem to work and therefore, bending tests were conducted in the laboratory in order to qualify the performance of these cables as a strain sensor. No full scale embedment test in mastic asphalt on a real road construction site, which would expose the cable solutions to an even more harsh environment, was conducted within in this study.

3 Temperature exposition and strain test

3.1 Introduction and purpose

Before subjecting the fibre optic cables to the embedment procedure in mastic asphalt, their behaviour under high temperatures is investigated by subjecting it to a heating cycle reaching 240°C. Before and after, the behaviour of the cables is investigated in a strain test. For these tests, pigtails are spliced to a 10m sample of every cable. In the strain test, a section of 2m is fixed and stretched in a box with a step motor. Meanwhile, OBR measurements are taken to see whether a uniform strain can be measured along the inner fibre. Besides the loss of inner bond, shrinkage is expected to have a detrimental effect on the cable and potentially cause a loss of signal. Therefore, one part of the cable is tensioned on a metal tube inside the oven to partially resist length changes during the temperature exposition. If a cable indicates a uniform strain before and after the temperature exposition it is likely to also perform well in realistic embedment conditions. However, even if a cable does not perform well in this test, it will not be excluded from the embedment test, as there is a chance that it indicates the strain correctly under realistic conditions, as the setup for the strain test (clamps) does not reflect the conditions of a continuous mastic asphalt embedment. The temperature exposition and strain test mainly serve the purpose of understanding the cables behaviour and identifying weaknesses while being able to visually investigate it.

3.2 Temperature exposition

To subject the cables to a temperature of 240°C they are placed into an oven (Binder ED 115) in the laboratory. The ends of the cable are lead through the ventilation hole to the outside, as they consist of regular pigtails and cannot resist high temperatures. Inside the oven, one section of the cable is tensioned on a metal tube covered with baking paper to prevent large shrinkage of the cable. It is fixed at the bottom and the top of the tube using an endless belt. The other half of the cable is loosely fitted into the oven and wrapped by baking paper as shown in Fig. 15. Temperature sensors are lead into the oven via the ventilation hole in order to validate the temperature indicated by the oven's display.



Fig. 15 Cable setup in the oven.



Fig. 16 Effects of temperature exposition.

The heating cycle starts with setting the temperature of the oven to 240°C. After about one hour the display indicates that it reached this temperature. The oven is left to preserve this state for 10 minutes, after which it is set to cool down to 180°C. Again, it takes about one hour until this temperature is indicated and afterwards it is left in this state for another ten minutes. The same step is repeated with 120°C. Afterwards the oven is set to 20°C and when the temperature is below 50°C the door of the oven can be opened. Overall the

temperature exposition takes about 7 to 8 hours. The evolution of the temperature along this cycle is presented in Fig. 17. It can be seen that the actual temperature inside the oven reaches only roughly 230°C, even though the temperature is set and indicated at 240°C. This is due to the massive metal tube which delays the rise of the temperature in the middle of the oven compared to the walls where the temperature is measured for the oven control system. Therefore, there is a lower temperature peak compared to the temperature curve shown in Fig. 5.

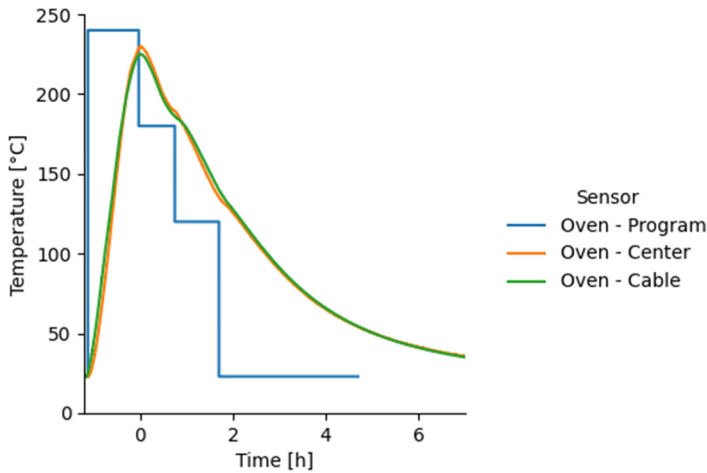


Fig. 17 Oven program and the measured inside temperatures.

3.3 Strain test

The strain test is conducted in the pull-out box shown in Fig. 18. A section of slightly more than two meters is taken and attached to the ends of the box with screwed fixations. On one side this fixation is located on a movable beam which is attached to a load cell and a step motor allowing for force and displacement measurements. The screws of the fixations are tightened with a moment approximately proportional to the diameter of the cable, as indicated by Fig. 18. Due to difficulties with the fixation of the thin PI and CO fibre, only the thicker 7 cable solutions are tested in this setup.



Fig. 18 Pull-out box and its step motor.

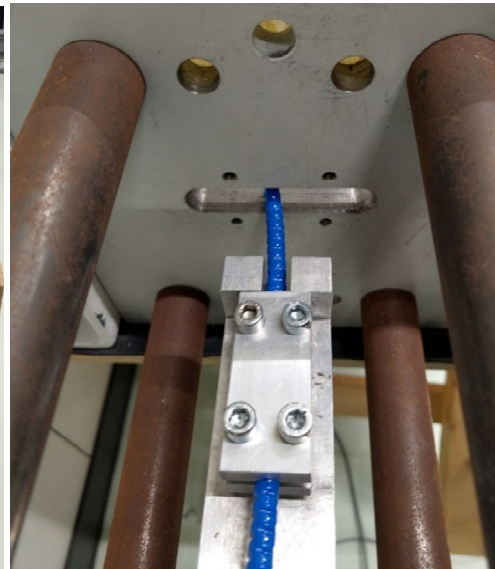


Fig. 19 The screwed fixation on the beam.

Tab. 3 Moments set for tightening the fixations screws.

Cable	NM1	NM2	PK	M1	M2	M3	M4
Moment	3kNm	3kNm	3kNm	3kNm	5kNm	5kNm	7kNm

Initially, the cable is fixed and stretched to an approximately straight line. Its length is noted and a reference measurement is taken. Afterwards it is pre-stressed until it follows a linear force-displacement curve. From this point on, increments of 0.21mm are applied through the step motor causing idealised strain increments of approximately $100\mu\epsilon$ in the cable. From the force increments, the stiffness of each cable can be roughly quantified. For each increment also a measurement with the OBR device is taken until $1000\mu\epsilon$ are reached ($1\mu\epsilon = 10^{-6}$). This device measures a spectral shift $\Delta\nu_s$ along the fibre, which is linearly dependent on the local change in axial strain $\Delta\epsilon$ and the change in temperature ΔT . The linearity is represented by the coefficients C_ϵ and C_T . Owing to the absence of relevant temperature changes, the whole spectral shift was converted to strain.

$$\Delta\nu_s = C_\epsilon \cdot \Delta\epsilon + C_T \cdot \Delta T$$

Afterwards the cable is loosened and taken out of the box. The displacement history as well as the measurement times of an example cable are shown in Fig. 20.

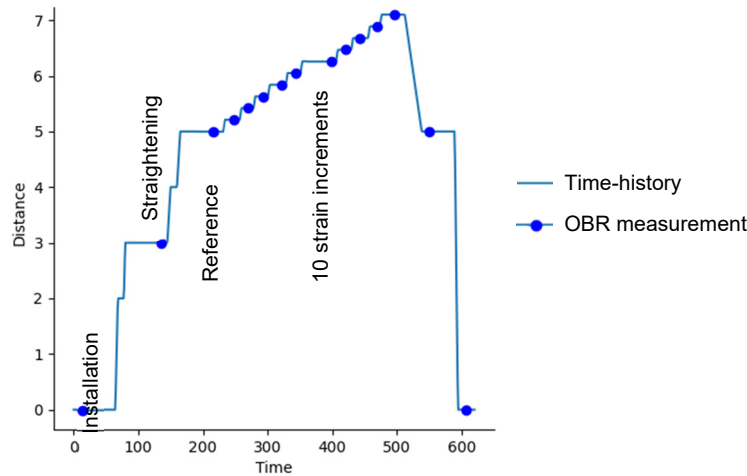


Fig. 20 Displacement and measurement times during the strain test.

In an ideal case, the OBR measurements indicate a precise rectangle of constant strains on the cable section that is fixed into the pull-out box, as shown in Fig. 21. This should be observed for every cable before subjecting it to the heating cycle. It indicates that the externally applied force causes a uniform strain distribution inside the cable and that the different cable layers transfer the necessary stress without relevant slippage. However, the temperature exposition can have a detrimental effect on this bond behaviour. The associated internal slippage is indicated by the OBR measurement if strains show up outside of the tensioned box section as shown in Fig. 22.

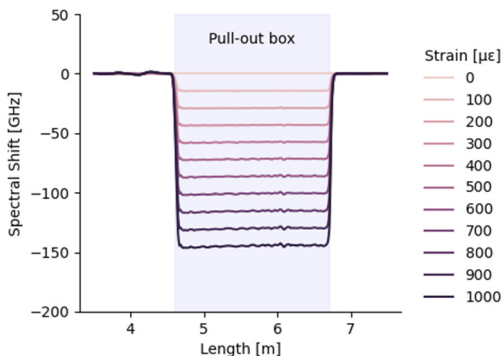


Fig. 21 Ideal strain test result.

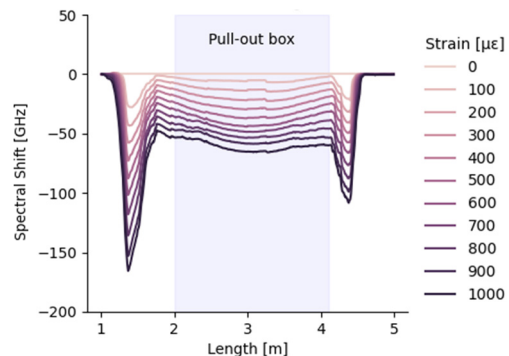


Fig. 22 Adverse stress test result.

However, also a variety of other problems can come up through the temperature exposition. Certain cables are stiff and melt into a deformed shape in the oven, so that they cannot be pulled straight again inside the pull-out box. In this case, the cross-section is no longer homogeneous and constant strains cannot be expected. Further, permanent shrinkage of the cable can cause a loss of signal which becomes visible in the decreasing amplitude of

the measured reflected signal. While these two problems make it hard to evaluate the strain test, they are only partially relevant for practical purposes as they may not appear to the full extent under realistic conditions. The inconstant strain due to cross-section changes only appears as there is a constant force in this strain test. Also, once exposed to the high temperatures in the embedment process the cable never has to undergo a large deformation. Therefore, only clear indications of a poor strain transfer, i.e. slippage, are considered a failure criterion.

It should be clearly mentioned, that the chosen strain test procedure is a simple method, which can only give some first hints on the real cable performance regarding strain transfer in mastic asphalt. The clamps form a local fixation of the cable, whereas in mastic asphalt, the cables are continuously embedded in the host material. The clamps introduce locally large radial stress on the cable which, depending on the cable type, may change its strain transfer owing to the shear stresses developing in the clamps when the cable is tested. In order to investigate the strain transfer in a more detailed manner, a more sophisticated setup would be required, which was out of the scope of the present study. However, the behaviour of the cable solutions regarding strain transfer was studied closer in chapter 4 using the cables embedded directly in laboratory mastic asphalt samples.

3.4 Results

The axial stiffness of each cable before and after the temperature exposition is presented in Tab. 4 (no tests were conducted for the thin coated fibres PI and CO). Further, also the diameter and the resulting apparent Young's modulus (dividing the axial stiffness by the total cross section area) of the cables are specified. The entire load-displacement curve for each cable can be found in the Appendix I.1. The resulting spectral shifts are following presented for each cable individually. Please note that the stiffness is in general strain rate and strain range dependent. In case of the M4 cable the initial prestrain was slightly too low what caused some deviations to values of similar older tests (in brackets).

Tab. 4 Stiffness of the cables before and after heat exposition.

Cable	NM1	NM2	PK	M1	M2	M3	M4	Unit
Initial stiffness	3	24	3	60	160	520	500	kN
Initial diameter	2.8	3x2	0.9	3.2	4.5	3.6	7.2	mm
Apparent Young's modulus	0.5	4.0	4.7	7.6	10	45	13	GPa
Stiffness after temp. exposition	3	24	3	45	130	430	300	kN

3.4.1 NM1

Before the temperature exposition, the NM1 cable showed an ideal spectral shift distribution in the pull-out box as can be seen in Fig. 23. During the setup of the tests after the temperature exposition, the sheath of the cable audibly cracked many times while being straightened. Both heat-exposed cable sections indicate a spectral shift outside the tensioned box section. Especially for the tight section, the slippage can be detected over multiple meters on the left side. Inside the box section a non-uniform spectral shift was measured with a significant gap in the middle of the tightened section. The expected spectral shift was not measured anywhere in the two heat-exposed cable sections.

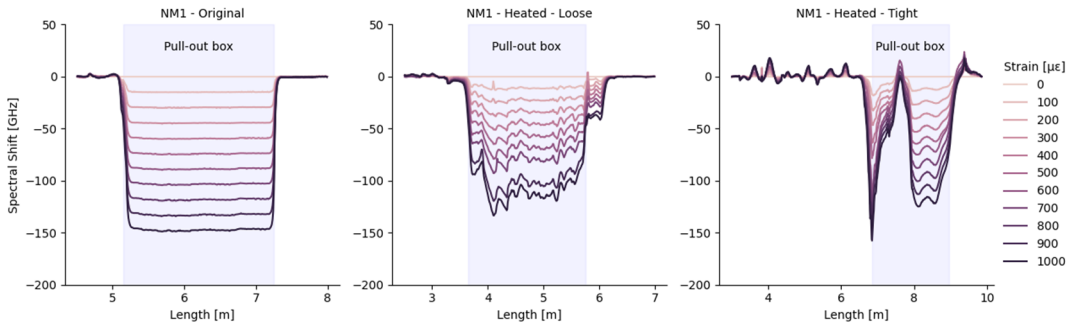


Fig. 23 Spectral shifts in the strain tests for NM1.

Further, the return amplitudes of the reference OBR measurement for each strain test, shown in Fig. 24, indicate significant loss caused by the temperature exposition. This loss is approximately linear along the loosely heated section from 3.8m to 6.4m and can be quantified to approximately 2dB/m. In the tightly heated section from 6.5m to 9.5m no significant loss of signal occurred.

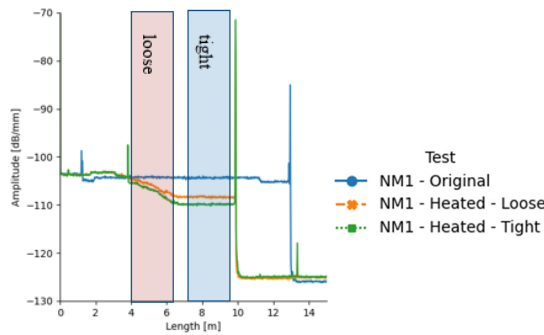


Fig. 24 Return amplitude in the strain tests for NM1.

3.4.2 NM2

The NM2 cable showed no visible effects of the temperature exposition and retained its flexibility. Also the return amplitude remained unchanged. The measured spectral shifts, shown in Fig. 25, initially indicate a perfect rectangle with the expected magnitude. For the heated sections they indicate a small non-uniformity and minor slippage on one side.

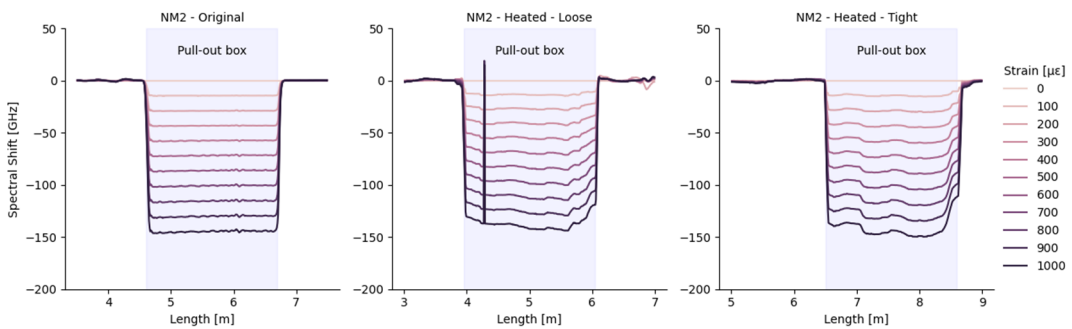


Fig. 25 Spectral shifts in the strain tests for NM2.

3.4.3 PK

The PK cable is characterised by its large cyclic variation of stiffness along the cable, which is potentially caused by its production process. This variation is also indicated in the strain tests shown in Fig. 26. Besides a few outliers in the measurements of the tight-heated section no relevant difference can be identified. However a temporary loss of signal is introduced by the screwed fixations corresponding to the positions of large point losses, as can be seen in Fig. 27.

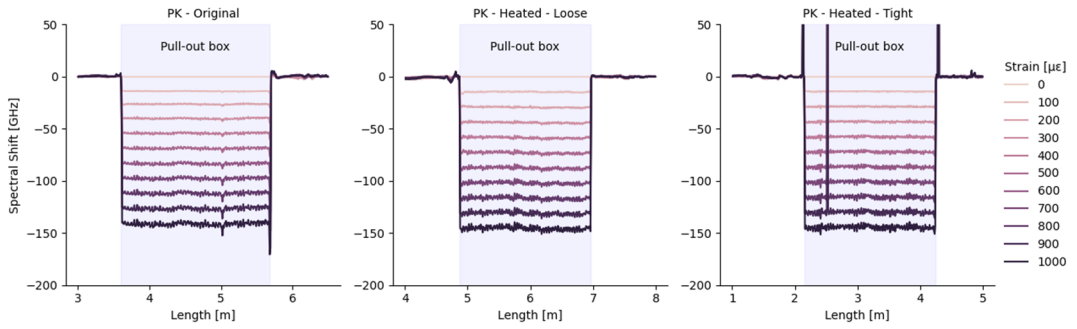


Fig. 26 Spectral shifts in the strain tests for PK.

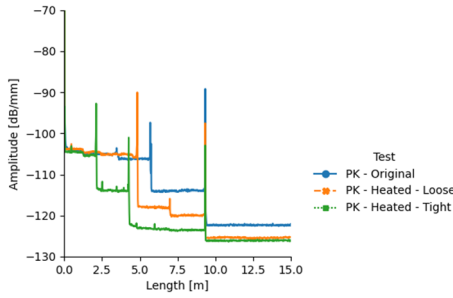


Fig. 27 Return amplitude in the strain tests for PK.

3.4.4 M1

The visible effect of the temperature exposition has already been shown in Fig. 15. The outer corrugated plastic jacket partially melted away and leaves a non-uniform cross-section. The return amplitude of the signal is not affected though. The end of the cable broke off during the installation in the pull-out box after the temperature exposition. Nevertheless, enough cable remained to test the tight and the loose section. The results of the strain test are shown in Fig. 28. Initially the cable indicated a uniform spectral shift with a few anomalies in the right half. The spectral shifts of the heated cables both clearly indicate slippage by the spectral shifts outside the strained section. While the spectral shifts in the tight-heated section are mostly uniform, they change strongly on the loose-heated section.

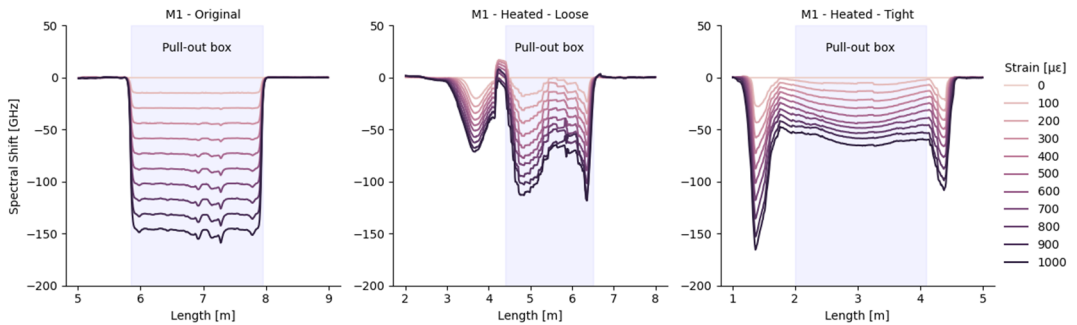


Fig. 28 Spectral shifts in the strain tests for M1.

3.4.5 M2

The cable showed strong visible changes from the temperature exposition as shown in Fig. 29. The outer PA jacket melted and the colourful coatings of the inner fibres appeared, also indicating to have melted away from their respective fibres. However, the signal in the tested fibre (blue coating) remained intact until the cable broke in the middle during the installation process of the strain test.



Fig. 29 Effects of temperature exposition on M2.

Despite the breakage, it was possible to test the loose-heated section of the cable. The results from the strain tests are shown in Fig. 30. The measurement under $500\mu\epsilon$ is disregarded for as it indicates an unrealistic offset. It can be seen that already the initial cable showed significant slippage. Additionally, the spectral shifts became less uniform by the heating process. It should be noted that potentially because of the helix shape of the inner fibres, the expected spectral shift is slightly lower compared to the previous cables. This is confirmed by the measured average strain coefficient C_ϵ of $-0.127\text{GHz}/\mu\epsilon$ as opposed to a usual value of $C_\epsilon \approx -0.147\text{GHz}/\mu\epsilon$.

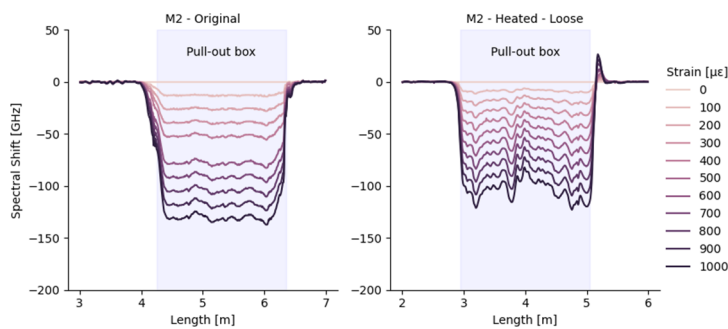


Fig. 30 Spectral shifts in the strain tests for M2.

3.4.6 M3

Due to the very high stiffness of 520kN, it was not attempted to pre-stress the cable on the metal tube inside the oven. Further, it was barely possible to fit the cable into the oven because of its high bending stiffness. From the outside, the cable showed no visible effects from the temperature exposition. The results from the strain test, shown in Fig. 31, indicate an ideal behaviour of the original cable. After the heat exposure, a little non-linear slippage can be seen on the right side and the tensioned section indicates a small non-uniformity.

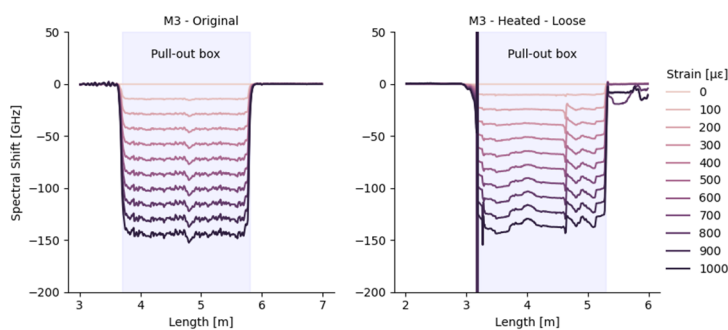


Fig. 31 Spectral shifts in the strain tests for M3.

3.4.7 M4

Because of the high stiffness of the cable, the section on the metal tube could not be adequately pre-stressed for the temperature exposition in the oven. Subsequently, it became loose under the high temperatures and shifted to the bottom of the tube where the different revolutions melted together. Even the inner metal spiral became visible, as can be seen in Fig. 32. Therefore, the tight section cannot be tested in the strain test.



Fig. 32 Effects of temperature exposition on the tight section of M4.

The initial strain test, allows a clear identification of the tensioned section. However, even before the heat exposure the measured spectral shifts, shown in Fig. 33, shifts are not entirely uniform. After heating the cable, it became a particular challenge to straighten the deformed molten cable. At a few locations the outer plastic jacket broke as a result, but the fibre remained intact thanks to the protective steel wires. Because of the resulting non-uniform cross-section, it has to be considered that the tested cable was not entirely straight. The measured spectral shifts only indicate about half of the expected strain along the fibre and slippage can be clearly identified along a length of 1.3m on the right side.

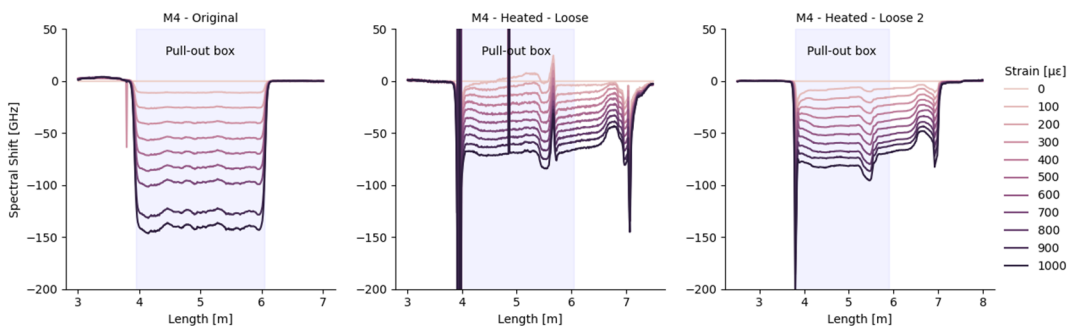


Fig. 33 Spectral shifts in the strain tests for M4.

3.5 Discussion

Even though the oven displayed to have reached 240°C for ten minutes during the temperature exposition, the temperature sensors which were applied to the steel tube and the cable only indicated roughly 230°C. This difference is due to the internal temperature measurement by the oven which is taken close to the heating elements. The oven would need to heat an extra 15 minutes to reach the desired temperature of 240°C at the centre where the cables are installed as the large mass of steel and the smoke outlet delay the rise of the temperature on the inside. For the purpose of investigating the applicability in mastic asphalt the longer heat exposition was disregarded for, since a realistic temperature exposition only exceeds 230°C for a very short time. To confirm this, the temperatures during the embedment are compared to the temperatures inside the oven in section 4.5.

The evaluation of the force measurements from the strained cables indicate a wide range of stiffness between around 3kN and 500kN. These results do not always conform with the specified characteristic of other sources as the strain rate is not controlled in this experiment. The apparent Young's moduli indicate very distinct characteristics for the cables, with some values much higher than expected for the mastic asphalt. This raises some doubts whether the cables can function as accurate sensors or whether they start to influence slightly the response of the host material.

The temperature exposition and its accompanying shrinkage have a detrimental effect on the signal inside the NM1 cable causing a continuous loss of amplitude along the length. This loss may be due to microbending inside the fibre as it does not shrink with the temperature exposition and keeps its original length by deforming into a curved shape. The respective radii are too small for the signal to undergo complete refraction inside the cable and certain ratio is continuously lost. By pre-tensioning the cable inside the oven during the temperature exposition, shrinkage is diminished. This is reflected in the amplitude trace in Fig. 24, indicating no loss of signal along the pre-tensioned section. Therefore, no loss of signal is expected for the considered application as the cable is embedded and supported by the surrounding asphalt, imposing similar conditions as for the tight-heated section. However, the strain tests of both sections show clear indications of slippage and of a deficient strain transfer as significant strains were measured outside of the pull-out box. Further, there is a strong variation of the spectral shift inside the tensioned box, implying a non-homogeneous cross-section. The average of the spectral shift inside the pull-out box is presented in Fig. 34. It confirms the previous observations of detrimental effects on the strain transfer by the temperature exposition, as the average spectral shift in the tensioned section is significantly smaller than in the original cable.

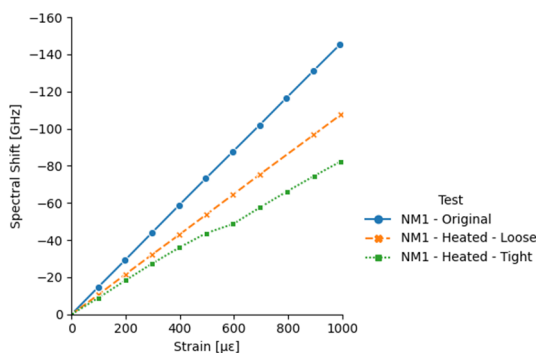


Fig. 34 Avg. spectral shift in the strain tests for NM1.

The NM2 and the PK cable show minor effects from the temperature exposition in Fig. 34 and Fig. 38. Therefore, also the average spectral shift shown in Fig. 35 remains practically identical to the original cable. Both cables seem suitable solutions for strain measurements under very high temperatures. However, their smooth surfaces could cause problems in the strain transfer from the asphalt to the cable. Further, the PK cable shows high return amplitude losses at the fixations in Fig. 27. This is an indication of an excessive force in the fixations for this thin cable, which probably improved the strain transfer artificially. However, considering the highly temperature resistant materials in the PK cable, a very good strain transfer can be expected nevertheless.

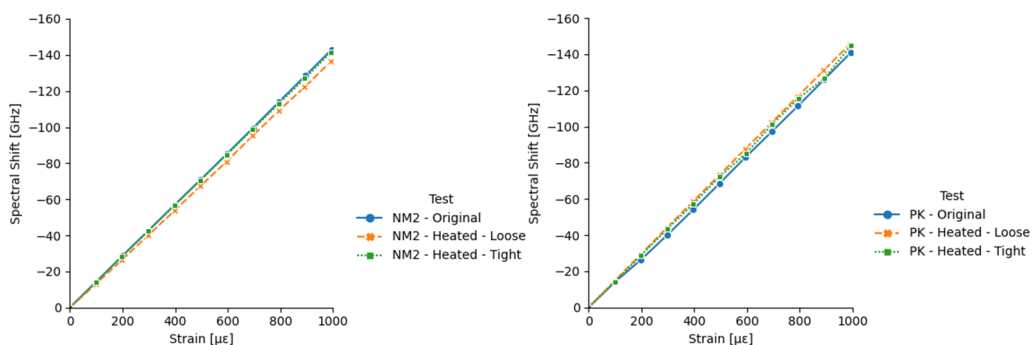


Fig. 35 Average spectral shift in the strain tests for NM2 and PK.

The strain tests of the M1 cable, seen in Fig. 28, show strong slippage in both the tensioned and the loose-heated section. This is also reflected in the lower average spectral shift presented in Fig. 36. The cable seems to react sensitive to the high temperatures in the oven test.

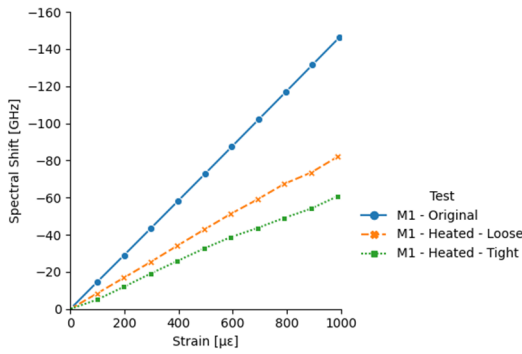


Fig. 36 Spectral shift in the strain tests for M1.

The cables M2 and M3 show minor slippage but a considerable non-homogeneity in Fig. 30 and Fig. 31 respectively. For M2, the non-homogeneity is due to the deformed molten cross-section. This is not an issue for the strain controlled application, but it is surprising that the fibre remained intact. It remains questionable, however, whether the unknown molten cross-section can guarantee an adequate strain transfer without the large pressure that is present at the fixations. No visible effects can be identified on the M3 cable, as the outer metal tube remains unaffected. The expanding gel cannot escape the intact tube, unlike what is seen in Fig. 7. The results indicate that the resolidified gel can guarantee a sufficient strain transfer, which is also seen in the average spectral shift, shown in Fig. 37, which follows almost the ideal inclination. However, large concerns remain about the workability of the very stiff and initially round cable.

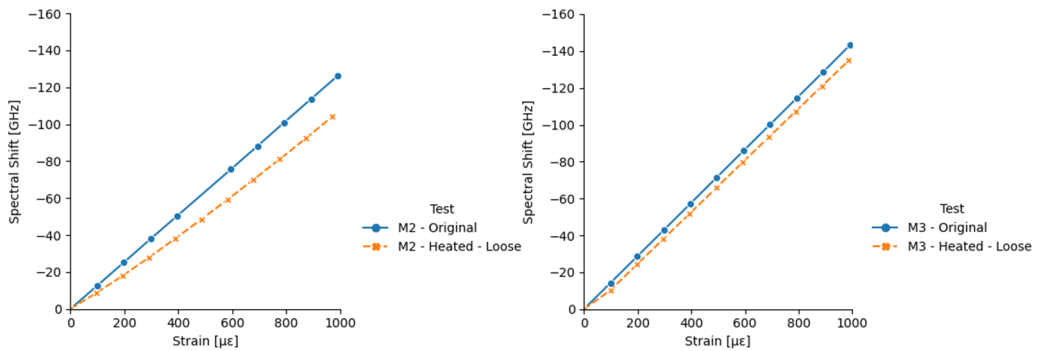


Fig. 37 Average spectral shift in the strain tests for M2 and M3.

The strain test of the original M4 cable already hints the limitation of the strain test setup by the variation of the measured spectral shift. It indicates that not entirely constant strains resulted in the cable, which are caused by the high stiffness and the initial curvature of the cable. However, the problem of setting up the cable as ideally intended is to be considered for the application in mastic asphalt. A straight embedment requires large forces which can impose an additional demand on the formwork. Further, the results of the heated cable section in Fig. 32 indicates a loss of bond inside the cable as significant slippage can be seen on the right side. Therefore, also the average spectral shift inside the pull-out box, presented in Fig. 38, does not have the ideal inclination for the heated cables.

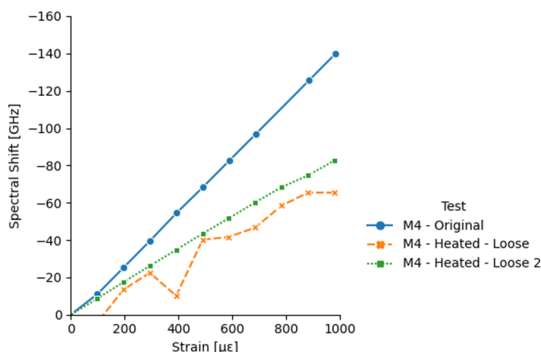


Fig. 38 Spectral shift in the strain tests for M4.

Both the M4 and the M3 cable indicate a very high stiffness which may change the behaviour of the surround mastic asphalt. The presence of a stiff cable inside a soft asphalt may act as a reinforcement and may have influence when characterising the material by using such measurement data. An overview of the discussion of this chapter is shown in Tab. 5, where the measured spectral shifts are divided by the strain to estimate the strain coefficient C_ϵ .

Tab. 5 Conclusions from the temperature exposition and strain test

Cable	Strain coefficient C_ϵ before exposition	Strain coefficient C_ϵ after exposition	Problems
NM1	-0.147 GHz/ $\mu\epsilon$	-0.108 GHz/ $\mu\epsilon$	Strain transfer, brittle
NM2	-0.142 GHz/ $\mu\epsilon$	-0.142 GHz/ $\mu\epsilon$	-
PK	-0.146 GHz/ $\mu\epsilon$	-0.146 GHz/ $\mu\epsilon$	-
M1	-0.147 GHz/ $\mu\epsilon$	-0.082 GHz/ $\mu\epsilon$	Strain transfer
M2	-0.127 GHz/ $\mu\epsilon$	-0.104 GHz/ $\mu\epsilon$	Strain transfer, brittle
M3	-0.145 GHz/ $\mu\epsilon$	-0.145 GHz/ $\mu\epsilon$	Stiffness/workability
M4	-0.146 GHz/ $\mu\epsilon$	-0.082 GHz/ $\mu\epsilon$	Strain transfer, stiffness/workability

Finally it should be mentioned, that the chosen simple procedure for the temperature exposure and the strain test reflect the conditions in mastic asphalt only to a limited extent. During the thermal exposure in mastic asphalt, the cables are surrounded by a material consisting from solids and liquids and they may be subjected to other geometrical boundary conditions. Furthermore, during the operating time in the cold mastic asphalt, the cables are continuously embedded and connected to the host material, instead of locally clamped by fixations. However, the chosen procedure may give already first hints on the later performance of the cables in mastic asphalt and, furthermore, their behaviour in mastic asphalt is analysed closer in the following chapter.

4 Embedment of cable solutions

4.1 Introduction and purpose

The fibre optic cables from section 2.2 and the modifications introduced in section 2.3 are embedded in mastic asphalt specimens to investigate their suitability as strain sensors in a bending test. Each cable solution is embedded along 0.8m on three different layers as proposed in section 2.3.3. These cables are embedded under realistic conditions with a shorter temperature exposition and the support of the cable by the embedment in the asphalt. After the casting it is investigated whether the cables are still usable as sensors. While the specimens are subjected to bending in a press setup, the measurements of the cables are compared to external strain sensors and a numerical calculation for different load levels. This comparison allows an assessment of the performance of the different cable solutions after having undergone realistic embedment conditions.

4.2 Embedment procedure

For the embedment of the cable solutions wooden casting boxes of the internal dimensions of 0.8m x 0.3m x 0.1m (length x width x height) are used to cast mastic asphalt specimens of roughly 60kg. A mastic asphalt MA 8 N with a bitumen 35/50 is used. Every asphalt specimen hosts four embedded cable solutions, each of which is installed on three different heights and embedment procedure types (refer to section 2.3.3), as show in Fig. 39:

1. On the bottom of the casting box ($h = 0\text{cm}$)
2. In a notch at the interface between two asphalt layers ($h = 2.75\text{cm}$)
3. In the middle of the second layer ($h = 7.25\text{cm}$).

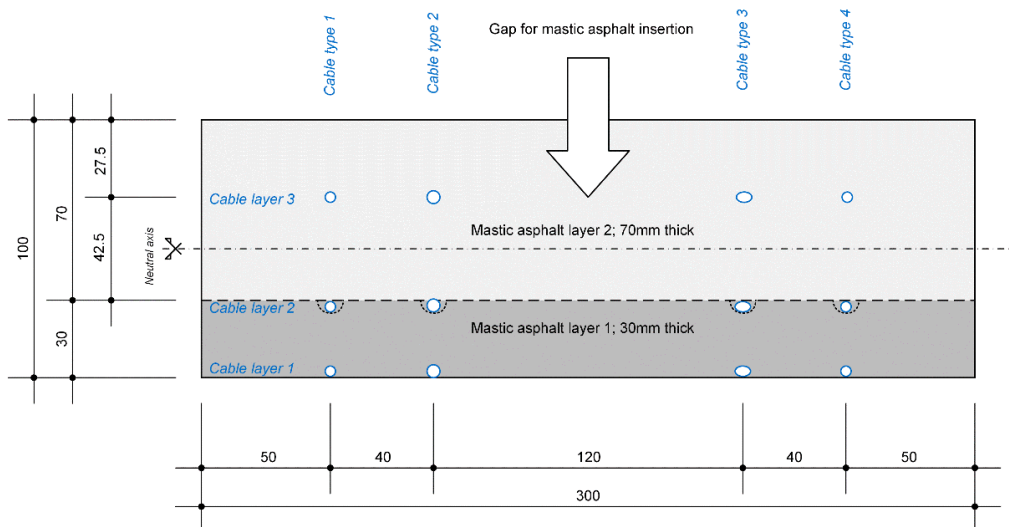


Fig. 39 Cross-section of the mastic asphalt specimen (dimensions in mm).

The cable solutions are previously tensioned along the length of the specimen using supporting tables and fixations. Thereby, the cable is stabilised at its initial position and partially takes away the thermal elongation of the embedment process. The casting box and the fixations are presented in Fig. 40. During the entire embedment procedure, OBR measurements are conducted to investigate the integrity of the cable solution. Also six temperature sensors are installed in one specimen in order to measure the evolution of the temperature at every embedment height.

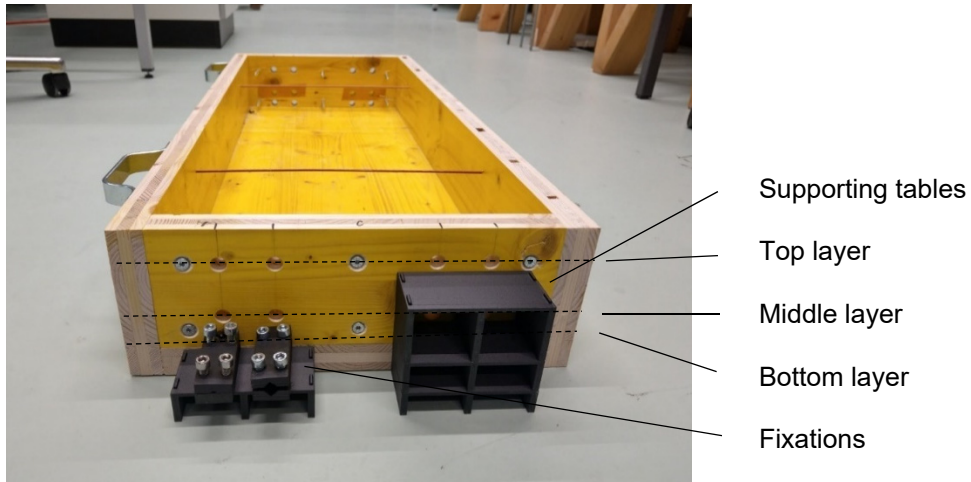


Fig. 40 Casting box, fixations and supporting tables.

Each specimen allowed for the embedment of four different cable solutions. 22 Cable solutions were chosen for the embedment procedure. In addition to the previously introduced modifications, the smooth metallic tube on the outside of the M3 cable is physically dented in order to increase the strain transfer (M3+RAU). However, the two self-fabricated cables (refer to section 2.3.2), broke immediately in the cold conditions during the installation. Hence, twenty cable solutions remained, which were distributed among five asphalt specimens as shown in Tab. 6 and Fig. 41.

Tab. 6 Embedded cable solutions

Specimen	Specimen 1	Specimen 2	Specimen 3	Specimen 4	Specimen 5
Cables	NM1+MDTA M1+MDTA PK+PEEK CO	PK+ATUM PK+ETW NM2+ATUM NM2+ETW	NM1 M1 NM2 PK	M2 NM1+PTFE M1+PTFE NM1+ETW	M4 M3 M4+MDTA M3+RAU

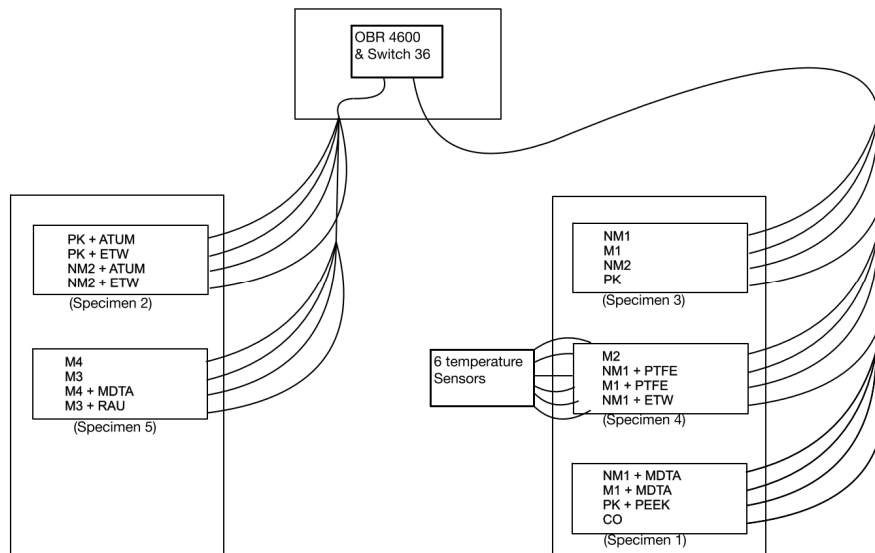


Fig. 41 Plan view of the setup

In the following, the detailed stepwise embedment procedure is introduced:

1. Installation and assembly of first cable layer

For the installation at the asphalt factory, the casting boxes are placed on tables and the first cable layer is assembled by pre-stressing it with the fixations on the first supporting table. Also the OBR device is installed on a separate table and all cables are connected to

it using a switch (Luna Fibre Optic Switch 036). For the rest of the embedment procedure measurements of each cable are taken every six minutes. After accomplishing the initial setup, the mastic asphalt boiler was brought by the operator of the factory. An impression from the installation is shown in Fig. 42.



Fig. 42 Installation at the asphalt factory.

2. Casting of first mastic asphalt layer

The first asphalt layer of a height of approximately 3.5cm is casted. The holes for the second cable layer are closed by a piece of Kapton tape. A measurement of the temperature of the asphalt indicated only 210°C for the first layer in Specimen 2, whereon the operator increased the heating of the boiler. For all other asphalt layers the temperature was between 235°C and 248°C. Fig. 43 illustrates the state of a specimen.

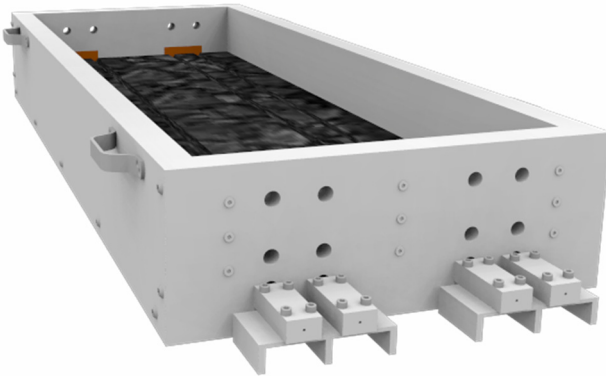


Fig. 43 First cable and asphalt layer.

3. Creation of notches

After the first asphalt layer cooled down and the asphalt behaved more viscous, the notch on top of the first asphalt layer was created using a self-made indentation gadget. It features a threaded bar which is attached to a wooden slat by clasps. On the upper surface two handles are attached as shown in Fig. 44.



Fig. 44 Indentation gadgets.

4. Assembly of second and third cable layer and

Two supporting table are stacked on top of the first one, in order to place the fixations at the respective heights of the second and third cable layers. This allows for their pre-stressed assembly as illustrated in Fig. 45. The third cable layer was also supported by two metal rods.

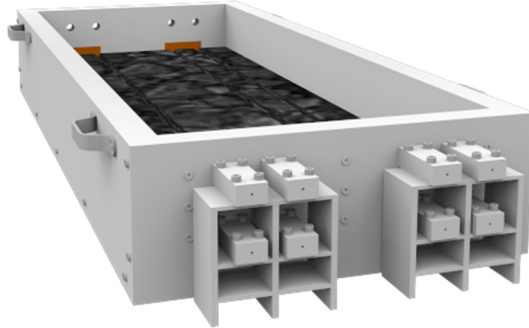


Fig. 45 Fixations for the second and third cable layer.

5. Embedment of second cable layer in bitumen

Bitumen (35/50) provided by the operator of the asphalt factory is used to cover the second cable layers. As the bitumen was rather liquid, it covered most of the surface of the first mastic asphalt layer as shown in Fig. 46. Measurements indicated a temperature of the bitumen between 135°C and 165°C.

6. Casting of second mastic asphalt layer

Ultimately the second layer of mastic asphalt is poured into the casting boxes. After filling the casting boxes almost to the top it was waited for the temperature to cool down. During this time a segregation at the top surface was detected as shown below on the right side. After four hours, when the specimen reached a suitable state, they were transported to the laboratories.

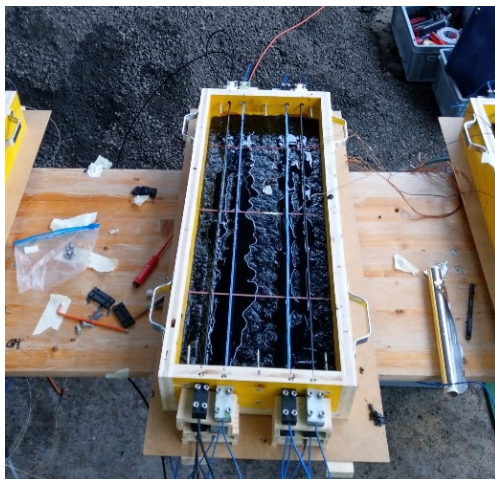


Fig. 46 Second cable layer.

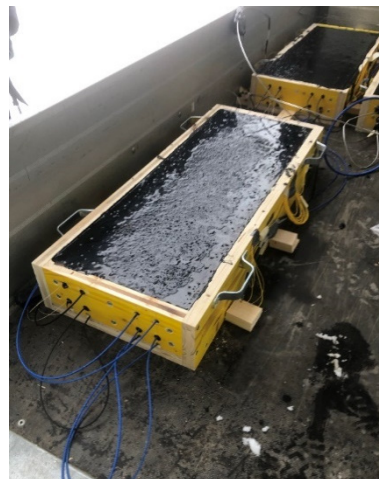


Fig. 47 Finished specimen.

4.3 Bending test

Three months after the embedment, the specimens were stripped of their formwork to be tested in a 3-point bending test. The specimens were loaded at different load levels to conduct OBR measurements in the strained embedded cables at the same time. Simultaneously, continuous strain measurements are obtained from a strain gauge attached to the centre of the bottom surface.

4.3.1 Test equipment

The 3-point bending test was conducted in a test laboratory of the institute for structural engineering with an electromechanical press (Zwick&Roell E-Series) with a capacity of 200kN. Roller bearings were mounted to the head as well as to the base of the press. The setup also featured two joints, one between the head of the press and its roller bearing and one between a base roller bearing and the base of the press. Thereby, it is guaranteed that the internal forces in the test specimen can be controlled and measured accurately. The setup of the press is presented in Fig. 48.



Fig. 48 Press configuration.

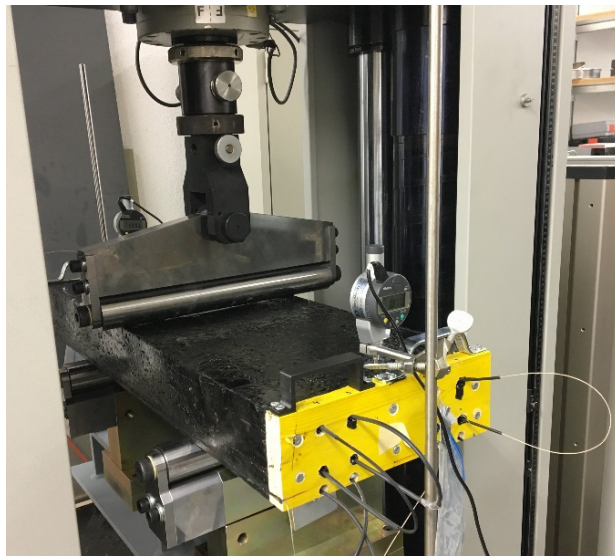


Fig. 49 Bending test in action.

In addition to the press measurements, the bending tests are monitored by the measurements from a strain gauge, external fibre optic sensors and displacement transducers. The strain gauge is attached to the centre of the bottom surface, where the highest strains are expected during the test. The external fibre optic sensors are attached to the side and the bottom surface of the specimen. In addition, displacement transducers are installed at both ends of the specimen. However, due to the very soft bitumen film on the top surface these measurements proved to be useless, as the pin penetrated into the layer with time. An illustration of the test setup and its instrumentation is seen in Fig. 50.

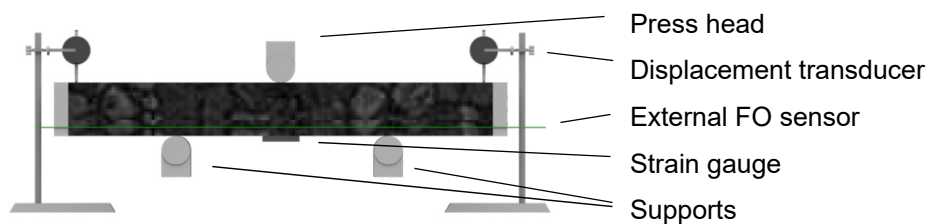


Fig. 50 Bending test and instrumentation setup.

As the asphalt was softer than expected, the span of the setup is set to 0.4m in order to prevent excessive strains under self-weight. Unfortunately the experiments had to be conducted in a warm environment of up to 28°C. This resulted in an expected strain

increment of $1\mu\epsilon/N$ and a stiffness of $3.75kN/mm$ as derived in the following equations assuming an elastic modulus of $200MPa$ for the mastic asphalt. This rather small elastic modulus, representing a secant stiffness to the real material behaviour, is explained by the high temperature ($23^{\circ}C < T < 28^{\circ}C$) and the slow loading rate ($f < 0.1Hz$):

$$\frac{\epsilon}{F} = \frac{3l}{2Eb h^2} = \frac{3 \cdot 0.4m}{2 \cdot 200MPa \cdot 0.3m \cdot (0.1m)^2} = 1 \frac{\mu\epsilon}{N}$$

$$\frac{F}{d} = \frac{48EI}{l^3} = \frac{48 \cdot 200MPa \cdot \left(\frac{0.3m \cdot (0.1m)^3}{12}\right)}{(0.4m)^3} = 3.75 \frac{kN}{mm}$$

4.3.2 Preparation

The formwork of the specimens was stripped and a strain gauge (HBM 1-LY41-20/120) was glued (HBM X60) to the roughened centre of the bottom surface of each specimen, as shown in Fig. 51. Only the formwork on the lateral side surface was kept and handles were mounted on it. Thereafter, the specimens were stored and transported on the longitudinal side surface. Further, grooves were created in order to glue an external fibre optic cable to the specimen as an additional reference as shown in Figs. 52 and 53.

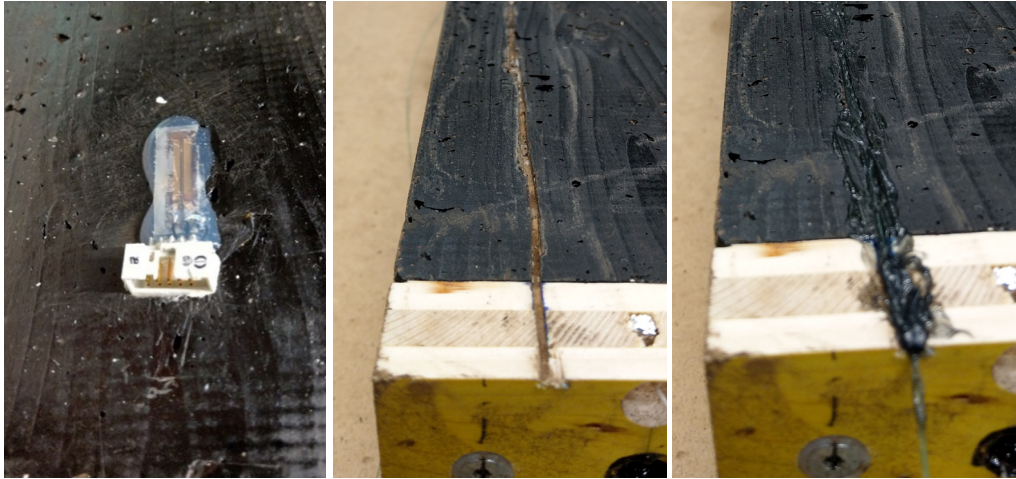


Fig. 51 Glued strain gauge. **Fig. 52** Groove on bottom. **Fig. 53** Glued external cable.

The external cables were spliced into a single series with the embedded cables to allow a simultaneous evaluation. An overview of the external fibre optic sensors and their positions is given in Tab. 7. As a final preparation step, the segregated binding layer on the top surface was locally removed to improve the load introduction.

Tab. 7 Overview of the external fibre optic cable sensors

Specimen	Name	Surface	Height
Specimen 1	S1 Bot 1	Bottom	0 cm
	S1 Bot 2	Bottom	0 cm
	S1 Side 1	Side	1 cm
	S1 Side 3	Side	3 cm
	S1 Side 9	Side	9 cm
Specimen 2	S2 Bot 1	Bottom	0 cm
	S2 Side 1	Side	1 cm
Specimen 3	S3 Bot 1	Bottom	0 cm
	S3 Side 1	Side	1 cm
Specimen 4	S4 Bot 1	Bottom	0 cm
Specimen 5	S5 Bot 1	Bottom	0 cm

4.3.3 Test procedure

Each bending test is performed according to the following the steps:

1. A reference OBR measurement and a measurement of the room temperature are taken.
2. The specimen is placed centrally into the press with a supernatant of 20cm on each side.
3. The strain gauge is connected to the amplifier and the measurements are taken at an interval of 0.5s.
4. A backing paper was placed between the specimen and the roller bearing of the head of the press.
5. The head of the press is lowered to close the gap and transmit a constant force of 50N. Also the value of the force and the displacement of the press are measured at an interval of 0.5s.
6. Before the further loading of the specimen it was waited until the creeping strain from the self-weight and the base load reached a sufficiently constant value.
7. The specimens were then loaded under different additional load levels ranging from 50 to 3200N, always increasing by a factor of two.
 - a. Just before the load application a reference OBR measurement is taken for the evaluation of the incremental strains.
 - b. The press head is lowered at a constant speed until the required force is reached. The speed is determined so that the force is reached within 3 seconds.
 - c. At this point the displacement is held constant and another OBR measurement is taken. Due to the relaxation of the mastic asphalt, the force in the sample decreases rapidly during this period.
 - d. After the measurement is taken the load is reduced to the base load of 50N. The specimen remained in this state until the strain increments measured by the strain gauge decreased below $1\mu\epsilon$ in 10s.
8. In the last load step (3200N), multiple measurements are taken.
9. The head of the press is lifted and the specimen is carried out of the press setup.

As an illustration, the history of the head displacement, the force measured by the press and the strain measured by the strain gauge of the third test specimen are shown in Fig. 54, where the blue markers indicate the moments when an OBR measurement was taken. It can be seen that the measurements are never taken at the peak of the press force, as it declines rapidly. However, the measurements are taken at the peak of the strain as indicated by the strain gauge. Further, it is seen how the displacement from the load steps is not entirely reversible.

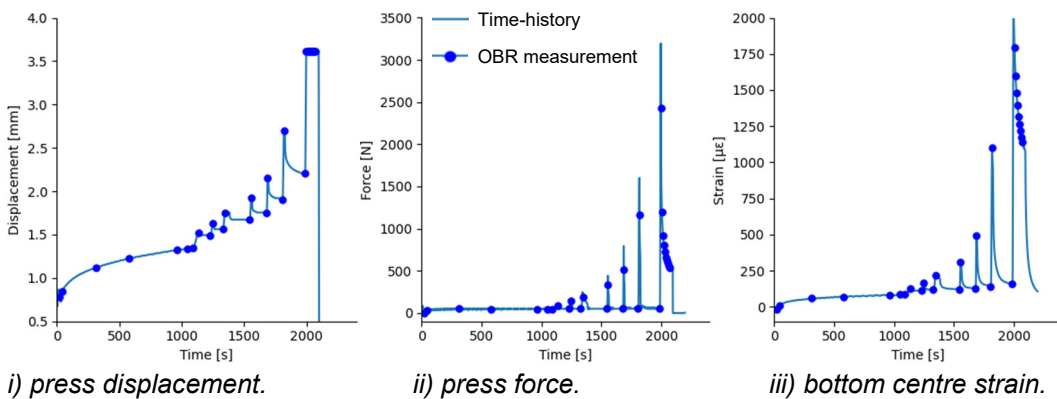


Fig. 54 Time-histories and OBR measurement times during the bending test.

4.3.4 Numerical comparison

The classical theory of structures and its assumptions for a Bernoulli beam predict a triangular bending moment distribution for the test setup introduced in section 4.3.1. Hence, also the curvature and the strain at a particular height in the cross-section would follow a triangular distribution. However, the underlying assumption that plane cross-sections remain plane under loading is a broad simplification for the considered bending test. The load introduction at the supports and at the centre create discontinuous zones which cover a large part of the specimen. Therefore, the bending test is modelled in a finite element software (Abaqus) in order to obtain a reasonable, comparative strain distribution. Considering that the specimen is supported and load along its entire width, a two-dimensional model using plane-stress elements is adequate. The specimen is divided into quadrilateral elements with a size of 5mm x 5mm and quadratic shape functions. The material was modelled as isotropic and elastic with an elastic modulus of 200MPa and a Poisson's ratio of 0.35. The specimen is supported at the lower quarter points and loaded by a unit load at the upper centre as shown in Fig. 55.



Fig. 55 Finite element model of the bending test.

The resulting two-dimensional distribution of longitudinal strain is shown in Fig. 56. It is verified by the peak strain at the centre of the bottom surface of approximately $10^{-6} = 1 \mu\epsilon$. This value matches the strain calculated in Eq. 1 under the assumption of a Bernoulli beam. The longitudinal strain at the relevant heights is extrapolated from the results and shown in Fig. 57. The respective shapes clearly indicate the discontinuous zones and the deviation from the triangular strain distribution at the quarter point and at the centre of the loaded span. The obtained curves are used for a comparison and validation of the measurements in the embedded cables and are referred to as “Elastic shape”. However, in reality the peaks are expected to be limited due to plastic behaviour.

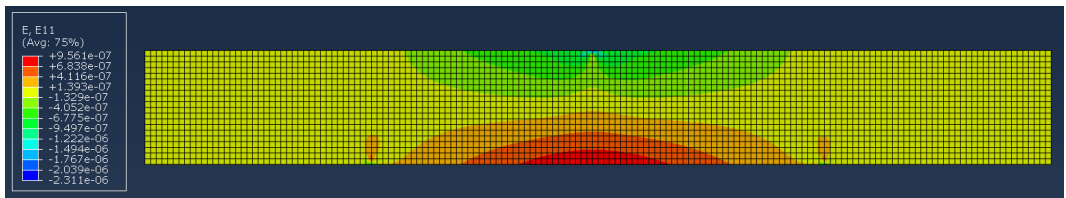


Fig. 56 Longitudinal strain distribution under centric unit load.

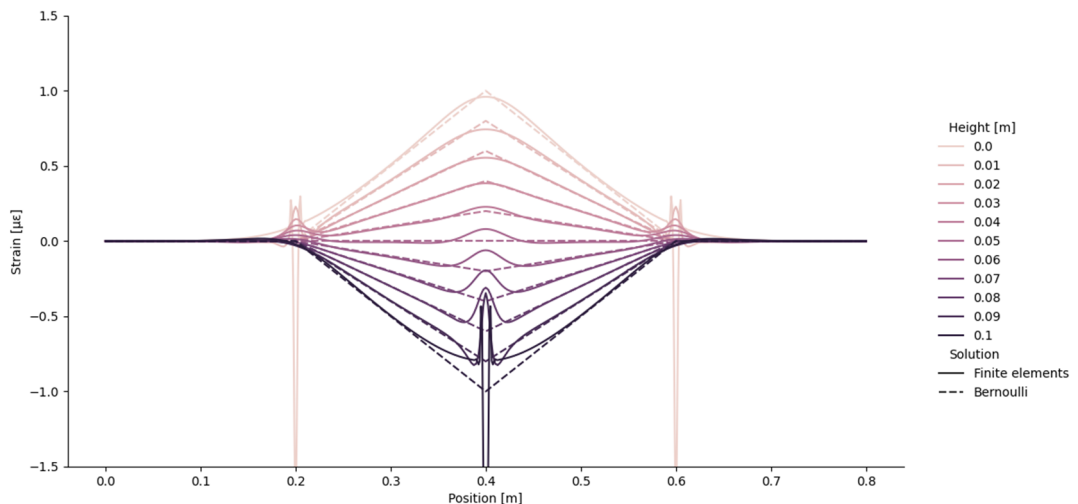


Fig. 57 Longitudinal strain distribution at different heights under centric unit load.

4.4 Results

4.4.1 Embedment

The two self-made cables using epoxy broke immediately in the cold conditions outside the asphalt factory. The preparation and pre-stressing of the remaining 20 cables in the formwork went without problems and the five asphalt specimen were created according to the plan. Specimen 2 was equipped with six temperature sensors, two on each layer. The respective measurements are presented in Fig. 58. The creation of the two asphalt layer can be clearly identified at 13:00 and 16:30. In the bottom layer the temperatures initially do not exceed 190°C and indicate a second peak at 130°C after the creation of the upper asphalt layer. The sensors in the middle cable layer at the interface between the lower and the upper asphalt layer show a very fast decline after initially reaching close to 200°C. Both sensors exceed 150°C for less than three minutes. The sensors in the top cable layer indicate the highest temperatures reaching 230°C. Within 10 minutes they cool down to 200°C and after 30 minutes they reach 150°C.

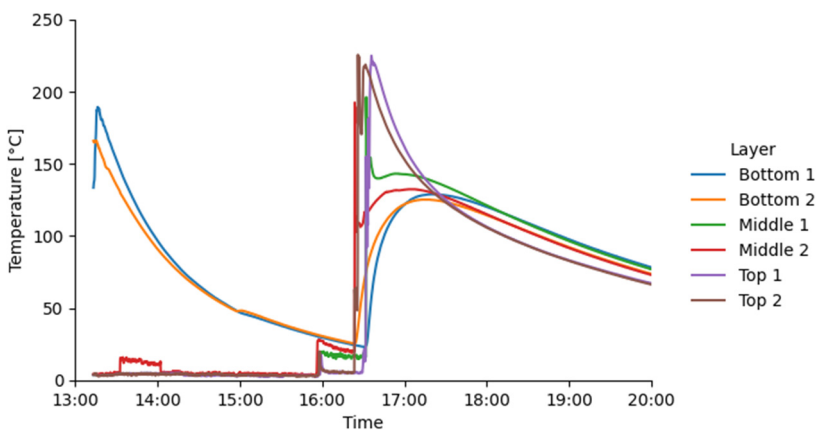


Fig. 58 Temperature measurements during the embedment.

The measured amplitude traces of the embedded cables do not show any signs of negative effects. Only the M3+RAU cable solution failed during the embedment procedure. Its problem is the weakened roughened cross-section which exhibited a plastic hinge when the cable was bended. The return amplitude indicated a total point loss at this position. Further the unprotected NM1 cable was lost. However, the amplitude trace indicates a pre-existing small point loss before the embedment in the mastic asphalt. Also the two self-made cable solutions immediately ruptured in the cold temperatures. Ultimately, 17 out of the 22 cable solutions were successfully embedded at the asphalt factory.

4.4.2 Bending test

The testing of the mastic asphalt samples took multiple days. Unfortunately, the conditions at the press could not be controlled and the temperature varied strongly between the different tests as shown in Tab. 8. It also indicates the static nature of the measurements which correspond to loading frequencies lower than 0.1Hz. Further, the first two specimens had to be tested multiple times to optimise the procedure, hence, at the time of the final tests, they had already undergone large strains before.

Tab. 8 Temperatures during the bending tests

Specimen	Specimen 1	Specimen 2	Specimen 3	Specimen 4	Specimen 5
Temperature	23.5°C	26.5°C	28.0°C	27.5°C	28°C
Frequency	<0.1Hz	<0.1Hz	<0.1Hz	<0.1Hz	<0.1Hz

External strain measurements

The external fibre optic strain sensors, which are glued to the side and the bottom surface, are used to determine the strain distribution in each specimen and for each load step. However, these measurements are not used directly, as neither they provide perfectly consistent measurements and further they are also not located at all the relevant heights of the cable layers. Therefore, the elastic strain distribution of the finite element analysis at the respective sensor height is scaled to fit the measurements of the external strain sensors as shown in Fig. 59. The respective scale factors can be expressed by the associated strain at the centre of the span at the bottom surface. These scale factors, which are obtained by a least-squares fit, allow for a direct comparison to the measurements by the strain gauge which is shown in Tab. 9. It can be seen that only for specimen 4 the external fibre optic measurements agree well with the strain gauge. For all other specimens the strain gauge indicates significantly less strain than the external fibre optic cables.

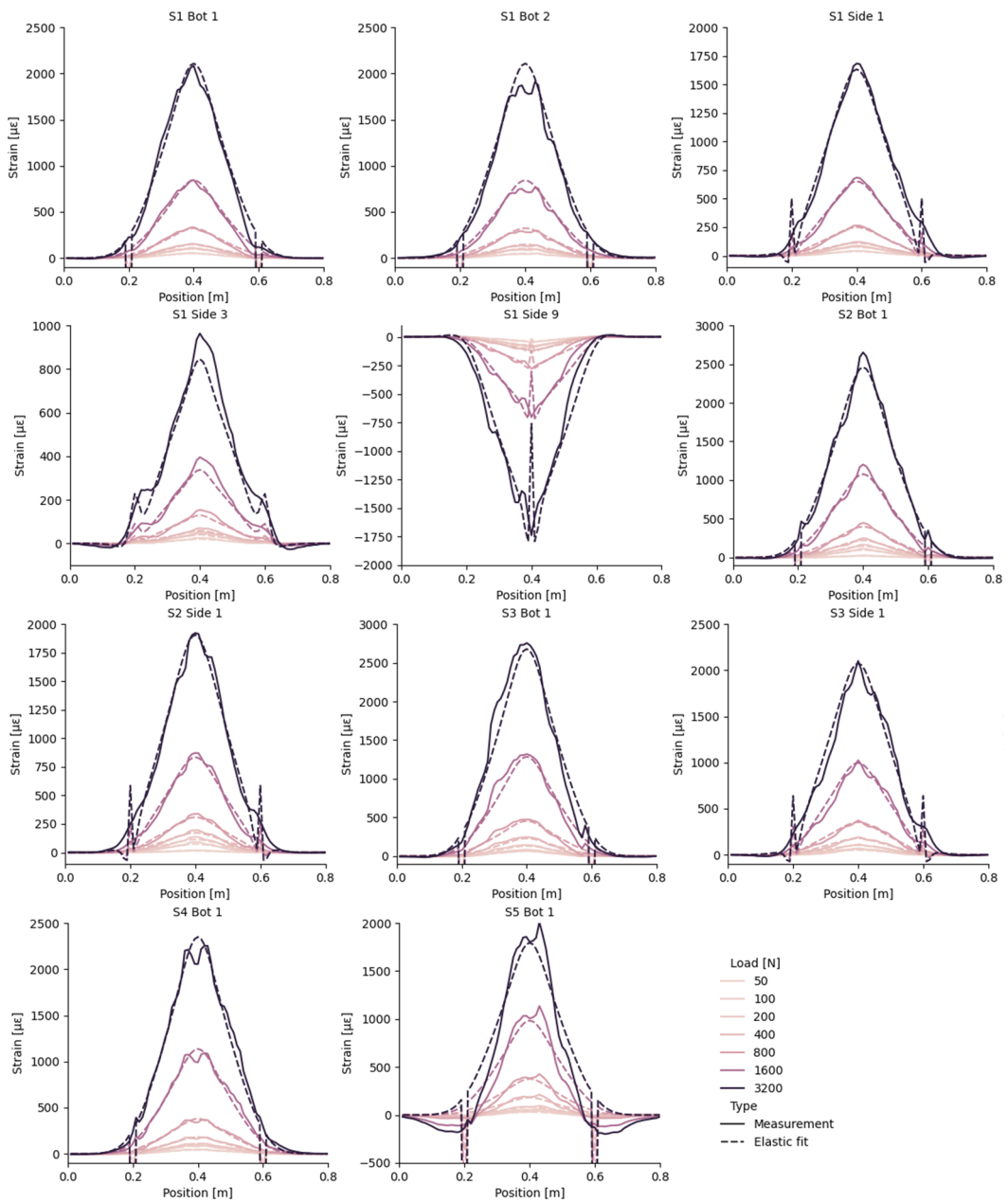


Fig. 59 Strain measurements in external fibre optic cables and fitted elastic curves.

Tab. 9 Comparison of external strain measurements

	Sensor	50 N	100 N	200 N	400 N	800 N	1600 N	3200 N
Specimen 1	S1 Bot 1	47.4 $\mu\epsilon$	97.4 $\mu\epsilon$	97.8 $\mu\epsilon$	142 $\mu\epsilon$	309 $\mu\epsilon$	806 $\mu\epsilon$	2020 $\mu\epsilon$
	S1 Bot 2	43.9 $\mu\epsilon$	90.9 $\mu\epsilon$	91.1 $\mu\epsilon$	133 $\mu\epsilon$	291 $\mu\epsilon$	761 $\mu\epsilon$	1911 $\mu\epsilon$
	S1 Side 1	48.4 $\mu\epsilon$	102 $\mu\epsilon$	96.1 $\mu\epsilon$	143 $\mu\epsilon$	315 $\mu\epsilon$	826 $\mu\epsilon$	2072 $\mu\epsilon$
	S1 Side 3	53.7 $\mu\epsilon$	114 $\mu\epsilon$	105 $\mu\epsilon$	158 $\mu\epsilon$	348 $\mu\epsilon$	916 $\mu\epsilon$	2289 $\mu\epsilon$
	S1 Side 9	49.8 $\mu\epsilon$	101 $\mu\epsilon$	96.3 $\mu\epsilon$	141 $\mu\epsilon$	309 $\mu\epsilon$	793 $\mu\epsilon$	1982 $\mu\epsilon$
	S1 DMS	37.7 $\mu\epsilon$	77.0 $\mu\epsilon$	88.3 $\mu\epsilon$	127 $\mu\epsilon$	287 $\mu\epsilon$	736 $\mu\epsilon$	1782 $\mu\epsilon$
Specimen 2	S2 Bot	19.7 $\mu\epsilon$	92.4 $\mu\epsilon$	141 $\mu\epsilon$	213 $\mu\epsilon$	386 $\mu\epsilon$	1059 $\mu\epsilon$	2417 $\mu\epsilon$
	S2 Side 1	19.7 $\mu\epsilon$	95.1 $\mu\epsilon$	146 $\mu\epsilon$	221 $\mu\epsilon$	391 $\mu\epsilon$	1041 $\mu\epsilon$	2379 $\mu\epsilon$
	S2 DMS	13.9 $\mu\epsilon$	58.4 $\mu\epsilon$	90.9 $\mu\epsilon$	149 $\mu\epsilon$	270 $\mu\epsilon$	720 $\mu\epsilon$	1671 $\mu\epsilon$
Specimen 3	S3 Bot	61.5 $\mu\epsilon$	76.2 $\mu\epsilon$	135 $\mu\epsilon$	233 $\mu\epsilon$	460 $\mu\epsilon$	1304 $\mu\epsilon$	2717 $\mu\epsilon$
	S3 Side 1	64.3 $\mu\epsilon$	73.5 $\mu\epsilon$	124 $\mu\epsilon$	215 $\mu\epsilon$	427 $\mu\epsilon$	1203 $\mu\epsilon$	2506 $\mu\epsilon$
	S3 DMS	43.2 $\mu\epsilon$	55.7 $\mu\epsilon$	99.0 $\mu\epsilon$	184 $\mu\epsilon$	360 $\mu\epsilon$	959 $\mu\epsilon$	1954 $\mu\epsilon$
Specimen 4	S4 Bot	43.9 $\mu\epsilon$	85.9 $\mu\epsilon$	108 $\mu\epsilon$	176 $\mu\epsilon$	369 $\mu\epsilon$	1107 $\mu\epsilon$	2290 $\mu\epsilon$
	S4 DMS	41.2 $\mu\epsilon$	85.2 $\mu\epsilon$	107 $\mu\epsilon$	178 $\mu\epsilon$	364 $\mu\epsilon$	1042 $\mu\epsilon$	2158 $\mu\epsilon$
Specimen 5	S5 Bot	29.5 $\mu\epsilon$	50.5 $\mu\epsilon$	80.5 $\mu\epsilon$	178 $\mu\epsilon$	367 $\mu\epsilon$	959 $\mu\epsilon$	1750 $\mu\epsilon$
	S5 DMS	24.0 $\mu\epsilon$	42.8 $\mu\epsilon$	69.1 $\mu\epsilon$	148 $\mu\epsilon$	306 $\mu\epsilon$	752 $\mu\epsilon$	1445 $\mu\epsilon$

Strain normalisation

In order to compare the cable solutions from different specimens and load levels, the measurements of the cable solutions are normalised by a reference strain. The respective reference strain is taken as the average of the estimated strain from the external fibre optic cables. Thereby, the normalised strains of each cable solution and each load level ideally follow the same shape only depending on the height in the cross-section. These reference strains are shown in Tab. 10. The normalisation procedure is illustrated in Fig. 60 for the measurements in the bottom layer of the NM2 cable. On the left side the measured strains are shown for each load level and the reference strain from the external fibre optic measurements is indicated by the respective horizontal line. By dividing the measured strains by the reference strain the normalised strains on the right side are obtained. They indicate a good consistency between the internal and the external fibre optic measurements for all load steps as the results are in a narrow range.

Tab. 10 Estimated reference strains at the centre of the bottom surface

	Load	50 N	100 N	200 N	400 N	800 N	1600 N	3200 N
Specimen 1	ϵ_{ref}	48.6 $\mu\epsilon$	101 $\mu\epsilon$	92.3 $\mu\epsilon$	144 $\mu\epsilon$	314 $\mu\epsilon$	821 $\mu\epsilon$	2055 $\mu\epsilon$
Specimen 2	ϵ_{ref}	19.7 $\mu\epsilon$	93.8 $\mu\epsilon$	143 $\mu\epsilon$	217 $\mu\epsilon$	389 $\mu\epsilon$	1050 $\mu\epsilon$	2398 $\mu\epsilon$
Specimen 3	ϵ_{ref}	62.9 $\mu\epsilon$	74.8 $\mu\epsilon$	129 $\mu\epsilon$	224 $\mu\epsilon$	444 $\mu\epsilon$	1253 $\mu\epsilon$	2611 $\mu\epsilon$
Specimen 4	ϵ_{ref}	43.9 $\mu\epsilon$	85.9 $\mu\epsilon$	108 $\mu\epsilon$	176 $\mu\epsilon$	369 $\mu\epsilon$	1107 $\mu\epsilon$	2290 $\mu\epsilon$
Specimen 5	ϵ_{ref}	29.5 $\mu\epsilon$	50.5 $\mu\epsilon$	80.5 $\mu\epsilon$	178 $\mu\epsilon$	367 $\mu\epsilon$	959 $\mu\epsilon$	1750 $\mu\epsilon$

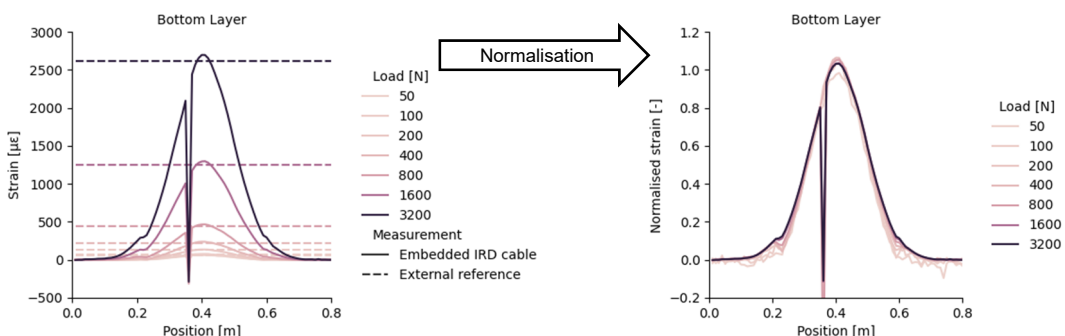


Fig. 60 Strain normalisation for the bottom layer of the embedded NM2 cable.

Strain measurements in embedded cables

In the following figures the normalised strain is shown for each cable and its modifications. The mean of the different load steps is shown by the coloured lines while the range of the obtained results is indicated by the respective shade. However, the measurements from the first load step are disregarded for this evaluation, as the noise of the respective measurement causes a large variation in the normalised strains. The results from the three different layers are shown separately along with the ideal elastic solution. This curve is identical for every test as the results are normalised by the reference strain. For the top and the middle layer it has a peak of 1.00 and 0.50 while indicating the discontinuous zones at the supports at 0.2m and 0.6m. In the top layer it has two peaks of -0.40 and clearly indicates the load introduction in between the peaks.

The cable NM1 was protected by three different shrinkage tubes. The respective normalised strains are shown in Fig. 61. However, the unprotected cable is missing as it broke during the embedment process. It is remarkable that the NM1+PTFE cable measured strains up to 25% higher than the elastic solution for the bottom and the middle layer. NM1+ETW indicates the expected strain very accurately for these two layer, only slightly missing the peak in the middle layer. The NM1+MDTA cable indicates less strain than the elastic fit for the bottom layer. Especially for the middle layer both cables correctly indicate the discontinuous zones from the support reactions. For the bottom layer all three cables measured larger strains than estimated for the corresponding height. This is particularly striking for the NM1+MDTA cable, which measured strains of almost the same magnitude as the reference strain.

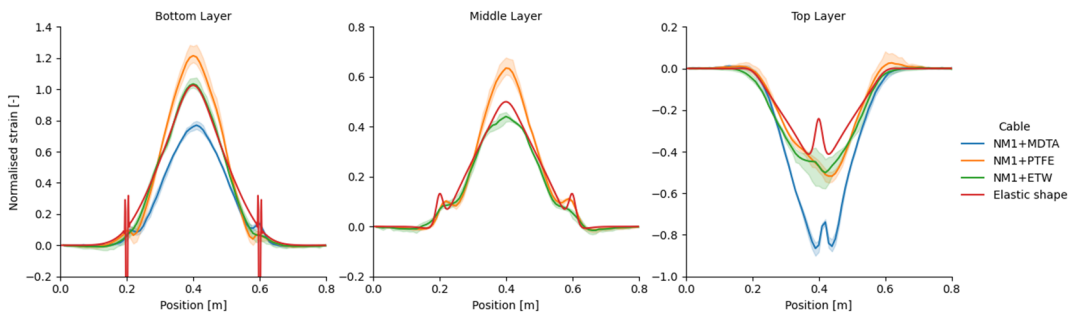


Fig. 61 Normalised strain distribution in the bending tests for NM1 and its modifications.

The measurements from the NM2 cable and its modifications, shown in Fig. 62, are characterised by a very strong agreement with the elastic estimation. Only the bare NM2 cable indicates slightly higher strains than expected in the middle layer. Further, all cables indicate the discontinuous zone at the supports in the middle and the top layers, even though with a lesser magnitude than expected from the elastic calculations. It can be noted that every cable solution also shows a few outliers in some measurements.

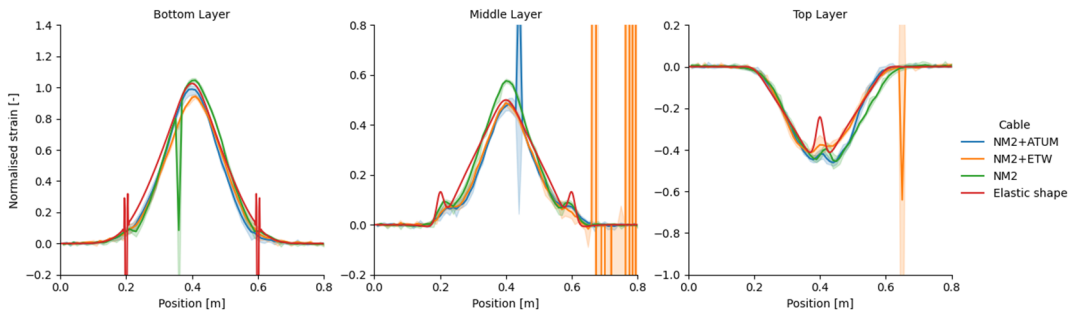


Fig. 62 Normalised strain distribution in the bending tests for NM2 and its modifications.

The results from PK cable and its modifications is presented in Fig. 63. The measurements show a significantly less smooth shape compared to the other cables. Nevertheless, the variation at the individual points is rather small. In the lower layers, the peaks are slightly higher than the estimate from the external measurements, except for the bare PK cable

which shows significantly larger strains in the middle layer. Also in the top layer the measured strains exceed the elastic estimation. Further, the PK cable and its modifications show strongly accentuated discontinuous zones in all layers.

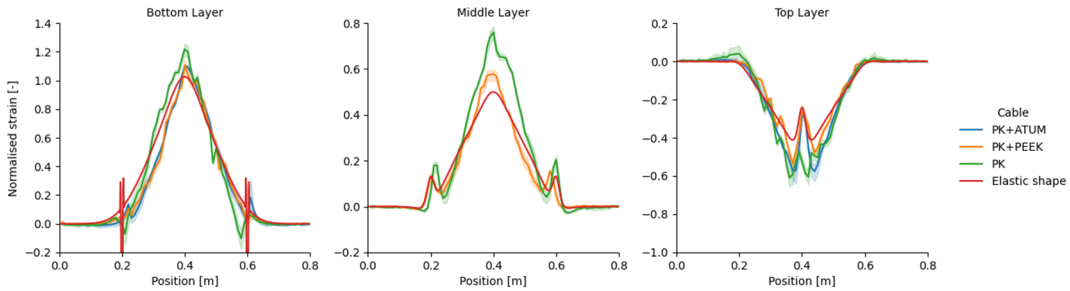


Fig. 63 Normalised strain distribution in the bending tests for PK and its modifications.

The normalised strains from the M1 cables and its modifications are shown in Fig. 64. The normalised measurements from the M1+PTFE cable show a large strain outside the supports paired with a very high variation between the different measurements. On the other hand, the M1 and the M1+MDTA cables both indicate a low variation while slightly underestimating the peak strain. All cables show a similar result for the top layer with normalised peak strains of approximately -0.4. However, no cable indicates the load introduction in the measurement of the top layer.

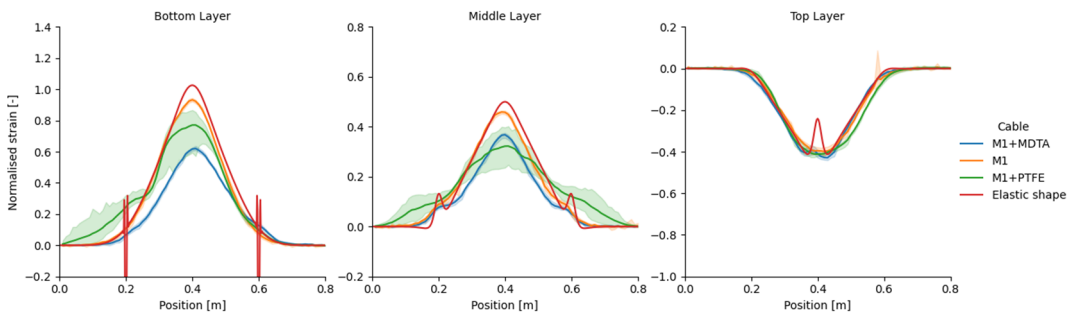


Fig. 64 Normalised strain distribution in the bending tests for M1 and its modifications.

The measurements from the M2 cable, shown in Fig. 65, show a very smooth curve with little variation between the different load steps. The measured strains in the lower layers are smaller than expected from the external measurements with peaks of 0.78 and 0.30 respectively. In the top layer, the normalised strain shows a peak normalised strain of 0.50, exceeding the elastic estimation. The measurements do not show any signs of the discontinuous zones. Further, it can be noted how in the upper layers strains are measured outside of the supported range.

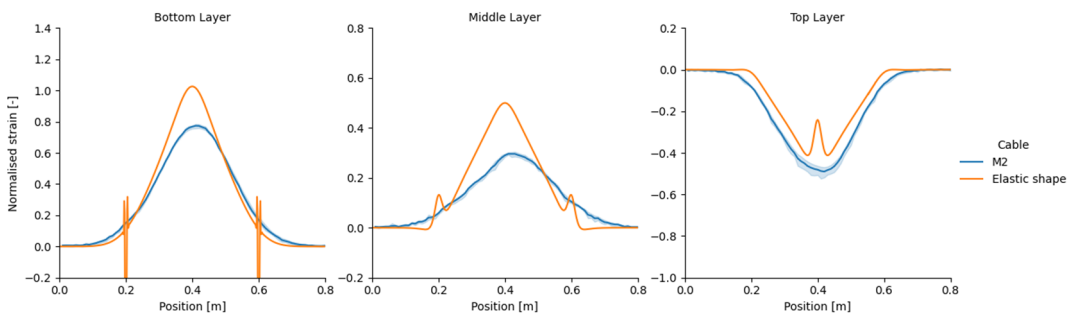


Fig. 65 Normalised strain distribution in the bending tests for M2.

The normalised strains for the bare M4 cable and the M4+MDTA cable are shown in Fig. 66. Both cables measured significantly less strain in the bottom and the middle layer than the respective elastic solution. Further, more strain appears outside of the two supports in the top and the middle layers while also slightly indicating the discontinuous zones. In the

top layer, the peaks of the measured strains come close to the estimation and indicate the load introduction.

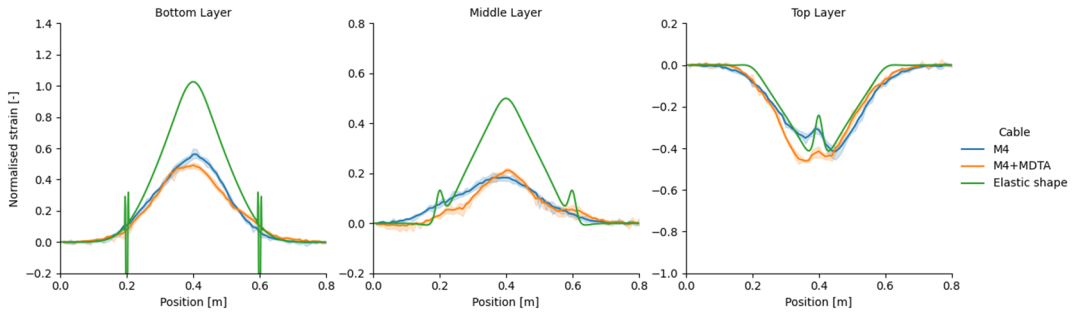


Fig. 66 Normalised strain distribution in the bending tests for M4 and its modification.

4.5 Discussion

4.5.1 Embedment

The temperature measurements in Fig. 58 show that the expected peak temperature of 240°C is not reached in any cable layer. A comparison to the temperature curve in the oven is shown in Fig. 67, where every curve is shifted to its peak time. It indicates that the temperature exposition in the oven is on the conservative side compared to the conducted embedment procedure. As a comparison, the temperature in the oven exceeds 200°C for more than an hour. Whereas only the top cable layer exceeds 200°C for a short time of less than ten minutes during the embedment.

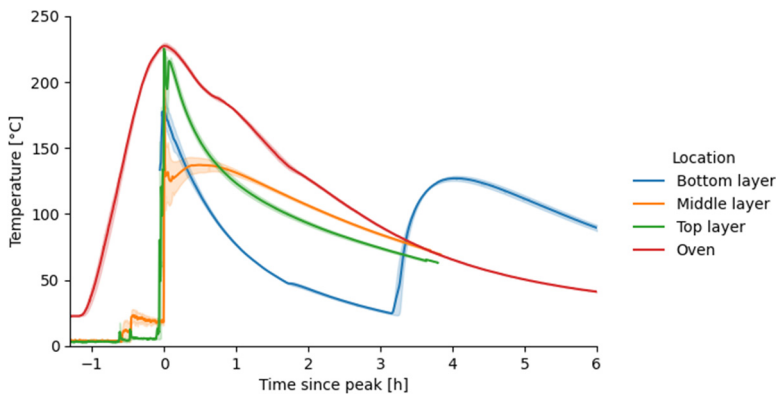


Fig. 67 Temperature evolution in the oven and during the embedment.

Only the NM1 and the M3+RAU cable solutions indicated a clear loss of signal during the embedment. The latter broke because of the roughened and weakened cross-section, which is not a practical modification. The reason for the failure of the NM1 cable is not clear as it failed within the respective specimen and cannot be investigated. However, it is possible that there was a pre-existing damage in the cable, which broke during the pre-stressing in the formwork. However, the amplitude traces do not indicate a continuous loss for the NM1 cable, which shows that the shrinkage of the cable is hindered.

4.5.2 Bending test

It is surprising that the external strain gauges in four out of five specimens significantly underestimate the strain in the centre of the bottom surface. There is little doubt of their appropriate setup, as they were installed by an experienced technician using optimal equipment. Potential problems could be their stiffness or the strain transfer by the glue. Considering that the external fibre optic sensors provide a very good fit to the ideal numerically derived elastic solution, it is legitimate to take their average scale factor as a reference strain. The thereby normalised results of most cables indicate a very low variation between the different load steps, which can be seen as a confirmation of the external fibre

optic strain sensors. The only significant deviation from the elastic solution is seen in the fifth specimen where the external fibre optic sensor even indicates compressive strains around the supports, as seen in the last plot in Fig. 59. This is the specimen featuring all the stiff cable solutions based on the M4 and M3 cables. Even though it was tested with the highest measured room temperature the measured strains at the bottom surface are lower than in the other specimens. Both of the observations may be due to the stiff cable solutions which act as a significant reinforcement on the specimen, making it locally stiffer and change the resulting strain distribution. Whether or not these cable solutions indicate the strain correctly is irrelevant in the scope of this project, since they potentially change the behaviour of at least soft asphalt material which they are supposed to measure.

The M1+PTFE and the M2 cable solutions measured significant strains in the supernatants of the tested specimens but less strain in the loaded span. This is a clear sign of an insufficient strain transfer or slippage as the fibre is basically pulled out from the unloaded sections. Another bad sign is a large variation of the normalised strains between the different load levels. This indicates a non-linear strain transfer and is observed for the cables solutions M1+PTFE, NM1+PTFE and NM1+ETW in the top layer.

Most embedded cable sections based on the NM1, M1, PK and NM2 cables indicate a very good fit to the scaled elastic solutions. This is surprising as already a change of position of 5mm approximately causes a change in the normalised peak strain of 0.1 as seen in Fig. 57. This indicates that most cables are accurately embedded at their respective heights even at the centre of the specimen. Thereby, they validate the embedment procedure. But it is unclear whether the remaining differences stem from an insufficient strain transfer or from slight changes in the heights of the cable. However, a few cables indicate significant deviations in the normalised strain. They are most notably the NM1+MDTA and the M1+MDTA cable solutions. Besides the thick and soft shrinkage tube and the associated challenge to pre-stress them, these cable solutions are naturally located a bit higher because of their large diameter. This offers an explanation why these two cables measure an accurate shape but of a lower magnitude. In the top layer of the NM1+MDTA cable normalised peak strains of 0.88 are measured, indicating potentially that the cable elongated and floated towards the surface as illustrated in Fig. 68. Further, there are also two cables, the PK and the NM1+PTFE, which measure larger strains than expected in the middle layer and even in the bottom layer. A change in position cannot serve as an explanation for the deviation in the bottom layer. It could be caused by an inhomogeneity of the specimen that locally undergoes larger strains. However, no clear answer can be offered for this phenomenon.

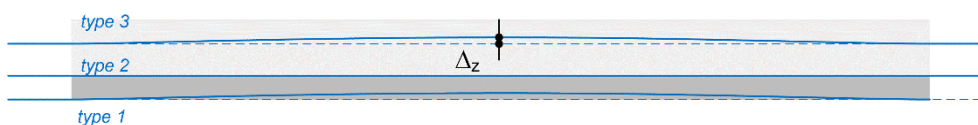


Fig. 68 Inaccurate cable position due to temporary thermal elongation.

Many cables indicate the strains in the bottom and the middle layer similar to the expected shape from the numerical model. This is already a good sign. However, the discontinuous zones which exist due to the concentrated load introductions allow to investigate the strain transfer on an even smaller scale. Especially in the middle layer many cables exhibit two sections around the supports with increased strains, as predicted by the elastic solution. Also in the top layer, many cables indicate a clear bump at the centre of the span. This strong local variation of strain, which is undoubtedly not just a theoretical phenomenon, is the ultimate measure for the quality of the strain transfer of the cable solutions as it requires large bond stresses. For example, all the NM2-based cable solutions, indicate the discontinuous areas to a certain extent. However, the PK-based cable solutions indicate strains in this area that actually correspond to the ones predicted by the theoretical model. This is a sign of an extraordinary strain transfer and a surprising accuracy of the numerical model.

An overview of the performance of each cable solution is presented in Tab. 11.

Tab. 11 Overview of the performance of the tested cable solutions in mastic asphalt environment

Cable solution	Strain distribution	Discontinuous zones	Rating
CO	Broken during embedment		
NM1	Broken during embedment		
NM1+PTFE	Insufficient bond	No indication	-
NM1+ETW	Accurate	Weak indication	+
NM1+MDTA	Instable position	No indication	-
NM2	Accurate	Moderate indication	++
NM2+ATUM	Accurate	Moderate indication	++
NM2+ETW	Accurate	Moderate indication	++
PK	Accurate	Pronounced indication	++
PK+ATUM	Broken during transportation		
PK+ETW	Accurate	Pronounced indication	++
PK+PEEK	Accurate	Pronounced indication	++
M1	Accurate	Weak indication	+
M1+PTFE	Slippage	-	-
M1+MDTA	Instable position	No indication	-
M2	Insufficient bond		-
M3	Broken during preparation		
M3+RAU	Broken during embedment		
M4	Changed specimen response	-	-
M4+MDTA	Changed specimen response	-	-

Please note, that none of the above cable was stated a priori to work in the rough environment of mastic asphalt. However, some of them perform in this particular environment surprisingly well. In addition it should be mentioned, that some effects, noted in the laboratory testing in the oven, are clearly occurring less pronounced in the more representative mastic asphalt embedment test owing to the faster cooling and the geometrical constraints. The embedment of the cables in the mastic asphalt samples (dimensions of 0.8m x 0.3m x 0.1m) is regarded to represent the real application in the field closer than the laboratory test in the oven.

5 Conclusions and recommendations

The project aims to answer the question whether commercially available fibre optic cables can be used as distributed strain sensors in mastic asphalt. Also, the feasibility and performance of simple modifications to improve the behaviour of the available cables in the rough environment is investigated. These questions are investigated by a temperature exposition and a strain test in the laboratory and by a bending test of realistically embedded cable solutions.

5.1 Conclusions

5.1.1 Cables

The commercially available cables which are used for strain sensing often guarantee an operating temperature resistance of less than 90°C. The strain tests of the heat-exposed cables show a significant loss of bond for practically all typically used cables. While some of these cables have been used in the past after a temporary exposure to temperatures which were above their indicated range, some of them are now showing to deteriorate with the even higher temperature exposure to more than 200°C in the oven. As expected, some cable sheaths are melting at these temperatures, which may not necessarily be a large drawback in a mastic asphalt embedment. Other cable sheaths underwent a change in material behaviour after the thermal exposure (from ductile to rather brittle) or tended to significantly shrink and many of these cables show reduced strain transfer properties after the temperature exposure in the oven. Only the NM2 and the PK cable show no visible impact from the temperature exposition and still indicates a good strain transfer. For the PK cable this is less surprising as it is made for applications in high temperature environments.

Besides the loss of bond a few other problems appeared in the embedment in mastic asphalt and the respective bending tests. For the M2 cable, some disadvantages are related to its stranded design which does not strain identical as the host material. Further, the cables M4 and M3 are rather stiff so that they tend to locally change the behaviour of the rather soft mastic asphalt sample in this project. Therefore, the mentioned cables are only to a limited extent suitable for the very specific purpose of an embedment in mastic asphalt and should be used with care in this case. It appeared to be difficult to assess the performance of the NM1 cable solution in the mastic asphalt sample, as the embedment seemed to have some difficulties, most likely owing to the thermal elongation of the cable and the difficulties to control its positioning in the sample.

On the other hand, the NM2 and PK cables perform very well and the M1 cable performs well in the bending test. For the M1 cable it is most likely the short exposure to high temperatures in the realistic embedment which allows it to keep its internal bond. All of these cables also indicate the zones of the load introductions. The M1 cable shows a little bump in the strains around the supports, whereas the NM2 cable even indicates inclinations of a different sign, as predicted by a numerical model. However, the PK cable shows the most pronounced strain discontinuities. This is the ultimate measure for the performance of a strain sensor as the large change in strain requires high bond stresses. On the other hand, M1 and NM2 in turn provide slightly more robustness for the embedment procedure.

There are also a few specialist cables (or rather coated fibres) with a small resistant coating that claim to survive temperatures of much more than 240°C. However, these cables are rather fragile and do not seem to provide the necessary robustness for this particular mastic asphalt field application.

5.1.2 Modification methods 1 and 2 (protective layers)

The M2, M3 and M4 cables seem to have a design which may be extremely favourable for other applications, but cannot be improved by a modification for the specific application discussed here. On the other hand, the NM2 and the PK cable already indicate a very accurate strain distribution without a modification. Only if the PK cable would need to be made more robust against mechanical damaging, additional protective layers would make sense for this cable. The design of the NM1 and M1 cables, on the other hand, may be improved by some modifications for the specific mastic asphalt application. Whereas the PTFE shrinkage tube offers a lot of protection against high temperatures, it causes severe strain transfer problems. Also the ETW and the MDTA shrinkage tube impair the strain transfer to a lesser extent. Additionally, the size of the MDTA protected cable tube becomes larger and harder to embed precisely. However, the shrinkage tubes do not generally deteriorate the performance of a cable. The PEEK and ATUM shrinkage tubes still allow for very precise measurements with the NM2 and the PK cables. Hence, they provide an option to improve the robustness of these cables locally in case they are used in very rough conditions. Please note that the additional protection using shrinkage tubes is only a local measure and may not be suitable for a cable embedment in mastic asphalt over longer distances.

The casting of cable solutions based on the very resistant coated fibres poses many challenges. While the chosen casting process worked well, the fast hardening of the adhesive requires a timely fabrication. Further, the casting for longer lengths would become challenging and the ends of the fibre remain weak and prone to rupture. Because of the breakage in the cold conditions, the bond between the cable and the adhesive has not been investigated. Ultimately, no real advantages are expected from these self-casted fibres over the PK and NM2 cables.

5.1.3 Modification method 3 (embedment procedure)

Most cable solutions were embedded successfully in the mastic asphalt samples, validating the procedure and the approach of pre-straining the cable solutions with fixations. Some cables tend to shrink after temperature exposure, but while being in the heating phase, some of them experience a significant thermal expansion. This may lead to a loss of pre-strain and the cables may deviate from their initial position. This problem may be tempered with embedment type 1 (fixed on a surface) or type 2 (casted in a notch) but can be pronounced in embedment type 3 (arbitrary height). This circumstance needs to be taken into account when embedding the cables in mastic asphalt. Another strategy might be a repetition of prestraining once the cable is surrounded by mastic asphalt but this requires a rather robust cable design.

In particular in the bottom and the middle layer, the temperature cools down much faster than anticipated. Therefore, the heat exposure obtained in the oven is on the conservative side.

5.2 Recommendations

The NM2 cable performed very well in all conducted tests and seems to be suitable and can be recommended, on basis of the present test results, for further applications as a strain sensor in mastic asphalt. The same applies in principle for the PK cable. It allows for the accurate measurement even of strong local changes in the strain distribution, which makes it very interesting for analysing the local behaviour. On the other hand, it possesses smaller robustness than the NM2 cable. Using the NM2 cable, no additional protection is necessary. Also the PK cable did not require additional protection in the present study. However, it was not applied in a full scale test on the construction site and therefore, future applications of this cable on construction sites will give more clarity whether its mechanical robustness results in satisfying survival rates. The M1 cable was performing well in the bending test, on the other hand its strain transfer showed some detrimental effects after the more conservative oven test in the laboratory. Hence its behaviour seems to depend on the duration of the high temperature exposure. It is slightly stiffer than other well-

performing cables, which potentially affects the behaviour of a soft asphalt, but provides in turn also more mechanical robustness. In further projects, the PK, the NM2 and potentially also the M1 cable could be used for distributed fibre optic measurements in mastic asphalt. The final cable choice should depend on the application purpose, embedment type, expected temperature and on a trade-off decision between most accurate local strain measurements and mechanical robustness or high survival rates. It is recommended to embed two or even three different types of cables in parallel in the first full scale field application in order to finally evaluate their performance under field conditions. Besides the favoured cable versions, also the other cable versions may have their special application purposes in the field of pavement monitoring. For the choice of the measurement type, the different fibre optic sensing technologies are to be considered, which also bring distinct requirements with respect to the necessary equipment and its setup.

The embedment at the bottom of a mastic asphalt layer, at the interface between two layers (type 1) or in notches between two layers (type 2) can be accomplished, even over longer distances, using rather simple fixations. However, the embedment over a long span at an arbitrary height in the middle of an asphalt layer (type 3), remains a challenge. In the scope of this project no procedure that works for a long range is developed. The usage of specific fixtures at the arbitrary heights or repeated re-tensioning in case of robust cables seems inevitable for this purpose. This particularly requires attention because the strain measurements in mastic asphalt could be limited by the accuracy of the embedment.

5.3 Outlook

The conclusions from this project show that the fibre optic technology to investigate the behaviour of mastic asphalt is available. Further, it is seen that the strain can be measured along a particular direction with an astonishing accuracy. The fact that discontinuous zones can be measured opens the door for the deeper investigation of the distribution of concentrated loads and for the behaviour of the material on a smaller scale. Further investigations are required when the fibre optic sensor should be embedded at an arbitrary height in the mastic asphalt layer. The results of this study were obtained using a measurement device based on Rayleigh scattering (SWI / c-OFDR; OBR 4600) enabling rather local measurements over several tens of meters with a data acquisition typically within a few seconds. If other technologies or devices are used, the cables should be tested in advance in the relevant temperature environment, in order to guarantee its applicability. In particular if a measurement over larger perimeters is considered, other fibre optic measurement technologies may potentially be more suitable (e.g. technologies based on Brillouin scattering), provided their spatial resolution (gauge length) and the required measurement duration can meet the requirements. In such a case, longer cable sections should be tested regarding their performance as well as potential detrimental effects of temporary high temperatures on the Brillouin gain spectra should be analysed.

5.4 Acknowledgement

The authors would like to thank the members of the accompanying committee for their valuable inputs, comments and hints which contributed to this project. Particular thanks goes to Samuel Probst and the personnel of the asphalt factory who enabled an efficient production of the mastic asphalt samples, as well as to Massimo Facchini for his hints regarding potential cable solutions.

Appendix

I	Test data.....	67
I.1	Strain test.....	67
I.2	Bending test.....	69

I Test data

I.1 Strain test

In the following, further test data from the strain tests is presented for each cable individually. The results consist the return amplitude of the reference measurement as well as the average spectral shift measured in the strained section. Ultimately, the force-strain relationship is also shown.

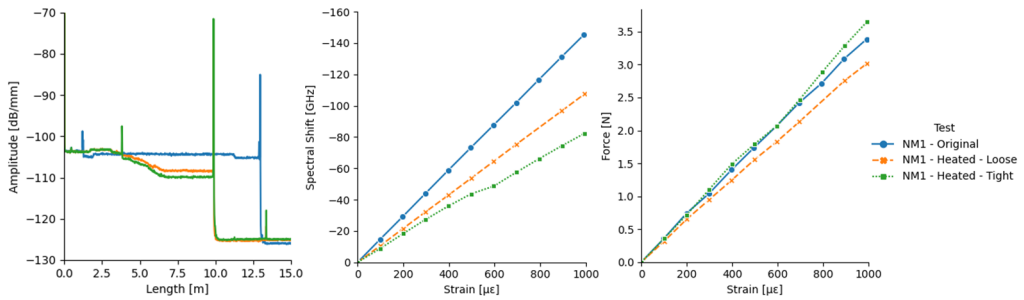


Fig. 1 Return amplitude, avg. spectral shift and force in the strain tests for NM1.

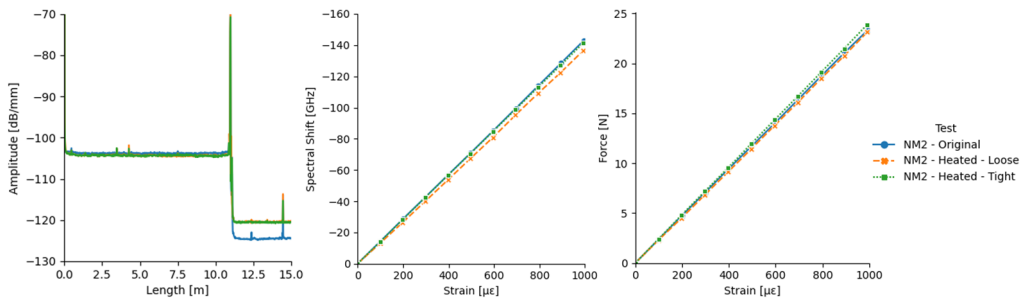


Fig. 2 Return amplitude, avg. spectral shift and force in the strain tests for NM2.

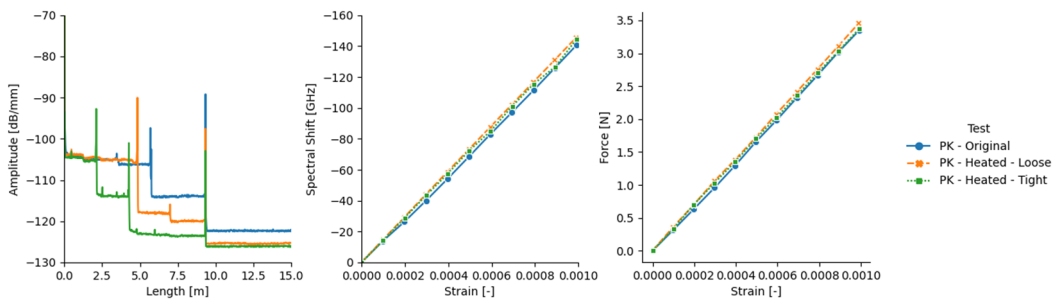


Fig. 3 Return amplitude, avg. spectral shift and force in the strain tests for PK.

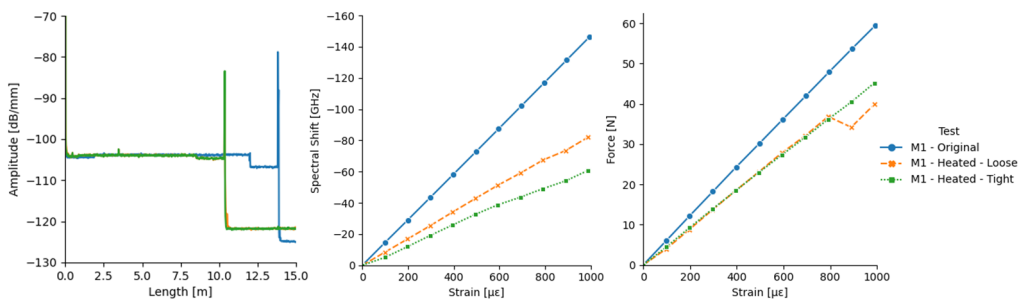


Fig. 4 Return amplitude, avg. spectral shift and force in the strain tests for M1.

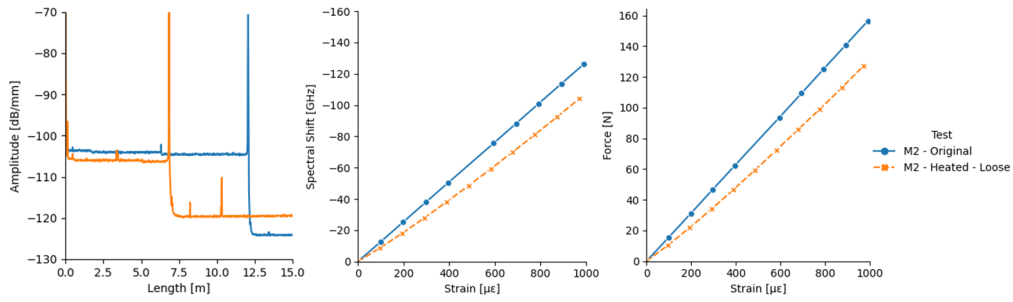


Fig. 5 Return amplitude, avg. spectral shift and force in the strain tests for M2.

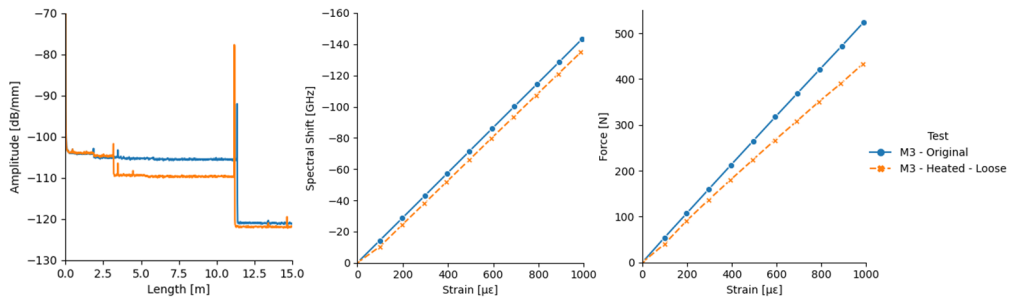


Fig. 6 Return amplitude, avg. spectral shift and force in the strain tests for M3.

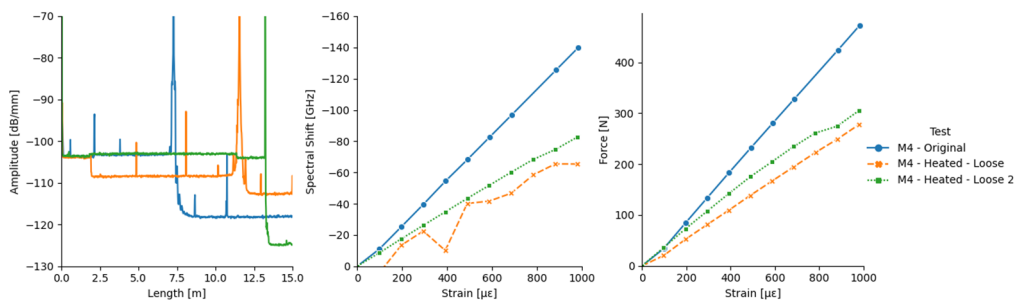


Fig. 7 Return amplitude, avg. spectral shift and force in the strain tests for M4.

I.2 Bending test

In this section the normalised results from the bending tests are shown for each mastic asphalt specimen.

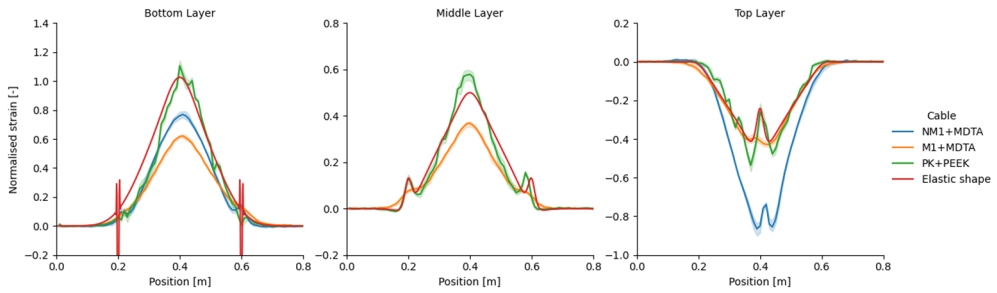


Fig. 8 Normalised strain measurements of Specimen 1.

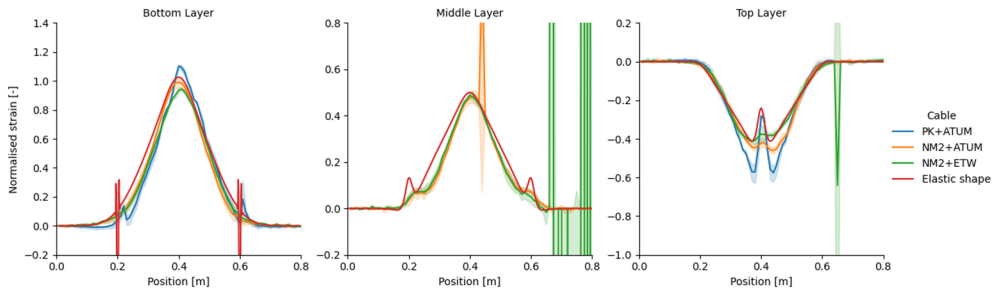


Fig. 9 Normalised strain measurements of Specimen 2.

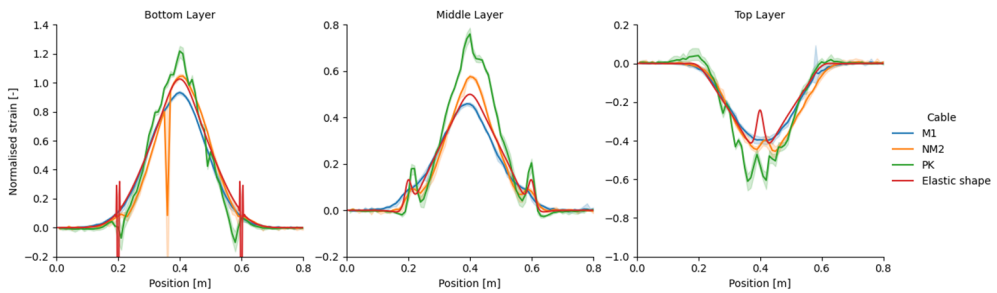


Fig. 10 Normalised strain measurements of Specimen 3.

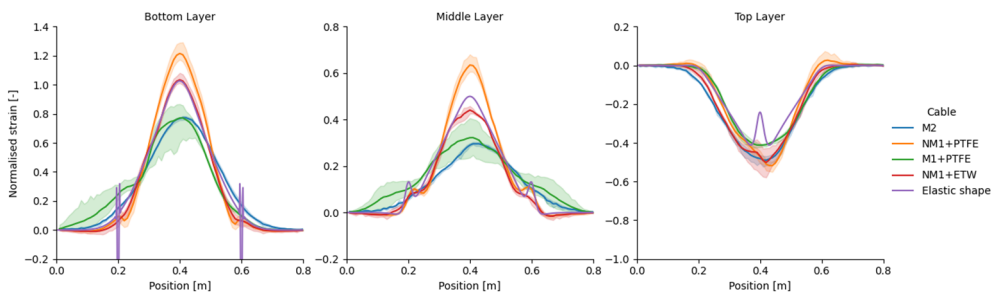


Fig. 11 Normalised strain measurements of Specimen 4.

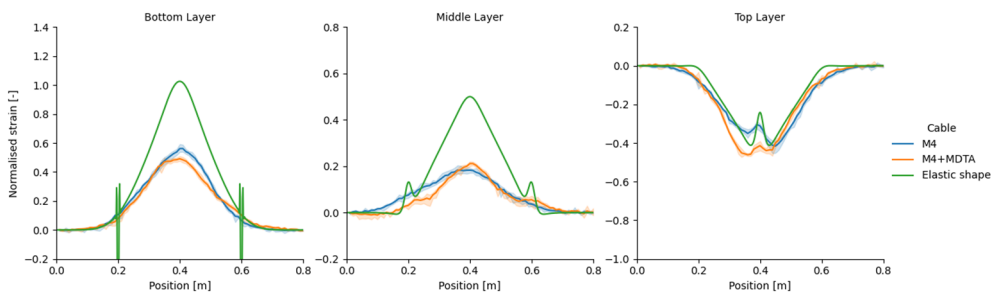


Fig. 12 Normalised strain measurements of Specimen 5.

Glossary

Term	Meaning
BOTDA	Brillouin Optical Time Domain Analysis
DTS	Distributed Temperature Sensing
DTSS	Distributed Temperature & Strain Sensing
DSS	Distributed Strain Sensing
MMF	Multi Mode Fibre
OBR	Optical Backscatter Reflectometer
(c)-OFDR	(coherent) - Optical Frequency Domain Reflectometry
OTDR	Optical Time Domain Reflectometry
PEEK	Polyetheretherketone
PTFE	Polytetrafluoroethylene
SMF	Single Mode Fibre
SWI	Swept Wavelength Interferometry.
$1\mu\epsilon = 10^{-6}$	Microstrain

References

Dokumentation

-
- [1] Puzrin, A.M., Rabaiotti, C., Hauswirth, D., Fischli, F., Tsirantonaki, D., Iten, M., Facchini, M., and Friedrich, E., (2019). «**Distributed fibre optic strain sensing in pavements**». Zurich, Schweizerischer Verband der Strassen- und Verkehrsfachleute VSS, www.mobilityplatform.ch.
-
- [2] Cosentino, P.J., Wulf von Eckroth, P.E. and Grossman, B.G., (2003), «**Analysis of Fibre Optic Traffic Sensors in Flexible Pavements**», Journal of Transportation Engineering, 129 (5), 549-557.
-
- [3] Malla, R.B., Sen, A. & Garrick, N.W., (2008), «**A special fibre optic sensor for measuring wheel loads of vehicles on highways**». Sensors 2008, 8, 2551-2568.
-
- [4] Iten, M. and Puzrin, A.M., (2009), «**BOTDA road-embedded strain sensing system for landslide boundary localization**», in: N.G. Meyendorf, K.J. Peters and W. Ecke, eds. Smart Sensor Phenomena, Technology, Networks, and Systems 2009, Proceedings of SPIE 7293, 7 April 2009 San Diego. Bellingham, WA: International Society for Optics and Photonics (SPIE), 729316.
-
- [5] Zhou, Z., Liu, W., Huang, Y., Wang, H., He, J., Huang, M. and Ou, J., (2012), «**Optical fibre Bragg grating sensor assembly for 3D strain monitoring and its case study in highway pavement**», Mechanical Systems and Signal Processing, 28, 36-49.
-
- [6] Dong, Z., Li, S., Wen, J. and Chen, H., (2012), «**Asphalt pavement structural health monitoring utilizing FBG sensors**», Advanced Engineering Forum, 5, 339-344.
-
- [7] Wu, J., Ye, F., Hugo, F. and Wu, Y., (2015), «**Strain response of a semi-rigid base asphalt pavement based on heavy-load full-scale accelerated pavement testing with fibre Bragg grating sensors**», Road Materials and Pavement Design, 16 (2), 316-333.
-
- [8] Liu, W., Wang, H., Zhou, Z., Xing, X., Cao, D. and Jiang, Z., (2015), «**Optical fibre-based sensors with flexible encapsulation for pavement behaviour monitoring**», Structural Control and Health Monitoring 2015, 22, 301-313.
-
- [9] Xiang, P. and Wang, H., (2016), «**Optical-fibre-based sensors for distributed strain monitoring in pavements**», International Journal of Pavement Engineering, 19 (9), 842-850.
-
- [10] Wang, H., Xiang, P. and Jiang, L., (2018), «**Optical Fibre Based In-Field Structural Performance Monitoring of Multilayered Asphalt Pavement**», Journal of Lightwave Technology, 36 (17), 3624-3632.
-
- [11] Bao, Y. and Chen, G., (2016), «**Strain distribution and crack detection in thin unbonded concrete pavement overlays with fully distributed fibre optic sensors**», Optical Engineering, 55 (1), 011008.
-
- [12] Chapeleau, X., Blanc, J., Hornych, J-L G. and Carroget, J., (2017), «**Assessment of cracks detection in pavement by a distributed fibre optic sensing technology**», Journal of Civil Structural Health Monitoring, 7 (4), 459-470.
-
- [13] Rabaiotti, C., Hauswirth, D., Fischli, F., Facchini, M. and Puzrin, A.M., (2017), «**Structural health monitoring of airfield pavement using distributed fibre-optic sensing**», in: Fourth Conference on Smart Monitoring, Assessment and Rehabilitation of Civil Structures – Proceedings of SMAR 2017, 13-15 September 2017, Zurich, www.smar2017.org.
-
- [14] Hauswirth, D., Fischli, F., Rabaiotti, C. and Puzrin, A.M., (2020), «**Distributed fibre optic strain measurements in an airfield pavement**», in: C. Raab, ed. Proceedings of the 9th International Conference on Maintenance and Rehabilitation of Pavements – Mairepav9, Lecture Notes in Civil Engineering 76, 1-3 July 2020 Dubendorf. Cham: Springer Nature Switzerland, 825-834.
-
- [15] De Maeijer, P.K., Luyckx, G., Vuye, C., Voet, E., Van den bergh, W., Vanlanduit, S., Braspeninckx, J., Stevens, N. and De Wolf, J., (2019), «**Fibre Optics Sensors in Asphalt Pavement: State-of-the-art Review**», Infrastructures 2019, 4 (36).
-
- [16] Thévenaz, L. ed., (2011), «**Advanced fibre optics – Concepts and technology**», Lausanne, Switzerland: EPFL Press.
-
- [17] Hartog, A.H., (2017), «**An introduction to distributed optical fibre sensors**», Taylor and Francis Group, Boca Raton, FL, USA: CRC Press.
-
- [18] Berghmans, F. and Geernaert, T., (2011), «**Optical fiber point sensors**», Advanced fiber optics – Concepts and technology, Thévenaz, L. (ed.), EPFL Press, Lausanne, pp. 309-344.
-
- [19] Polytec., (2012). «**Faseroptische Sensorik**», Polytec GmbH, Waldbronn.
-
- [20] Thévenaz, L., (2011), «**Inelastic scatterings and applications to distributed fiber optic sensing**», Advanced fiber optics – Concepts and technology, Thévenaz, L. (ed.), EPFL Press, Lausanne, pp. 263-344.
-

- [21] Wuilpart, M., (2011), «**Rayleigh scattering in optical fibers and applications to distributed measurements**»,. Advanced fiber optics – Concepts and technology, Thévenaz, L. (ed.), EPFL Press, Lausanne, pp. 207-262.
-
- [22] Dakin, J.P., Pratt, D.J., Bibby, G.W. and Ross, J.N., (1985), «**Distributed optical fibre Raman temperature sensor using a semiconductor light source and detector**», Electronics Letters, Vol. 21, No. 13, pp. 569-570.
-
- [23] Cotter, D., (1983), «**Stimulated Brillouin Scattering in monomode optical fiber**», J. Opt. Commun. Vol. 4, No. 1, pp. 10-19.
-
- [24] Horiguchi, T., Kurashima, T., and Tateda, M., (1989). «**Tensile strain dependence of Brillouin frequency shift in silica optical fibers**», IEEE Photonics Technology Letters, Vol. 1, No. 5, pp. 107-108.
-
- [25] Kurashima, T., Horiguchi, T. and Tateda, M., (1990), «**Thermal effects on the Brillouin frequency shift in jacketed optical silica fibers**», Applied Optics, Vol. 29, No. 15, pp. 2219-2222.
-
- [26] Horiguchi, T., Shimizu, K., Kurashima, T., Tateda, M. and Koyamada, Y., (1995), «**Development of a distributed sensing technique using Brillouin scattering**», Journal of Lightwave Technology, Vol. 13, No. 7, pp. 1296-1302.
-
- [27] Niklès, M., Thévenaz, L. and Robert, P.A., (1997), «**Brillouin gain spectrum characterization in single-mode optical fibers**», Journal of Lightwave Technology, Vol. 15, No. 10, pp. 1842-1851.
-
- [28] Niklès, M., (2007), «**Fibre optic distributed scattering sensing system: Perspectives and challenges for high performance applications**», 3rd European Workshop on Optical Fibre Sensors (EWOFS), Proc. of SPIE, Vol. 6619, pp. 0D-1-0D8.
-
- [29] Kishida, K., Che-Hien, L. and Nishiguchi, K., (2005), «**Pulse pre-pump method for cm-order spatial resolution of BOTDA**», 17th Int. Conf. on Optical Fibre Sensors (OFS-17), Voet, M., Willsch, R., Ecke, W., Jones, J. & Culshaw, B. (eds.), Proc. of SPIE, Vol. 5855, pp. 559-562.
-
- [30] Froggatt, M. and Moore, J., (1998), «**High-spatial-resolution distributed strain measurement in optical fiber with Rayleigh scatter**», Applied Optics, Vol. 37, No. 10, pp. 1735-1740.
-
- [31] Gifford, D.K., Soller, B.J., Wolfe, M.S. and Froggatt, M.E. (2005). «**Distributed fibre-optic temperature sensing using Rayleigh backscatter**», Proc. of ECOC 2005, Vol. 3, Paper We4.P.005.
-
- [32] Gifford, D.K., Kreger, S.T., Sang, A.K., Froggatt, M.E., Duncan, R.G., Wolfe, M.S. and Soller, B.J., (2007), «**Swept-wavelength interferometric interrogation of fiber Rayleigh scatter for distributed sensing applications**», Fiber Optic Sensors and Applications V, Udd, E. (ed.), Proc. of SPIE, Vol. 6770, pp. 0F-1-0F-9.
-

Project closure



Schweizerische Eidgenossenschaft
Confédération suisse
Confederazione Svizzera
Confederaziun svizra

Eidgenössisches Departement für
Umwelt, Verkehr, Energie und Kommunikation UVEK
Bundesamt für Strassen ASTRA

FORSCHUNG IM STRASSENWESEN DES UVEK

Version vom 09.10.2013

Formular Nr. 3: Projektabschluss

erstellt / geändert am: 27.09.22

Grunddaten

Projekt-Nr.: TRU_20_01B_01
 Projekttitel: Applicability of existing fibre optic cable solutions for strain measurements in mastic asphalt
 Enddatum: 30.09.22

Texte

Zusammenfassung der Projektergebnisse:

Verteilt messende faseroptische Sensoren erlauben es, Grössen wie z.B. Dehnungen oder Temperaturen mit hoher räumlicher Auflösung kontinuierlich entlang von dünnen Glasfasern zu messen. Diese Eigenschaft macht diese Technologie, neben vielen anderen Anwendungen, auch für die Messung des Tragverhaltens von Strassenbelägen unter Belastung interessant. Das vorliegende Projekt hatte dabei zum Ziel, mögliche Glasfaserkabelösungen zu identifizieren, welche auch im Gussasphalt, nach temporär hohen Einbautemperaturen, als Dehnungssensoren eingesetzt werden könnten.

Dazu wurden in einem ersten Schritt verschiedene Kabel ausgewählt. Diese Kabel wurden zuerst im Labor vor und nach einer Temperatureinwirkung hinsichtlich ihrer Eigenschaften als Sensoren untersucht. Nach diesem ersten Test wurden diverse Kabelösungen (inkl. deren Modifikationen) in unterschiedlichen Prozeduren in Gussasphaltproben eingebaut. Dies um ausgewählte Lösungen unter realistischeren Bedingungen eingehender zu testen. Diese Gussasphaltproben wurden anschliessend im Labor einem 3-Punkt-Biegeversuch unterworfen und dabei die Dehnungen entlang der Glasfaserkabel gemessen. Diverse Kabelösungen konnten die erwartete Dehnungsverteilung gut messen, wie ein Vergleich mit nachträglich an den kalten Proben angebrachten Sensoren und einfachen numerischen Simulationen zeigte. Andere Kabelösungen erwiesen sich als mechanisch zu wenig robust, zeigten Mängel bei der Dehnungsübertragung oder beeinflussten lokal das Tragverhalten der Gussasphaltprobe. Bezüglich Einbauverfahren wurden insbesondere Lösungen an Schichtgrenzen als praktikabel bewertet, während die Positionierung auf beliebiger Höhe in der Gussasphaltprobe noch weitergehende Untersuchungen bezüglich Sicherstellung der Lagestabilität benötigt. Abschliessend kann gefolgert werden, dass kommerziell erhältliche Kabelösungen für eine verteilte Dehnungsmessung im Gussasphalt existieren. Die Wahl der einzubauenden Kabelösung hängt dabei vom jeweiligen Anwendungszweck ab. Der Schlussbericht enthält dazu die entsprechenden Resultate und Hinweise.



Schweizerische Eidgenossenschaft
Confédération suisse
Confederazione Svizzera
Confederaziun svizra

Eidgenössisches Departement für
Umwelt, Verkehr, Energie und Kommunikation UVEK
Bundesamt für Strassen ASTRA

Zielerreichung:

Die Frage, ob zur Zeit Kabel für eine Dehnungsmessung im Gussasphalt kommerziell verfügbar sind, kann positiv beantwortet werden. Einige Kabel übertrafen die Erwartungen bei einer Dehnungsmessung in einem Biegeversuch deutlich. Die Hauptzielsetzung dieses Projektes konnte damit erreicht werden. Bezüglich der allgemeinsten Einbauprozedur auf beliebiger Höhenlage im Gussasphalt müssen noch weitere Überlegungen angestellt werden, um eine optimale Lagestabilität zu erreichen. Andere Einbauverfahren z.B. an Schichtgrenzen, erwiesen sich als einfacher realisierbar.

Folgerungen und Empfehlungen:

Es zeigte sich, dass die Dehnungsverteilung im Gussasphalt mit faseroptischen Sensoren mit hohem Detaillierungsgrad gemessen werden kann. Dies eröffnet, in Kombination mit anderen Messverfahren und der Modellierung, verschiedene Möglichkeiten um das Tragverhalten von Gussasphalt unter Belastung zu untersuchen.

Einige der getesteten Kabel liefern sowohl im Dehnungsversuch als auch im Biegeversuch sehr gute Ergebnisse - mit und ohne Modifikationen als zusätzlichen Schutz. Vor allem diese Kabel können für weiterführende Versuche empfohlen werden. Wenn in Feldanwendungen von Gussasphalt der Einsatz anderer faseroptischer Messtechnologien (als der hier verwendeten) vorgesehen ist, sollte vorab die Übertragbarkeit der Resultate punktuell überprüft werden.

Publikationen:

-

Der Projektleiter/die Projektleiterin:

Name: Puzrin

Vorname: Alexander M.

Amt, Firma, Institut: Institut für Geotechnik, ETH Zürich

Unterschrift des Projektleiters/der Projektleiterin:



Schweizerische Eidgenossenschaft
Confédération suisse
Confederazione Svizzera
Confederaziun svizra

Eidgenössisches Departement für
Umwelt, Verkehr, Energie und Kommunikation UVEK
Bundesamt für Strassen ASTRA

FORSCHUNG IM STRASSENWESEN DES UVEK

Formular Nr. 3: Projektabschluss

Beurteilung der Begleitkommission:

Beurteilung:

Die vorgeschlagene Forschung hatte zum Ziel, herauszufinden, ob bestehende handelsübliche Glasfaserkabelösungen für den Zweck der Dehnungsmessung in Gussasphalt verwendet werden können, auch wenn beim Einbau von Gussasphalt vorübergehend hohe Temperaturen von über 200°C auf sie einwirken. Darüber hinaus sollte geprüft werden, ob Kabelkonstruktionen, die für den vorliegenden Anwendungszweck unzureichend sind, durch kleiner Modifikationen verbessert werden können.

Das durchgeführte Forschungsprojekt konnte zeigen, dass einerseits bereits Glasfaserkabel für die beabsichtigte Anwendung vorhanden und andererseits allerdings nur bedingt Modifikationen ungenügender Kabel möglich sind. Die Zielsetzung des Projekts konnte damit erreicht werden.

Umsetzung:

Zusammenfassend lässt sich sagen, dass die faseroptische Technologie zur Untersuchung des Verhalten von Gussasphalt kommerziell verfügbar ist und somit auch für die entsprechenden Anwendungen eingesetzt werden kann. Es kann davon ausgegangen werden, dass sich im Laufe solcher Anwendungen sogar weiteres Entwicklungs- und Anwendungspotential ergibt.

weitergehender Forschungsbedarf:

Die Ergebnisse zeigen, dass die genaue Positionierung eines Kabels über große Spannweiten eine praktische Herausforderung bleibt, die weiteren Forschungsbedarf erfordert.

Einfluss auf Normenwerk:

Das Projekt hat keinen direkten Einfluss auf die Normung.

Der Präsident/die Präsidentin der Begleitkommission:

Name: Raab

Vorname: Christiane

Amt, Firma, Institut: Empa, Dübendorf

Unterschrift des Präsidenten/der Präsidentin der Begleitkommission: